

Project Report No. 98

MODEL STUDIES - FOOTHILL FEEDER PROJECT  
METROPOLITAN WATER DISTRICT OF SOUTHERN CALIFORNIA  
PART III. MORRIS RESERVOIR TURNOUT STRUCTURE

by  
Alvin G. Anderson  
and  
David J. Anderson

Prepared for  
HARZA ENGINEERING COMPANY  
Chicago, Illinois

August 1968

Project Report No. 10

MOBILE WATER TREATMENT PLANT  
METRO WATER DEPARTMENT OF METRO POLICE  
MAY 1964

by

John E. Anderson

and

David L. Anderson

Prepared for  
METRO WATER DEPARTMENT  
Chicago, Illinois

April 1964

## CONTENTS

	Page
Preface	
I. INTRODUCTION.....	1
A. Description of Model.....	2
II. EXPERIMENTAL RESULTS.....	3
A. Operational Characteristics.....	3
1. Theoretical Considerations.....	3
2. Experimental Results.....	5
B. Velocity Profiles in the Jets Issuing from Partially Opened Upstream and Downstream Gates.....	6
C. Distribution of Discharge Through Downstream Gates...	15
D. The Nature of Deposition in the Morris Drift.....	17
E. Pressure Fluctuations in Gate Structure.....	19
1. Apparatus for Measuring Pressure Fluctuations..	20
2. Pressure Fluctuations on Control Gates.....	21
3. Pressure Fluctuations for Various Flow Conditions.....	23
4. Pressure Fluctuations with Blind Flange on Morris Drift.....	24
III. CONCLUSIONS.....	24

List of Photos (for 14 Accompanying Photos)

List of Charts (for 24 Accompanying Charts)

ATP 1970

1970

1970

- 1. ....
- 2. ....
- 3. ....
- 4. ....
- 5. ....
- 6. ....
- 7. ....
- 8. ....
- 9. ....
- 10. ....
- 11. ....
- 12. ....
- 13. ....
- 14. ....
- 15. ....
- 16. ....
- 17. ....
- 18. ....
- 19. ....
- 20. ....
- 21. ....
- 22. ....
- 23. ....
- 24. ....
- 25. ....
- 26. ....
- 27. ....
- 28. ....
- 29. ....
- 30. ....
- 31. ....
- 32. ....
- 33. ....
- 34. ....
- 35. ....
- 36. ....
- 37. ....
- 38. ....
- 39. ....
- 40. ....
- 41. ....
- 42. ....
- 43. ....
- 44. ....
- 45. ....
- 46. ....
- 47. ....
- 48. ....
- 49. ....
- 50. ....

.....

.....

.....

## PREFACE

This report is the third in a series dealing with the gated control structures to be used in the Foothill Feeder of the Metropolitan Water District of Southern California. The report describes the model experiments pertaining to the operation of the Morris Reservoir Turnout Structure. This structure will provide flow control in the tunnel and in addition will incorporate the Morris Drift connected to Morris Reservoir. By means of this structure the Morris Reservoir will float on the Santa Anita Tunnel No. 2, and thus serve as a reservoir that will supply water to or receive water from the foothill feeder as needed.

Experiments have been carried out to establish the operating characteristics of the two independent sets of gates. The results show that the gates provide consistent control of the flow and could be set to provide almost any combination of head differentials desired for arbitrary elevations of Morris Reservoir.

Experiments were also carried out to delineate the flow pattern within the gate structure when it is operating at high discharges. These consisted of measurements of velocities and current directions within the structure. The measurements of vibratory pressures on the gates in the model were carried out with the Morris Drift open and closed in order to examine the effect of the additional mass of water on the fluctuations.

The Morris Reservoir Turnout Structure was similar in some respects to the Regular Gate Structure<sup>(1)</sup> and the Big Tujunga Gate and Spillway Structure<sup>(2)</sup> previously tested. This is particularly true with regard to the shape, size, and method of mounting of the gates. Many of the results obtained in the

---

(1) Model Studies - Foothill Feeder Project. Metropolitan Water District of Southern California - Part I. Regular Gate Structure. Project Report No. 91. St. Anthony Falls Hydraulic Laboratory, February 1967.

(2) Model Studies - Foothill Feeder Project. Metropolitan Water District of Southern California - Part II. Big Tujunga Gate and Spillway Structure. Project Report No. 93. St. Anthony Falls Hydraulic Laboratory, February 1968.

PATENT

The present invention is a method for the control of the flow of water in a water supply system. It is an improvement over the prior art in that it provides a means for automatically adjusting the flow of water to meet the varying demands of the system. This is accomplished by means of a control valve which is actuated by a sensor which is sensitive to the pressure of the water in the system. The sensor is connected to the control valve by means of a pipe and the control valve is connected to the water supply system by means of another pipe. The control valve is actuated by the sensor in such a manner that the flow of water is increased when the pressure of the water in the system is low and decreased when the pressure is high. This arrangement provides a means for automatically maintaining the flow of water in the system at a constant level.

The invention also provides a means for automatically adjusting the flow of water to meet the varying demands of the system. This is accomplished by means of a control valve which is actuated by a sensor which is sensitive to the pressure of the water in the system. The sensor is connected to the control valve by means of a pipe and the control valve is connected to the water supply system by means of another pipe. The control valve is actuated by the sensor in such a manner that the flow of water is increased when the pressure of the water in the system is low and decreased when the pressure is high. This arrangement provides a means for automatically maintaining the flow of water in the system at a constant level.

The invention also provides a means for automatically adjusting the flow of water to meet the varying demands of the system. This is accomplished by means of a control valve which is actuated by a sensor which is sensitive to the pressure of the water in the system. The sensor is connected to the control valve by means of a pipe and the control valve is connected to the water supply system by means of another pipe. The control valve is actuated by the sensor in such a manner that the flow of water is increased when the pressure of the water in the system is low and decreased when the pressure is high. This arrangement provides a means for automatically maintaining the flow of water in the system at a constant level.

The invention also provides a means for automatically adjusting the flow of water to meet the varying demands of the system. This is accomplished by means of a control valve which is actuated by a sensor which is sensitive to the pressure of the water in the system. The sensor is connected to the control valve by means of a pipe and the control valve is connected to the water supply system by means of another pipe. The control valve is actuated by the sensor in such a manner that the flow of water is increased when the pressure of the water in the system is low and decreased when the pressure is high. This arrangement provides a means for automatically maintaining the flow of water in the system at a constant level.

The invention also provides a means for automatically adjusting the flow of water to meet the varying demands of the system. This is accomplished by means of a control valve which is actuated by a sensor which is sensitive to the pressure of the water in the system. The sensor is connected to the control valve by means of a pipe and the control valve is connected to the water supply system by means of another pipe. The control valve is actuated by the sensor in such a manner that the flow of water is increased when the pressure of the water in the system is low and decreased when the pressure is high. This arrangement provides a means for automatically maintaining the flow of water in the system at a constant level.

The invention also provides a means for automatically adjusting the flow of water to meet the varying demands of the system. This is accomplished by means of a control valve which is actuated by a sensor which is sensitive to the pressure of the water in the system. The sensor is connected to the control valve by means of a pipe and the control valve is connected to the water supply system by means of another pipe. The control valve is actuated by the sensor in such a manner that the flow of water is increased when the pressure of the water in the system is low and decreased when the pressure is high. This arrangement provides a means for automatically maintaining the flow of water in the system at a constant level.

previous studies are also applicable to this structure. This is particularly true with regard to the gate vibrations and fluctuating pressures.

The model tests described in this report were sponsored by the Harza Engineering Company of Chicago, Illinois, which was represented by Dr. David Louie. The experiments were performed at the St. Anthony Falls Hydraulic Laboratory under the immediate direction of Alvin G. Anderson. The models were fabricated in the Laboratory shop, and much of the experimentation was carried on by David J. Anderson.





MODEL STUDIES - FOOTHILL FEEDER PROJECT  
METROPOLITAN WATER DISTRICT OF SOUTHERN CALIFORNIA  
PART III. MORRIS RESERVOIR TURNOUT STRUCTURE

I. INTRODUCTION

The Foothill Feeder Project of the Metropolitan Water District of Southern California incorporates a long tunnel through which water will be supplied to a large area in southern California. In this system head control devices are needed to regulate the discharge through the tunnels and the appurtenant structures. For this purpose gated control structures open to the atmosphere were chosen. The gate structures were circular in plan and fitted with gates for flow control. The research described in this report was carried out to study in detail the hydraulic characteristics for a wide variety of flow conditions for one of these structures, the Morris Reservoir Turnout Structure. More specifically, the items of special interest were:

- (1) The head differentials through each set of gates for various combinations of headwater, tailwater, and reservoir elevations.
- (2) Fluctuating pressures and gate vibrations that might result from various modes of operation.
- (3) The flow patterns within the structure and the effect of the Morris Drift directly connected to the Morris Reservoir on this flow pattern.

The Morris Reservoir Turnout Structure is designed to provide both flow control in the tunnel and facilities for regulating flow into or out of Morris Reservoir. It is the junction of the so-called Morris Drift with the Santa Anita Tunnel No. 2, the general features of which are shown on Chart 1. It consists essentially of a circular shaft 56 ft in diameter into which the three tunnels are directed. The upstream control consists of a full height dividing wall fitted with control gates and high level weirs for emergency operation. The tunnel leading to Morris Reservoir is uncontrolled at the structure so that the water level in the turnout structure will be essentially the same as that in Morris Reservoir. The downstream leg of the Santa Anita Tunnel No. 2, however, is controlled by another set of three gates at the point where it



leaves the control structure. The upstream and downstream sets of gates each consist of two outside gates 6 ft 3 in. wide and a center gate 2 ft wide. The maximum gate opening of each set is 18.5 ft. They are controlled from the upper deck by relatively rigid gate stems. The tunnels which enter or leave the structure are 17.5 ft in diameter.

#### Description of Model

The model was fabricated of a clear plastic at a scale of 1:38.3. This scale ratio was chosen so that standard plastic tubes could be used for the tunnel and at the same time provide a model of reasonable size. Photo 1 is a general view of the model setup showing the Santa Anita Tunnel No. 2 entering and leaving the structure and the Morris Drift leaving the structure at the left. The proper pressure in the Santa Anita tunnel downstream of the turnout structure is maintained at prescribed values by the water level in the downstream tank. The other tank to which the Morris Drift is connected is maintained at prescribed Morris Reservoir elevations. In addition, the photo shows the manometer board holding the piezometers that are attached by tubing to taps along the several tunnels at which piezometric pressures are measured. Photo 2 is a view from above showing the lower portions of the turnout structure, the gates, dividing wall, and the arrangements of the tunnel connections.

The design of the model was based upon the Froudian Law of Similarity, since the flow pattern within the structure is a gravitational phenomenon which is characterized by the free surfaces in the structure and in the reservoir. Utilizing this law the discharges in the model corresponding to specified prototype discharges can be computed and observations made in the model of pressures, water surface elevations, and flow patterns can be transferred to the prototype by the following relations:

$$V_r = L_r^{1/2}$$

$$Q_r = L_r^{5/2}$$

$$P_r = L_r$$

$$T_r = L_r^{1/2}$$

From the control elements, the upstream and downstream ends of gates, each  
 consists of two outer gates 6 ft. in width and a center gate 4 ft. wide. The  
 maximum gate opening at each end is 15 ft. They are controlled from the  
 upper bank by cables with 24 ft. gate stops. The middle gate can be raised  
 to 15 ft. or lowered to 10 ft.

*Construction of Gates*

The model was fabricated of a clear plastic of a scale of 1:30. The  
 gate ribs were chosen as flat standard plate glass which could be used for the  
 model and at the same time provide a model of reasonable size. Photo 3 is a  
 general view of the model setup showing the gate ribs spaced at 1 ft. intervals  
 and leaving the structure and the water level in the channel. The proper  
 gate opening for the flow is shown. The gate ribs were spaced at the same  
 intervals as indicated in the photograph. The water level in the channel  
 was raised. The other gate ribs were raised to the same level as water  
 level as presented for the flow. In addition, the gate ribs  
 were spaced at the same intervals as indicated by the photograph. The  
 gate ribs were spaced at the same intervals as indicated by the photograph.  
 In a view from the channel, the gate ribs were spaced at the same  
 intervals as indicated by the photograph. The gate ribs were spaced at the  
 same intervals as indicated by the photograph. The gate ribs were spaced at  
 the same intervals as indicated by the photograph. The gate ribs were spaced  
 at the same intervals as indicated by the photograph. The gate ribs were  
 spaced at the same intervals as indicated by the photograph. The gate ribs  
 were spaced at the same intervals as indicated by the photograph. The gate  
 ribs were spaced at the same intervals as indicated by the photograph. The  
 gate ribs were spaced at the same intervals as indicated by the photograph.  
 The design of the model was based upon the Froude law of similarity.  
 When the flow pattern which the channel is a conventional phenomenon which  
 is characterized by the flow pattern in the channel and in the model.  
 Utilizing this law the discharge in the model corresponding to a given  
 type discharge can be computed and observations made in the model of a given  
 water surface elevation, and flow pattern can be transferred to the prototype  
 by the following relationship:

$$\frac{V}{\sqrt{gH}} = \frac{V_m}{\sqrt{gH_m}}$$

$$\frac{Q}{\sqrt{gH^3}} = \frac{Q_m}{\sqrt{gH_m^3}}$$

$$\frac{V}{\sqrt{gH}} = \frac{V_m}{\sqrt{gH_m}}$$

$$\frac{Q}{\sqrt{gH^3}} = \frac{Q_m}{\sqrt{gH_m^3}}$$

The water supply was taken from the Mississippi River through the Laboratory supply system. The discharge was measured by means of two calibrated orifices arranged in parallel so that both large and small model discharges could be accurately measured.

## II. EXPERIMENTAL RESULTS

### A. Operational Characteristics

#### 1. Theoretical Considerations

The operating characteristics of this structure involve the coupled effect of the two sets of gates and three closely related water surface elevations. When both gate sets are combined in the same structure the calibration characteristics of one set depend to a certain degree on the relative position of the gates in the other set. In order to investigate this interrelationship as a guide to the interpretation of the physical measurements, a simplified and idealized condition is considered. The simplifying assumptions were made with the expectation that effects of neglected characteristics would be noted in the experimental data. It was initially assumed that the gates were far enough apart that the flow pattern generated by the upstream gates did not affect the operation of the downstream gates. It was further assumed that the losses of energy were negligible and that the discharge coefficients were equal. Under these circumstances the discharge through the sluice gate can be written in terms of the head differential and the gate opening as

$$Q = C_d b d (2g\Delta H)^{1/2} \quad (1)$$

in which  $Q$  is the discharge in cfs,  $C_d$  is the discharge coefficient,  $b$  is the total gate width of all the gates in feet,  $d$  is the gate opening in feet,  $g$  is the acceleration due to gravity ( $g = 32.2$  ft per sec<sup>2</sup>), and  $\Delta H$  is the head difference across the gate. Assuming that the water surface elevation in the structure is equal to that of the Morris Reservoir, so that there is no flow into or out of the reservoir, continuity requires that the flow entering the structure through the upstream set of gates be equal to the discharge leaving by the downstream set of gates so that

The water vapor in the atmosphere is a mixture of water vapor and other gases. The water vapor is a mixture of water vapor and other gases. The water vapor is a mixture of water vapor and other gases.

1. WATER VAPOR

The atmosphere

1. Physical Properties

The physical properties of water vapor are determined by the temperature and pressure. The physical properties of water vapor are determined by the temperature and pressure. The physical properties of water vapor are determined by the temperature and pressure.

$$p = \frac{2}{3} n \langle \epsilon \rangle$$

In addition to the atmospheric pressure, the total gas pressure is the sum of the partial pressures of all the gases. The total gas pressure is the sum of the partial pressures of all the gases. The total gas pressure is the sum of the partial pressures of all the gases.

$$C_d b d_1 (2g \Delta H_1)^{1/2} = C_d b d_2 (2g \Delta H_2)^{1/2}$$

or

$$d_1 \sqrt{\Delta H_1} = d_2 \sqrt{\Delta H_2} \quad (2)$$

since the discharges, the gate width, and the discharge coefficients are equal for both sets of gates. Now if  $\alpha$  is defined as the relative gate opening, so that

$$\alpha_1 = \frac{d_1}{d_T} \quad \text{and}$$
$$\alpha_2 = \frac{d_2}{d_T} \quad (3)$$

where  $d_T$  is the same maximum gate opening for each set of gates, and if  $\beta$  is defined as the relative head differential such that

$$\beta = \frac{\Delta H_1}{\Delta H_T} \quad \text{and} \quad 1 - \beta = \frac{\Delta H_2}{\Delta H_T}$$

where  $\Delta H_T$  is the total head differential across both sets of gates, then Eq. (2) can be written in dimensionless form as

$$\alpha_1 = \alpha_2 \left( \frac{1 - \beta}{\beta} \right)^{1/2} \quad (4)$$

Eq. (4), giving the relationship between  $\alpha_1$  and  $\alpha_2$ , the relative gate openings, for any particular  $\beta$  or relative head differential, represents a family of straight lines radiating from the origin. This family of curves is shown on Chart 2(a) for values of  $\beta$  ranging from 0.05 to 0.95. In addition, the graph shows a series of curves for various values of the total head differential,  $\Delta H_T$ . These are obtained for any prescribed values of  $Q$ ,  $\Delta H_T$ , and  $\beta$  by substitution in Eq. (1), using Eq. (3) in the form

$$\alpha_1 = \frac{Q}{C_d b d_T (2g \beta \Delta H_T)^{1/2}}$$

where  $C_d \approx 1.0$ . The family of curves for various total head differentials can then be computed for a given discharge. From such curves, given the

(3)

$$\frac{d}{dx} \left( \frac{1}{x} \right) = -\frac{1}{x^2}$$

Using the relationship between the derivative and the integral, we can show that the derivative of the integral of a function is the function itself. Let  $f(x)$  be a function and  $F(x)$  be its antiderivative. Then  $F'(x) = f(x)$ .

$$\frac{d}{dx} \int f(x) dx = f(x)$$

$$\frac{d}{dx} \int f(x) dx = f(x)$$

Let  $f(x) = \frac{1}{x}$ . Then  $F(x) = \ln|x|$ . The derivative of  $\ln|x|$  is  $\frac{1}{x}$ . This shows that the derivative of the integral of  $\frac{1}{x}$  is  $\frac{1}{x}$ .

$$\frac{d}{dx} \int \frac{1}{x} dx = \frac{1}{x}$$

Let  $f(x) = \frac{1}{x^2}$ . Then  $F(x) = -\frac{1}{x}$ . The derivative of  $-\frac{1}{x}$  is  $\frac{1}{x^2}$ . This shows that the derivative of the integral of  $\frac{1}{x^2}$  is  $\frac{1}{x^2}$ .

$$\frac{d}{dx} \int \frac{1}{x^2} dx = \frac{1}{x^2}$$

(3)

Let  $f(x) = \frac{1}{x^3}$ . Then  $F(x) = -\frac{1}{2x^2}$ . The derivative of  $-\frac{1}{2x^2}$  is  $\frac{1}{x^3}$ . This shows that the derivative of the integral of  $\frac{1}{x^3}$  is  $\frac{1}{x^3}$ .

$$\frac{d}{dx} \int \frac{1}{x^3} dx = \frac{1}{x^3}$$

Let  $f(x) = \frac{1}{x^4}$ . Then  $F(x) = -\frac{1}{3x^3}$ . The derivative of  $-\frac{1}{3x^3}$  is  $\frac{1}{x^4}$ . This shows that the derivative of the integral of  $\frac{1}{x^4}$  is  $\frac{1}{x^4}$ .



discharge and the total head drop, as well as the elevation of Morris Reservoir, the relative gate openings for the upstream and downstream gates can be determined. The actual curves as measured in the model should be somewhat similar to those in Chart 2, but will include such effects as the spacing between gate sets, flow pattern, energy loss, and discharge coefficients.

## 2. Experimental Results

Charts 3, 4, and 5 present the results of actual measurements of relative gate openings as measured in the model for different discharges and total head differential. The tests were conducted with three different values of the tailwater elevations downstream of the structure in the Santa Anita Tunnel No. 2 of 1130, 1150, and 1170 ft in order to determine among other things if such a variation in tailwater elevation influenced the calibration curves. The charts present data for three different discharges; that is, Chart 3 gives the results for a discharge of 420 cfs, Chart 4 for 1,000 cfs, and Chart 5 for 1,550 cfs. The two graphs shown on each chart are presentations of the same data. The logarithmic plot serves to spread out the data for the larger total head differentials, and facilitates the determination of the gate openings. The curves delineate a pattern which is similar to the idealized computed curves. The differences are principally that the  $\beta$  curves are not actually straight lines but are somewhat curved and shifted closer together. This curvature and shift is due to the non-ideal flow pattern, which is the result of the non-symmetrical gate arrangement and the irregular flow pattern between gate sets. In addition, there is a transition zone for each set of gates beyond which the relative gate opening exerts no influence upon the generated head differentials. In this region the total head differential is controlled by one gate set only.

The experiments have shown that a point exists beyond which a particular gate set has no influence upon the head differential through the structure. The lines-of-no-control represent the practical values for  $\beta = 0$  and  $\beta = 1.0$ . That is to say, for a given total head differential when the upstream gate is sufficiently closed, all the head differential occurs at the upper gate and is independent of the position of the downstream gate provided the downstream gate is above the line-of-no-control. On the other hand, when the downstream gate

the energy and the total head drop, as well as the elevation of the reservoir. The relative gas openings for the upstream and downstream gases can be determined. The actual curves as measured in the actual model are compared with the theoretical curves. In the case of the total head drop between the two reservoirs, the energy loss and discharge coefficients are determined.

### 4. Experimental Results

Graphs 5, 6, and 7 present the results of actual measurements of relative gas openings as measured in the model for different discharge and total head coefficients. The data were recorded with three different values of the discharge coefficient,  $C_{d1}$ ,  $C_{d2}$ , and  $C_{d3}$ , in the range of the discharge coefficient from 0.5 to 1.0. In order to determine the effect of the relative gas openings on the total head drop, the measurements were taken for  $C_{d1} = 0.5$ ,  $C_{d2} = 0.7$ , and  $C_{d3} = 0.9$ . The results for a discharge coefficient of 0.5 are shown in Graph 5 for  $C_{d1} = 0.5$ ,  $C_{d2} = 0.7$ , and  $C_{d3} = 0.9$ . The results for a discharge coefficient of 0.7 are shown in Graph 6 for  $C_{d1} = 0.5$ ,  $C_{d2} = 0.7$ , and  $C_{d3} = 0.9$ . The results for a discharge coefficient of 0.9 are shown in Graph 7 for  $C_{d1} = 0.5$ ,  $C_{d2} = 0.7$ , and  $C_{d3} = 0.9$ . The results for a discharge coefficient of 0.5 are shown in Graph 5 for  $C_{d1} = 0.5$ ,  $C_{d2} = 0.7$ , and  $C_{d3} = 0.9$ . The results for a discharge coefficient of 0.7 are shown in Graph 6 for  $C_{d1} = 0.5$ ,  $C_{d2} = 0.7$ , and  $C_{d3} = 0.9$ . The results for a discharge coefficient of 0.9 are shown in Graph 7 for  $C_{d1} = 0.5$ ,  $C_{d2} = 0.7$ , and  $C_{d3} = 0.9$ .

The measurements have shown that a point exists beyond which a certain discharge coefficient cannot be maintained through the contraction. The discharge coefficient represents the practical value for  $C_{d1}$  and  $C_{d2}$ . The discharge coefficient for a given total head difference between the two reservoirs is determined by the head difference between the two reservoirs and the relative gas openings of the upstream gas and the downstream gas. On the other hand, when the discharge coefficient is above the theoretical value, the discharge coefficient is determined by the relative gas openings of the upstream and downstream gases.

is nearly closed, the upstream gate may be drowned out, so that any position above that given by the line-of-no-control again has no influence upon the flow pattern.

Computations of the discharge coefficient defined by

$$C_d = \frac{Q}{bd (2g \Delta H + V^2)^{1/2}} \quad (5)$$

show that they are less than one in all cases. In Eq. (5) the velocity of approach was included in order to approximate the flow patterns existing in the structure. The approach velocity at the upstream gates was assumed to be the velocity in the upstream tunnel, while the approach velocity at the downstream gates was assumed to be the discharge divided by the area of the upstream gate opening, since the gates were so close together that the jet under the upstream gates did not have room to expand to the full depth. The computed discharge coefficients ranged between 0.72 and 0.98 for the upstream gates and between 0.56 and 0.88 for the downstream gates.

It will be observed in Charts 3, 4, and 5 that the calibration curves are independent of the tailwater elevation in Santa Anita Tunnel No. 2 within the range of values tested. The reason for this is that for these tailwaters the gates are very deeply submerged and the precise tailwater elevation in the structure does not influence the flow pattern through and between the gate sets. This means that a single calibration curve for each discharge will be applicable to all reservoir elevations within the prescribed range of variation.

#### B. Velocity Profiles in the Jets Issuing from Partially Opened Upstream and Downstream Gates

Chart 1 shows that the streamlines for the flow through the turnout structure are curved, and one might expect that the discharges through the respective downstream gates would not be equal and that the flow pattern might be complicated by the presence of the Morris Drift. In order to help determine the distribution of the flow at the downstream gates in comparison with the pattern in the upstream gates, the measurement of velocities within the structure was undertaken.

to study the effect of the system on the system. The system is a linear system and the input is a step function. The output is a step function with a delay. The delay is due to the system's response time.

Transfer function of the system is given by

$$G(s) = \frac{1}{s(s+1)}$$

where  $s$  is the Laplace transform variable. The transfer function is a rational function. The denominator is a second-order polynomial. The numerator is a constant. The system is a second-order system. The system is a linear system. The system is a time-invariant system. The system is a causal system. The system is a stable system. The system is a minimum phase system. The system is a BIBO stable system. The system is a BIBO unstable system. The system is a BIBO marginally stable system. The system is a BIBO asymptotically stable system. The system is a BIBO unstable system. The system is a BIBO marginally stable system. The system is a BIBO asymptotically stable system.

The system is a linear system. The system is a time-invariant system. The system is a causal system. The system is a stable system. The system is a minimum phase system. The system is a BIBO stable system. The system is a BIBO unstable system. The system is a BIBO marginally stable system. The system is a BIBO asymptotically stable system. The system is a BIBO unstable system. The system is a BIBO marginally stable system. The system is a BIBO asymptotically stable system.

The system is a linear system. The system is a time-invariant system. The system is a causal system. The system is a stable system. The system is a minimum phase system. The system is a BIBO stable system. The system is a BIBO unstable system. The system is a BIBO marginally stable system. The system is a BIBO asymptotically stable system. The system is a BIBO unstable system. The system is a BIBO marginally stable system. The system is a BIBO asymptotically stable system.

The system is a linear system. The system is a time-invariant system. The system is a causal system. The system is a stable system. The system is a minimum phase system. The system is a BIBO stable system. The system is a BIBO unstable system. The system is a BIBO marginally stable system. The system is a BIBO asymptotically stable system. The system is a BIBO unstable system. The system is a BIBO marginally stable system. The system is a BIBO asymptotically stable system.

In the first set of experiments measurements of the vertical velocity profiles were made downstream of the left and right upstream gates and downstream of the left and right downstream gates. These velocities were measured on the vertical centerline of each gate for the maximum discharge of 1550 cfs. In order to gain greater insight into the velocity patterns, additional measurements were made at the successive stations along the same centerline downstream of the respective gates.

At the time that the velocity measurements were taken an attempt was made to photograph the flow pattern in the vicinity of the upstream gates. For this purpose a streamer of dye was introduced through an upstream port and permitted to move downstream into the structure. Photo 5 was taken just as the dye flowed under the gate. The streamlines upstream of the gate are clearly shown and the downstream jet is confined to a thickness about equal to the gate opening. This photo was taken before the dye was diffused into the overlying water in the structure and into the Morris Drift. The high velocity flow near the bottom extends to and through the downstream gates. Photo 6 is another view of the gate section a short time later, when the dye has diffused throughout the region upstream of the gates. The jet, however, is still well-defined and the dye has not yet begun to mix with the surrounding water.

The velocities at each station were measured by means of special pre-calibrated Pitot-static tubes that could be inserted into the structure at prescribed points. For velocity profiles downstream of the upstream gates the measuring points were located within the turnout structure and were easily reached. Normally, access to the transition section downstream of the downstream gates was not possible, but special fittings were installed so that the Pitot tubes could be inserted through the upper wall of the transition section.

The velocity measurements were made for a discharge of 1550 cfs, the maximum flow for this structure. The difference in elevation between the headwater and the tailwater was also fixed at the maximum in order that the velocities would represent the most extreme flow situation. The headwater was maintained at elevation 1180 ft and the tailwater was lowered to elevation 1130 ft. The gate openings of the upstream and downstream outside gates were made the same, each being open 4 ft (21.5 per cent). The center gates were closed. The water level in the chamber, and hence in the Morris Reservoir, was

In the first set of experiments measurements of the vertical velocity profiles were made downstream of the left and right upstream gates and downstream of the left and right downstream gates. These velocities were measured at the vertical centerline of each gate for the maximum thickness of 1.50 ft. In order to gain greater insight into the velocity patterns, additional measurements were made at the successive stations along the same centerline downstream of the respective gates.

At the time that the velocity measurements were taken an attempt was made to photograph the flow pattern in the vicinity of the upstream gates. For this purpose a streamer of dye was introduced through an upstream port and permitted to move downstream into the apparatus. Photo 5 was taken just as the dye flowed under the gate. The streamlines upstream of the gate are clearly shown and the thickness of the dye is confined to a thickness about equal to the gate opening. This photo was taken before the dye was diffused into the overlying water in the structure and into the Morris Unit. The high velocity flow near the bottom extends to and through the downstream gates. Photo 6 is another view of the gate section a short time later when the dye has diffused throughout the region upstream of the gates. The dye, however, is still well-defined and the dye has not yet begun to mix with the surrounding water.

The velocities at each station were measured by means of optical resistance probes which were inserted into the structure at prescribed points. For velocity profiles downstream of the upstream gates the measurements were located within the tunnel structure and were easily accessed. However, access to the transition section downstream of the downstream gates was not possible, but special fittings were installed so that the Pitot tubes could be inserted through the upper wall of the transition section.

The velocity measurements were made for a discharge of 1.50 cfs, the maximum flow for this structure. The difference in elevation between the head water and the tailwater was also fixed at the maximum in order that the velocities would represent the most extreme flow situation. The headwater was maintained at elevation 1180 ft and the tailwater was lowered to elevation 1150 ft. The gate openings of the upstream and downstream gates were made the same, each being open 4-ft (2.5 per cent). The center gates were closed. The water level in the chamber, and hence in the Morris Reservoir, was

permitted to seek the equilibrium elevation. In normal operation the gates would have to be adjusted to take into account the pre-existing water surface elevation in Morris Reservoir. However, for this experiment with equal gate openings the water level in the chamber between the gates was in equilibrium at elevation 1150 ft. This water surface elevation indicates that the head drop through the upstream gates was 30 ft, while the head drop through the downstream gates was only 20 ft. This difference is probably due to the very high velocity of approach directed toward the downstream gates as compared to the velocity of approach of the upstream gates. The approach velocity for the upstream gates is approximately the mean velocity in the approach tunnel, while that for the downstream gates is of the same order of magnitude as the jet velocity under the upstream gates. If one assumes equal head losses through the upstream and downstream gates respectively and neglects the kinetic energy factor,

$$\Delta(\Delta H) = \frac{V_3^2}{2g} - \frac{V_1^2}{2g}$$

where  $\Delta(\Delta H)$  is the difference between the head differentials of the upstream and downstream gates,  $V_3$  is the velocity of approach of the downstream gates, and  $V_1$  is the velocity of approach of the upstream gates. A study of the velocity profiles generated at the upstream gates indicates that the difference of the measured head differentials is on the same order as the difference in respective velocity heads.

It was felt initially that sufficient information regarding the patterns of flow could be obtained by measuring the vertical velocity profiles of the centerline of the gates. It was recognized, however, that because of the non-symmetry of the flow pattern in the turnout structure the discharge in the individual downstream gates might not be the same, but it was not possible to predict the distribution of the discharge through the downstream gates.

In addition to the measurements of the discharge rates and gate velocities for the normal geometry, velocity measurements were also made with the entrance to the Morris Drift closed by means of a blank flange. The purpose of these measurements was to determine whether the volume of water enclosed within the Morris Drift would have measurable influence upon the energy dissipation and





the velocity pattern within the turnout structure. It had been observed that the high velocity flow from the upstream left gate (Photos 5 and 6) moving past the entrance to the Morris Drift was able to generate and maintain vortex motion that extended for a considerable distance into Morris Drift before it was dissipated. The purpose of these measurements was to determine whether the creation and maintenance of the vortex motion would have any measurable influence upon the energy dissipation or velocity pattern within the turnout structure.

The results of these measurements are shown in Charts 6, 7, 8, and 9. Chart 6 shows the vertical velocity profiles for stations along the downstream centerline of the right upstream gate; Chart 7 shows similar profiles for the left upstream gate, while Charts 8 and 9 show corresponding vertical profiles at several stations on the longitudinal centerlines downstream of the right and left downstream gates respectively. On each chart the velocity profiles obtained with the Morris Drift entrance closed by the blind flange are plotted for comparison.

It should be noted that the velocity profiles for the right and left upstream gates are practically identical and show that the flow entering the turnout structure is very uniformly divided, and the flow patterns are highly symmetrical whether the Morris Drift is closed or open. It appears, however, that the velocities measured when the entrance to the Morris Drift was closed are consistently less than those obtained when the Morris Drift was open. This difference is probably due to errors in re-establishing a discharge for the consecutive tests.

The velocity patterns developed at the right and left downstream gates, however, show somewhat greater differences in velocity between the right and left gates and for the two conditions of the Morris Drift entrance. It will also be observed that for these profiles, in contrast to those measured at the upstream gates, the velocities with the entrance to the Morris Drift closed are slightly greater than those observed when the Morris Drift was open. Combining these observations with the profiles obtained from the upstream gates indicates that the effect of Morris Drift on the velocity profiles is greater than first appears on the charts. In spite of this, however, the velocity patterns

the velocity pattern within the current structure. It had been observed that the high velocity flow from the upstream left gate (labeled 1 and 2) moving past the entrance to the Morris Mill was due to generate and maintain velocity pattern that extended for a considerable distance into Morris Mill before it was dissipated. The purpose of these measurements was to determine whether the erosion and maintenance of the vortex would have any measurable influence upon the energy dissipation or velocity pattern within the current structure.

The results of these measurements are shown in Figures 4, 5, 6, and 7. Figure 4 shows the vertical velocity profile for station above the downstream end of the right upstream gate. Figure 5 shows similar profile for the left upstream gate, while Figure 6 and 7 show corresponding vertical profiles at various stations on the longitudinal centerline downstream of the right and left downstream gates respectively. In each case the velocity profiles obtained with the Morris Mill entrance closed by the blind flange are plotted for comparison.

It should be noted that the velocity profiles for the right and left gates are very similar, indicating that the flow from the right gate is very similar to that from the left gate. It was also observed that the velocity pattern above the Morris Mill was very similar to that observed in the Morris Mill when the Morris Mill was open. This indicates that the velocity pattern above the Morris Mill was very similar to that observed in the Morris Mill when the Morris Mill was open. The overall picture is that the velocity pattern above the Morris Mill is very similar to that observed in the Morris Mill when the Morris Mill was open.

The velocity patterns developed at the right and left downstream gates, however, show somewhat greater differences in velocity between the right and left gates and for the two conditions of the Morris Mill entrance. It will also be observed that for these profiles, as contrasted to those measured at the upstream gates, the velocities with the entrance to the Morris Mill closed are slightly greater than those observed when the Morris Mill was open. Comparing these observations with the profiles obtained from the upstream gates indicates that the effect of Morris Mill on the velocity profiles is greater than that appears on the charts. In spite of this, however, the velocity patterns

obtained with the Morris Drift open and closed are remarkably similar. It will also be observed that the maximum velocity just downstream of the left downstream gate is several feet per second larger than the maximum velocity along the centerline of the right downstream gate. This is to be expected from the geometry of the gate structure and the direction of curvature of the streamlines. If for any reason the velocity of approach to the gate is reduced, the velocity under the gate will be correspondingly reduced.

Some comparisons between these results can be made by integrating the area of each velocity profile as an indication of the unit discharge at the centerline. It must be remembered, however, that because of the curvature of the streamlines approaching the downstream gates the velocity pattern--that is, the transverse velocity profile--will not be symmetrical and consequently the discharges measured at the centerline will not necessarily be proportional to the total discharge. They will, however, give a good indication of the effects of asymmetry upon the individual discharges, if these areas can be compared with each other. The relative discharges through the several gates based upon these computations are given in Table I. Any lack of balance between the discharges could be caused by the non-uniformity of the transverse velocity profiles resulting from the forced curvature of the streamlines between the upstream and downstream gate sets. This becomes apparent when the sum of the unit discharges for the upstream gates (301 cfs/ft) is compared to that of the downstream gates (285 cfs/ft). The tests showed, however, relatively little difference in the discharge through the left and right downstream gates.

Additional velocity measurements within the turnout structure and between the upstream and downstream gates are shown in Charts 10 through 14. For the measurements shown in Charts 10, 11, and 12 the upstream gates were set at a 15 per cent opening and the downstream gates were fully open. In addition, all the gates in each set were opened equally. This arrangement of gates for a discharge of 1550 cfs results in a head differential across the upstream gates of 39 ft, while the head differential across the downstream gates was only about 1 ft. The headloss in the downstream gates is due entirely to the effect of the structure geometry, since Chart 5 shows that the downstream gates lose control when the gates are open over 50 per cent. The velocity measurements were made at various points within the turnout structure using a Pitot-static

The first part of the paper is devoted to a discussion of the general principles of the theory of the structure of the atom. It is shown that the structure of the atom is determined by the laws of quantum mechanics and the laws of electrodynamics. The second part of the paper is devoted to a discussion of the structure of the nucleus. It is shown that the structure of the nucleus is determined by the laws of quantum mechanics and the laws of electrodynamics. The third part of the paper is devoted to a discussion of the structure of the molecule. It is shown that the structure of the molecule is determined by the laws of quantum mechanics and the laws of electrodynamics.

The fourth part of the paper is devoted to a discussion of the structure of the crystal. It is shown that the structure of the crystal is determined by the laws of quantum mechanics and the laws of electrodynamics. The fifth part of the paper is devoted to a discussion of the structure of the liquid. It is shown that the structure of the liquid is determined by the laws of quantum mechanics and the laws of electrodynamics. The sixth part of the paper is devoted to a discussion of the structure of the gas. It is shown that the structure of the gas is determined by the laws of quantum mechanics and the laws of electrodynamics.

The seventh part of the paper is devoted to a discussion of the structure of the plasma. It is shown that the structure of the plasma is determined by the laws of quantum mechanics and the laws of electrodynamics. The eighth part of the paper is devoted to a discussion of the structure of the solid. It is shown that the structure of the solid is determined by the laws of quantum mechanics and the laws of electrodynamics. The ninth part of the paper is devoted to a discussion of the structure of the liquid crystal. It is shown that the structure of the liquid crystal is determined by the laws of quantum mechanics and the laws of electrodynamics.

The tenth part of the paper is devoted to a discussion of the structure of the polymer. It is shown that the structure of the polymer is determined by the laws of quantum mechanics and the laws of electrodynamics. The eleventh part of the paper is devoted to a discussion of the structure of the composite material. It is shown that the structure of the composite material is determined by the laws of quantum mechanics and the laws of electrodynamics. The twelfth part of the paper is devoted to a discussion of the structure of the nanomaterial. It is shown that the structure of the nanomaterial is determined by the laws of quantum mechanics and the laws of electrodynamics.

The thirteenth part of the paper is devoted to a discussion of the structure of the quantum dot. It is shown that the structure of the quantum dot is determined by the laws of quantum mechanics and the laws of electrodynamics. The fourteenth part of the paper is devoted to a discussion of the structure of the quantum wire. It is shown that the structure of the quantum wire is determined by the laws of quantum mechanics and the laws of electrodynamics. The fifteenth part of the paper is devoted to a discussion of the structure of the quantum well. It is shown that the structure of the quantum well is determined by the laws of quantum mechanics and the laws of electrodynamics.

TABLE I  
 Comparison of Unit Discharges Through Control Gates  
 Morris Drift Open and Closed

<u>Combination of Gates</u>	<u>Unit Discharges</u>	<u>Ratio of Discharges</u>
$\frac{\text{USL}}{\text{USL} + \text{USR}} (1)$	$\frac{147}{301}$	0.49
$\frac{\text{DSR}}{\text{DSL} + \text{USR}} (1)$	$\frac{154}{301}$	0.51
$\frac{\text{DSL}}{\text{DSL} + \text{DSR}} (1)$	$\frac{147}{285}$	0.51
$\frac{\text{DSR}}{\text{DSL} + \text{DSR}} (1)$	$\frac{138}{285}$	0.49
$\frac{\text{USL open}}{\text{USL closed}}$	$\frac{147}{136}$	1.08
$\frac{\text{USR open}}{\text{USR closed}}$	$\frac{154}{154.5}$	1.00
$\frac{\text{DSL open}}{\text{DSL closed}}$	$\frac{147}{153}$	0.96
$\frac{\text{DSR open}}{\text{DSR closed}}$	$\frac{138}{138}$	1.00

USL Upstream left gate  
 USR Upstream right gate  
 DSL Downstream left gate  
 DSR Downstream right gate  
 (1) Morris Drift Open

TABLE I  
Comparison of the observed and theoretical values of the ratio of the number of particles in the ground state to the total number of particles

Ratio of Observed to Theoretical Values	Observed Values	Theoretical Values
0.95	$\frac{100}{105}$	(1) $\frac{100}{105}$
0.90	$\frac{90}{100}$	(1) $\frac{90}{100}$
0.85	$\frac{85}{100}$	(1) $\frac{85}{100}$
0.80	$\frac{80}{100}$	(1) $\frac{80}{100}$
0.75	$\frac{75}{100}$	$\frac{75}{100}$
0.70	$\frac{70}{100}$	$\frac{70}{100}$
0.65	$\frac{65}{100}$	$\frac{65}{100}$
0.60	$\frac{60}{100}$	$\frac{60}{100}$

The observed values are compared with the theoretical values calculated from the Boltzmann distribution. The theoretical values are calculated from the Boltzmann distribution using the observed values of the number of particles in the ground state and the total number of particles.

tube. It was located at successive stations on a longitudinal centerline of the right upstream gates and at various points on a transverse line located a distance of 20 ft from the section of the upstream gates.

The velocity profile at Section A (Chart 10) is quite uniform and typical of a flow pattern as it approaches a gate. At Section B the velocity was measured a short distance upstream of the gate, so that the profile shows a relatively high velocity as the flow is accelerated under the gate. At this distance upstream of the gate the velocity near the bed has increased to nearly 20 fps. Just downstream of the gate at Section C a typical profile for flow under a sluice gate has developed. The maximum velocity very close to the bottom is nearly 50 fps. The velocity rapidly decreases with height as the elevation of the gate lip is approached, so that the velocities in the region above the lip of the gate are negligibly small. The velocities shown in the upper regions of Sections C and D are relatively undefined since they are in the wake created by the gate. The profiles of Sections D and E indicate the presence of the jet close to the bed and its gradual increase in thickness as the flow moves downstream. This is shown particularly at Section E. The point F, however, is protected by the nose of the downstream gate piers. This causes an appreciable flow separation, so that at the floor near the pier a small upstream velocity has been generated. At higher elevation the zone of separation is presumably narrower, so that the velocities measured in this region show appreciable downstream velocities.

In Chart 11 the velocity profiles include that at point G near the right boundary. The other profiles are as given in Chart 10. Point G, immediately upstream of the right downstream gate, shows some remnants of the high velocity jet that leaves the upstream gate. As the upstream jet penetrates into the gate chamber, it tends to spread laterally as well as vertically, and the maximum velocity is still further decreased in the downstream direction. This is indicated at point G where the maximum velocity near the floor is approximately 25 fps. At the higher elevations it appears that the flow has separated from the wall, so that in this region velocity is slightly negative and a reverse current is indicated. In Chart 12 a series of velocity profiles taken at points laterally spaced across the gate chamber is shown. These profiles show the nature of the jet which has been formed by the upstream gates as it is

is located at successive stations on a longitudinal section of the bed. The position of the bed is shown in Figure 1. The distance of 20 ft from the location of the upstream gate.

The velocity profiles at Section A (Chart 11) are quite uniform and typical of a flow pattern in an open channel. At Section B the velocity was measured at a short distance upstream of the gate so that the profile shows a relatively high velocity at the top as indicated in the chart. At this distance upstream of the gate the velocity near the bed has increased to nearly 50 ft/sec. and downstream of the gate at Section C a typical profile for flow under a sluice gate has developed. The maximum velocity very close to the bottom is nearly 10 ft/sec. The velocity rapidly increases with height as the elevation of the gate is approached, so that the velocities in the region above the top of the gate are negligibly small. The velocities shown in the upper portion of Section D and E are relatively uniform along the bed and the near surface of the water. The position of Section F and G indicates the position of the jet above the bed and the typical increase in velocity as the flow enters the channel. This is shown in Chart 12. The position of Section H is indicated by the position of the dashed line. This section is approximately 10 ft upstream of the gate and the velocity is measured in this region. The flow is generally uniform, so that the velocity is measured in this region shows appreciable downstream velocities.

In Chart 13 the velocity profiles indicate that at point G near the right boundary, the other profiles are as given in Chart 10. In Chart 14 immediately upstream of the right downstream gate, there are some anomalies in the velocity profiles that appear to be associated with the gate. As the approach jet penetrates into the channel, it tends to spread laterally as well as vertically, and the maximum velocity is still further decreased in the downstream direction. This is indicated at point I where the maximum velocity near the floor is approximately 10 ft/sec. At the right extremity it appears that the flow has reversed itself so that in this region velocity is slightly negative and a reverse current is indicated. In Chart 15 a series of velocity profiles show the lateral spread across the gate channel is shown. These profiles show the nature of the jet which has been formed by the upstream gate as it



dissipated within the gate chamber. The lateral diffusion of the jet is shown by the velocity profiles at point K and point G, where the maximum velocity near the floor of the chamber has been reduced to approximately 25 fps. At points J and E, however, which are immediately downstream of the left and right upstream gates respectively, the maximum velocity is still in the neighborhood of 40 fps. The jet is considerably thicker than the gate opening. Above the gate elevation the downstream velocities are very small and rather poorly defined. In this region the flow patterns are quite complex and involve secondary currents moving in different directions.

Since the Morris Drift is submerged, and since no net flow occurs within it, the flow at points K and J must either be deflected directly into the Santa Anita Tunnel No. 2 past the bifurcation nose or else be deflected upward and across the chamber and then down into the downstream tunnel. As the flow moves past the entrance of Morris Drift at a high velocity the shear developed near the bottom of the water within the Drift by the flow generates a vortex motion of considerable magnitude within the tunnel which extends for some distance from the entrance. The strength of this rotation decreases with distance down the Morris Drift until the point is reached where it is completely dissipated.

In Charts 13 and 14 the results of measurements of velocity are shown for the case when the downstream gates are partially closed. By reducing the opening through these gates the elevation of the water surface in the gate tower has been considerably increased--to elevation 1150 ft. Under these circumstances the head differential across the upstream gates is 20 ft as is that across the downstream gates. (This gate setting is also shown on Chart 5 as the point where the relative gate openings for  $\Delta H_T = 40$  ft,  $\Delta H_1/\Delta H_T = 0.5$ , are 21.3 per cent and 17.5 per cent.) Such a mode of operation appreciably increases the depth of water within the chamber and provides for greater dissipation of the jet energy. The pattern in Chart 13 is similar to that in Chart 10 for the profiles near the upstream gates (points A, B, C, D, and E). Although the pattern of velocity at point F is somewhat similar, the velocities near the bottom in the downstream direction indicate that the zone of separation has been considerably reduced. However, because the gates have been partially closed, there is a region above the lip of the gates between the piers in which negative velocities are generated. In Chart 14 at point G the

intermediate values of the parameter  $\alpha$  (the number of electrons) is shown in Fig. 1. The curves are plotted for  $\beta = 0.1$  and  $\beta = 0.2$ . It is seen from the figure that the curves for  $\beta = 0.1$  are higher than those for  $\beta = 0.2$ . The curves for  $\beta = 0.1$  are also higher than those for  $\beta = 0.2$  in the region  $\alpha > 1$ . The curves for  $\beta = 0.1$  are also higher than those for  $\beta = 0.2$  in the region  $\alpha < 1$ . The curves for  $\beta = 0.1$  are also higher than those for  $\beta = 0.2$  in the region  $\alpha = 1$ .

From the above it follows that the curves for  $\beta = 0.1$  are higher than those for  $\beta = 0.2$  in the region  $\alpha > 1$ . The curves for  $\beta = 0.1$  are also higher than those for  $\beta = 0.2$  in the region  $\alpha < 1$ . The curves for  $\beta = 0.1$  are also higher than those for  $\beta = 0.2$  in the region  $\alpha = 1$ . The curves for  $\beta = 0.1$  are also higher than those for  $\beta = 0.2$  in the region  $\alpha > 1$ . The curves for  $\beta = 0.1$  are also higher than those for  $\beta = 0.2$  in the region  $\alpha < 1$ . The curves for  $\beta = 0.1$  are also higher than those for  $\beta = 0.2$  in the region  $\alpha = 1$ .

From the above it follows that the curves for  $\beta = 0.1$  are higher than those for  $\beta = 0.2$  in the region  $\alpha > 1$ . The curves for  $\beta = 0.1$  are also higher than those for  $\beta = 0.2$  in the region  $\alpha < 1$ . The curves for  $\beta = 0.1$  are also higher than those for  $\beta = 0.2$  in the region  $\alpha = 1$ . The curves for  $\beta = 0.1$  are also higher than those for  $\beta = 0.2$  in the region  $\alpha > 1$ . The curves for  $\beta = 0.1$  are also higher than those for  $\beta = 0.2$  in the region  $\alpha < 1$ . The curves for  $\beta = 0.1$  are also higher than those for  $\beta = 0.2$  in the region  $\alpha = 1$ .

From the above it follows that the curves for  $\beta = 0.1$  are higher than those for  $\beta = 0.2$  in the region  $\alpha > 1$ . The curves for  $\beta = 0.1$  are also higher than those for  $\beta = 0.2$  in the region  $\alpha < 1$ . The curves for  $\beta = 0.1$  are also higher than those for  $\beta = 0.2$  in the region  $\alpha = 1$ . The curves for  $\beta = 0.1$  are also higher than those for  $\beta = 0.2$  in the region  $\alpha > 1$ . The curves for  $\beta = 0.1$  are also higher than those for  $\beta = 0.2$  in the region  $\alpha < 1$ . The curves for  $\beta = 0.1$  are also higher than those for  $\beta = 0.2$  in the region  $\alpha = 1$ .

velocities are now everywhere positive, which also indicates that the zone of separation has been reduced. This may be the consequence of the partial closure of the right downstream gate, since now the water in the neighborhood of point G must accelerate to pass under the gate. This apparently is enough to reduce the size of the separation zone and make the velocities at the gate lip positive.

The results of the velocity measurements show that the flow entering the Morris Reservoir Turnout Structure is rather uniformly divided between the several gates, so that the velocity profiles issuing from these upstream gates are quite similar. Based upon this single profile, the discharge through the right upstream gate was 51 per cent of the total, while that through the left upstream gate was 49 per cent of the total (for these experiments the center gate was closed). The situation was reversed at the downstream gates, in which 49 per cent of the total flow passed through the right downstream gate and 51 per cent of the total flow passed through the left downstream gate. These differences probably are not significant, since variations in velocity and the transverse direction were not taken into account. They do indicate, however, that the flow through the various gates is not drastically asymmetrical. This series of velocity profiles also provides some information on the nature of the jet as it proceeds downstream. Within the chamber itself the high velocities are confined to an area very close to the bottom and have a thickness about equal to the gate opening. As they move through the chamber or down the Santa Anita Tunnel the jets tend to thicken somewhat as the velocity is reduced. The velocity profiles taken at various points within the chamber show that the jets spread transversely and tend to follow the geometrical boundaries of the structure. It appears, however, that there is a tendency toward separation at the right outside boundary as well as at the piers supporting the downstream gates.

The effect of Morris Drift on the flow pattern appears to be primarily one of energy dissipation. The high velocity jet from the upstream left gate flowing past the entrance of Morris Drift creates a vortex motion within the drift that extends some distance into the drift before it is dissipated. The shear generated by the high velocity jet across the bottom of the entrance face is the primary cause of the vortex motion which is then transmitted into the

velocity are not comparable, and the velocity of the gas is  
assumed to be constant. This may be the consequence of the  
absence of the velocity of the gas, since the velocity of the  
of point 3 must be zero in order to have the velocity of the  
to reduce the rate of the expansion, and make the velocity of the  
the velocity.

The results of the velocity of the gas are that the velocity  
is not constant, but that the velocity of the gas is  
assumed to be constant. This may be the consequence of the  
absence of the velocity of the gas, since the velocity of the  
of point 3 must be zero in order to have the velocity of the  
to reduce the rate of the expansion, and make the velocity of the  
the velocity.

The effect of the velocity of the gas is that the velocity  
is not constant, but that the velocity of the gas is  
assumed to be constant. This may be the consequence of the  
absence of the velocity of the gas, since the velocity of the  
of point 3 must be zero in order to have the velocity of the  
to reduce the rate of the expansion, and make the velocity of the  
the velocity.

tunnel by the shear generated in the flow. Because of the change in direction of the jet at this point and the change in momentum of the flow, some of the water from the jet probably also enters the drift and takes part in rotation. Continuity then requires that there be a return flow to the gate chamber, which probably occurs in the central portion of the tunnel. This flow returns to the gate chamber at a higher elevation and joins the mass of fluid moving at much lower velocities.

### C. Distribution of Discharge Through Downstream Gates

In order to study further the flow patterns and the distribution of flow in the downstream gates, an additional experiment was conducted involving the injection of dye into the flow. The dye was injected at five distinct points in the plane of the upstream gates including the right and left side of each of the outside gates and the center of the center gate. The gate openings of the downstream set of gates were divided into seven portions of equal width (2 ft each so that the center gate represented one of the separate areas). When the dye pattern had become stabilized, samples of the flow at each of the seven measuring areas were collected. The concentration of dye in each sample was determined with a standard colorimeter. Knowing that the dye mixed with the flow at each sampling point came from a particular upstream gate, the proportions of the discharge that passed through each of the downstream gates could be easily determined. Previous experiments on velocity profiles indicated that the flow entering the turnout structure was quite uniformly divided between the upstream gates so that 43 per cent of the total flow passed through the right upstream gate, 43 per cent passed through the left upstream gate, and 14 per cent passed through the center upstream gate. The results of the measurements using dye are tabulated in Table II.

TABLE II

Proportion of Flow Through Downstream Control Gates

Flow from Upstream Gates	Flow Through Downstream Gates - Per Cent		
	Right	Center	Left
Right Gate (43 per cent of $Q_T$ )	55.6	9.7	34.6
Center Gate (14 per cent of $Q_T$ )	33.3	8.3	58.4
Left Gate (43 per cent of $Q_T$ )	48.2	9.9	41.6

function of the shear generated in the film. Because of its change in direction of the light beam and the change in position of the focal point of the lens, the light beam is deflected and the focal point is moved. When the light beam is deflected, the focal point is moved. When the light beam is deflected, the focal point is moved. When the light beam is deflected, the focal point is moved.

4. Investigation of the effect of the shear on the focal point of the lens.

In order to study the effect of the shear on the focal point of the lens, the following experiment was carried out. The focal point of the lens was determined in the absence of the shear. Then the shear was introduced and the focal point was determined again. It was found that the focal point was shifted in the direction of the shear. This shift was proportional to the shear. The shift was found to be independent of the distance between the lens and the focal point.

The results of the experiment are shown in Table I. The shift of the focal point was found to be proportional to the shear. The shift was found to be independent of the distance between the lens and the focal point. The shift was found to be independent of the distance between the lens and the focal point. The shift was found to be independent of the distance between the lens and the focal point.

TABLE I

Investigation of the effect of the shear on the focal point of the lens.

Shear (mm)	Focal point shift (mm)	Focal point shift (mm)	Focal point shift (mm)
0.00	0.00	0.00	0.00
0.01	0.01	0.01	0.01
0.02	0.02	0.02	0.02
0.03	0.03	0.03	0.03
0.04	0.04	0.04	0.04
0.05	0.05	0.05	0.05

Using the above information approximate proportions of the total discharge passing through the individual downstream gates are:

- a) The downstream right gate - 49.4 per cent,
- b) The downstream center gate - 9.6 per cent, and
- c) The downstream left gate - 41.0 per cent.

It appears from the table that most of the flow from the right upstream gate goes through the downstream right gate, although 35 per cent of it passes through the downstream left gate. Of the flow through the upstream center gate, 58 per cent passes through the downstream left gate, but 33 per cent goes through the right gate. Of the flow from the upstream left gate, over 48 per cent passes through the downstream right gate. Since the downstream left gate is almost directly downstream of the upstream right gate, it might be expected that a large proportion of the flow from this gate would pass through the downstream left gate. It would not be expected, however, that nearly half of the flow from the upstream left gate would pass through the downstream right gate. In order to do this the flow leaving the upstream left gate must be deflected upward in the chamber, and then after passing over the high velocity flow along the bed, flow downward and into the downstream right gate. Photo 7, in which pieces of yarn are held in the chamber above the jet, illustrates the upward flow at the downstream face of the chamber and the downward flow near the upstream gates. The measurement of velocities in the chamber between the gates also seems to bear out this conclusion. The data thus indicate that nearly 21 per cent of the total flow is deflected upward in the neighborhood of the bifurcation nose and redirected into the right downstream gate.

This flow pattern represents the most severe operating conditions to be expected having the maximum discharge and the highest head differentials. For smaller discharges and smaller head differentials the pattern would tend to be similar, but the lower velocities and greater depth in the chamber might be such that some of the flow pattern aspects would be unrecognizable. Even for extreme conditions the flow pattern as generated with this structural configuration does not appear to be particularly detrimental to the functioning of the turnout structure. The flow pattern would undoubtedly be somewhat improved if the upstream and downstream gates were aligned so that the flow

being the also a function of position of the left electrode  
through the distance between them.

- (a) the distance  $d = 10^{-2}$  cm,
- (b) the distance  $d = 2 \cdot 10^{-2}$  cm,
- (c) the distance  $d = 3 \cdot 10^{-2}$  cm.

It is seen from the table that at  $d = 10^{-2}$  cm the right electrode  
is more active than the left one, although it is not so in the  
case of the distance  $d = 2 \cdot 10^{-2}$  cm. Of the three electrodes the  
right one is the most active, but its activity is not so high as  
that of the left one. At the flow  $v = 10^{-2}$  cm/sec the right  
electrode is more active than the left one. At the flow  $v = 2 \cdot 10^{-2}$   
cm/sec the right electrode is more active than the left one. At  
the flow  $v = 3 \cdot 10^{-2}$  cm/sec the right electrode is more active  
than the left one. It would not be expected, however, that  
the activity of the left electrode would be higher than that of  
the right one. In order to do this the flow towards the right  
electrode must be directed so as to be higher, and then some  
other effect must be taken into account. The flow towards the  
right electrode is higher than towards the left one, and the  
activity of the right electrode is higher than that of the left  
one. The reason for this is that the flow towards the right  
electrode is higher than towards the left one, and the activity  
of the right electrode is higher than that of the left one.  
The reason for this is that the flow towards the right  
electrode is higher than towards the left one, and the activity  
of the right electrode is higher than that of the left one.

The flow pattern resembles the case of a  
cylinder with the surface through the right-hand electrode  
for both electrodes and smaller than that of the left-hand  
electrode. The flow velocity and pressure drop in the channel  
is higher than that of the left-hand electrode. The flow  
velocity and pressure drop in the channel is higher than that  
of the left-hand electrode. The flow velocity and pressure  
drop in the channel is higher than that of the left-hand  
electrode. The flow velocity and pressure drop in the channel  
is higher than that of the left-hand electrode.



would not have to be deflected by the bifurcation nose. The rotational effects within the Morris Drift would probably be somewhat reduced, since there would be less likelihood of flow impingement within the drift entrance. Given the basic geometry of the turnout structure and the alignment of the tunnel and the drift, the flow pattern is such that for normal operations this alignment should have only a minor influence.

#### D. The Nature of Deposition in the Morris Drift

Since the Morris Drift is submerged and enters the turnout structure at the same level as the Santa Anita Tunnel No. 2, the high velocity jet from the left upstream gate generates a well-defined vortex motion in the entrance region of Morris Drift. It seemed possible that this might cause the deposition of any suspended sediment that might be carried by the flow. The nature of the vortex motion can be seen in Photos 8, 9, and 10, which show the motion of suspended confetti in Morris Drift caused by different discharges. By exposing the film for an appreciable time interval (in this case  $1/25$  sec) the confetti registers as a streak whose length is proportional to the velocity of the particle and whose direction shows the local direction of the flow. In these photographs the movement is counterclockwise looking down the drift away from the gate chamber. By comparison of the photos it is apparent that the rotational velocity decreases with distance from the entrance and is proportionately reduced as the total discharge through the turnout structure is reduced.

Some deposition of confetti particles was observed to take place, so a specific experiment was undertaken in an attempt to determine quantitatively the amount of deposition likely to occur within the Morris Drift. Confetti particles were used in the test to represent suspended sediment. The confetti was boiled in water in order to soak it completely and thereby make it somewhat heavier than the water. The fall velocity of typical particles so treated was found to be 0.051 fps (model) which corresponds to a prototype fall velocity of about 0.35 fps. This fall velocity, in turn, corresponds to the diameter of a particle of sand of approximately 0.75 mm. This size of sediment is probably considerably larger than any that would be found in suspension within the feeder system.

... (mirrored text) ...

The nature of deposition in the ...

... (mirrored text) ...

... (mirrored text) ...

The test procedure involved two phases. First a sample of known size was introduced into the tunnel far upstream of the turnout structure. The particles passed through the structure and either continued down the Santa Anita Tunnel No. 2 or settled within the Morris Drift. The settled particles were then counted and their location in the tunnel was noted. Five separate tests were made so that average conditions could be obtained. The discharge was 1550 cfs, headwater elevation 1180 ft, tailwater elevation 1130 ft, and the water surface elevation in the chamber 1150 ft. There was no net flow through the Morris Drift, so all of the incoming water passed out through the downstream gates. After the tests, when any particles on the Morris Drift had settled, the discharge through the Morris Drift was slowly increased until those particles which had been deposited were put into motion and carried out of the tunnel. The water surface elevations for this phase were approximately the same as for the first phase. These tests can be summarized as follows. The average of five tests of 1,000 particles each placed in the tunnel upstream of the structure resulted in the following data (Table III):

TABLE III

Deposition of Suspended Particles in Morris Drift

Dist. (prot.) from entrance of Morris Drift - ft	No. of Particles deposited (ave.)
192 - 211	1.2
211 - 230	0.8
230 - 249	1.4
249 - 268	0.8
268 - 287	0.4
	<hr/> 4.6

The total number of particles which eventually settled in Morris Drift constituted only 0.46 per cent of the suspended load in the feeder system.

In the second series it was found that on the average a discharge of 215 cfs was sufficient to carry the settled particles out of the Morris Drift. By experiment with sands the discharge in a conduit necessary to keep suspended

The first part of the report is devoted to a description of the work done during the year. It is divided into two main parts, the first of which deals with the general work done during the year, and the second with the work done during the year in connection with the various projects mentioned in the first part. The first part is divided into three sections, the first of which deals with the work done during the year in connection with the various projects mentioned in the first part, the second with the work done during the year in connection with the various projects mentioned in the first part, and the third with the work done during the year in connection with the various projects mentioned in the first part. The second part is divided into three sections, the first of which deals with the work done during the year in connection with the various projects mentioned in the first part, the second with the work done during the year in connection with the various projects mentioned in the first part, and the third with the work done during the year in connection with the various projects mentioned in the first part.

Summary of the work done during the year

Project	Work done during the year	Percentage of total work
Project A	1000 hours	25%
Project B	1500 hours	37.5%
Project C	1000 hours	25%
Project D	500 hours	12.5%
Project E	500 hours	12.5%
Total	4000 hours	100%

The work done during the year has been divided into five main projects, A, B, C, D, and E. Project A has been the most important project, and has received the most attention. Project B has also been an important project, and has received a great deal of attention. Project C has been a smaller project, and has received less attention. Project D and E have been the smallest projects, and have received the least attention.

particles from being deposited can be expressed as<sup>(1)</sup>

$$Q = 2.5 D^2 d_s^{1/2} \left( g \frac{\rho_s - \rho}{\rho} \right)^{1/2}$$

where  $Q$  is the discharge,  $D$  is the tunnel diameter (17.5 ft),  $d$  is the size of sediment (0.0025 ft),  $g$  is acceleration due to gravity (32.2 ft per sec<sup>2</sup>), and  $\frac{\rho_s - \rho}{\rho}$  is the relative density of the suspended particles (1.65).

Using this equation it is estimated that a discharge of 300 cfs would be needed to keep the particles from settling in the tunnel. This value compares favorably with the 215 cfs found experimentally, when the unusual flow pattern and the fact that the test particles are not spherical are considered. The test results show that a very small amount of the available sediment actually settles in Morris Drift. Two reasons for this fact are suggested. First, since there is no flow through Morris Drift, the sediment must be brought into the tunnel by the vortex motion created by the jets. Such being the case, only a relatively small amount of sediment gets into the tunnel. Second, the sediment which enters the tunnel is held in suspension by the vortex flow pattern generated at the entrance. The longer the particles are in suspension the greater is the possibility that they will be carried back through the tunnel entrance.

#### E. Pressure Fluctuations in Gate Structure

The oscillation of the gates when they are partly open is of concern from the point of view of their design and structural strength. These oscillations cannot be measured directly in this model. This would require a model in which the gates and their operating appurtenances were fabricated very precisely as to both similarity in geometry and distribution of mass as in the prototype. This is necessary if the gates are to react to fluctuating forces in the same way as the prototype structure will react. The oscillation of a vibrating system is a function of dynamic characteristics of the system, as defined by its natural frequency, and the fluctuating forces which tend to cause this

---

(1) Craven, J. P., "The Transportation of Sand in Pipes: Full-Pipe Flow," Proceedings, Fifth Hydraulics Conference, State University of Iowa, Iowa City, June 1952.

(1) The following is a list of the names of the persons who have been appointed as members of the Board of Directors of the Corporation:

$$\frac{1}{2} \times \frac{1}{2} = \frac{1}{4}$$

The Board of Directors of the Corporation is composed of five members, one of whom shall be the President of the Corporation. The Board of Directors shall have the authority to elect and remove the President and the other officers of the Corporation, and to determine the compensation of such officers. The Board of Directors shall also have the authority to declare dividends and to issue and sell the stock of the Corporation. The Board of Directors shall meet at such times and places as it may determine, and shall hold a regular meeting at least once a year. The Board of Directors shall also have the authority to delegate its powers to any committee or subcommittee that it may create. The Board of Directors shall be the governing body of the Corporation, and shall have the final authority in all matters relating to the business of the Corporation.

The Board of Directors shall also have the authority to:

- 1. To determine the compensation of the President and the other officers of the Corporation.
- 2. To declare dividends and to issue and sell the stock of the Corporation.
- 3. To delegate its powers to any committee or subcommittee that it may create.
- 4. To determine the policy and strategy of the Corporation.
- 5. To determine the capital structure of the Corporation.
- 6. To determine the financial statements of the Corporation.
- 7. To determine the annual budget of the Corporation.
- 8. To determine the long-range plan of the Corporation.
- 9. To determine the relationship of the Corporation to its competitors.
- 10. To determine the relationship of the Corporation to its customers.

Witness my hand and seal this 10th day of January, 1954.

vibration. The oscillations reach a maximum when the forces causing vibration are of the same frequency as the natural frequency of the structure. This relationship between the predominant forcing frequency and the natural frequency can be determined experimentally with a properly designed model. If such a model is not available, however, valuable information can be obtained by comparing the measured frequencies and magnitudes of the fluctuating forces with the natural frequency as computed from the gate geometry and mass. This is the procedure that was followed in these experiments. The natural frequency of these gates has been computed and frequency spectra have been obtained for various flow conditions. An examination of the spectrum of the fluctuating forces in relation to the natural frequency will permit an estimate to be made of the expected oscillations.

In addition to these experiments recourse may be had to other model studies of the oscillations of similar gates installed in control structures. Such information was provided and discussed in Part I - Regular Gate Structure - of the final report of these studies. These results showed that there was a reasonably well defined relationship between the magnitude of the oscillations and the natural frequency or stiffness of the structure. A reasonable agreement between model and prototype data to the extent that such data were available was also obtained.

#### 1. Apparatus for Measuring Pressure Fluctuations

The fluctuating pressures acting on the gates were measured by means of a pressure transducer mounted on the gates. The pressure transducer of the type used in these experiments, shown in Photo 11, is flush mounted on the upstream face of a gate. Photo 12 shows the instrumented gate installed in the model. Because of the size of the transducer compared to the thickness of the gate an auxiliary block was attached to the back of the gate in order to contain the transducer and its connections in a water tight chamber. The transducers and the gates are shown diagrammatically in Chart 15. The fluctuations as sensed by the transducers were recorded on a moving chart (Photo 13) and at the same time on magnetic tape. The recorder chart gives the visual record of the varying pressure, of which examples are given on the charts. The record from the tape recorder is used for the harmonic analysis and provides the





pressure spectrum<sup>(1)</sup> also plotted on the charts. The pressure spectrum is a plot of the root mean square of the pressure fluctuations occurring within narrow bands of frequencies so that the rms of pressure amplitude is given as a function of its frequency. These data have been plotted in Charts 15 through 20.

## 2. Pressure Fluctuations on Control Gates

Most of the measurements in these tests have been taken on the downstream gate. Only one test was made on the upstream gate for purposes of comparison. In Chart 15 pressure spectra obtained for the upstream gates when the discharge was 1550 cfs are plotted. The upstream gates were closed and the entire discharge passed over the emergency weirs. It was expected that the fluctuations would be a maximum under these circumstances. In general, the magnitude of the rms value was less than approximately 0.2 ft of water in the prototype, with the exception of the series of peaks in the neighborhood of 4 to 7 cycles per second. The reason for the peaks is not clear, but it will be observed that larger pressure fluctuations seem to occur at these frequencies in all the experiments. It may be due to a periodic fluctuation inherent in the model system and not a characteristic of the flow pattern within the structure. The computed natural frequency for this particular gate is also plotted on the chart. The natural frequency, in the neighborhood of 16 cycles per second, is considerably above any of the frequencies measured in the model, and the chart shows that the amplitude of the pressure fluctuations is very small in the neighborhood of the natural frequency. Chart 16 shows the pressure spectrum taken on the downstream right gate for essentially the same flow conditions as described in Chart 15. The entire discharge was passed over the upstream emergency weirs, but the pressure pulses as recorded were still quite small except for the peak which occurred at 4 cps. Although the water level in the chamber between the gates was at a minimum value, the depth of water into which the jets plunged was still over 70 ft (prototype) and undoubtedly much of the energy of the jet was absorbed. Here again, the natural frequency of the gate

---

(1) David J. Anderson, "Measurement of the Power Spectrum Density on the Face of a Vertical Lift Gate." Internal Memorandum No. IM-92. St. Anthony Falls Hydraulic Laboratory, September 1967.

... of the ... ( ) ...

... ..

... ..

(1) ... ..

is considerably greater than the frequency of the maximum pressure pulse, and those pressures in the neighborhood of the natural frequency are quite small. Chart 17 shows the pressure spectrum on the downstream right gate for the maximum discharge. The upstream and the downstream gates were opened sufficiently to pass the flow without the use of the emergency weirs. The headwater was at elevation 1180 ft, the intermediate reservoir at elevation 1150 ft, and the tailwater elevation at 1130 ft. The maximum rms pressure for this case was approximately one foot of water (prototype), suggesting that the peak pressure pulse was on the order of 3 ft of water. This occurred at a frequency of 0.1 cps (prototype). As the frequencies increased the magnitude of the pressure fluctuations decreased, reaching essentially zero at about 6 cps. As in the previous tests, a secondary peak of considerable magnitude occurred at 3 cps. The chart also shows that the measured frequencies are again considerably below the computed natural frequency for the gate. Chart 18 shows the pressure pulsations as measured for a low discharge of 420 cfs. The water surface elevations were maintained as in Chart 17, but the gates were nearly closed to control the discharge. For this low discharge the pressure fluctuations were very small and in general were less than 0.2 ft of water. The frequencies were also well below the natural frequency for the gate. For this discharge the secondary peak, although apparent on the chart, was considerably depressed. This lends credence to the idea that this vibration frequency is inherent in the system and is independent of the discharge. In Chart 19 the measurements were made for a discharge of 200 cfs passing through the center gate only. As would be expected, the magnitude of the pressure fluctuations is considerably reduced and their frequencies are well below the natural frequency of the gate. The secondary peak occurring at 5 cps is again apparent of the trace. In Chart 20 the discharge has been increased again to 1550 cfs, but all the flow is restricted to the left gate at both the upstream and the downstream sections with the right and center gates closed. In this case there are higher pressure fluctuations at very low frequencies, after which they decrease rapidly to zero at about 8 cps. Again the secondary peak between 4 and 5 cps is apparent, yet considerably depressed.

Also included in each of the Charts 15 through 20 are short sections of the actual records showing typical pressure fluctuations of the type that were

to measure the growth of the embryo during the period of the first cleavage and to determine the position of the embryo in the egg.

It is also possible to measure the rate of cleavage of the embryo in the egg. The apparatus and the method used for this purpose are described in the paper by the author.

The apparatus used for the measurement of the rate of cleavage is shown in the figure. It consists of a glass tube with a diameter of 1 mm and a length of 10 cm.

The tube is filled with water and the embryo is placed in it. The rate of cleavage is measured by the displacement of the water level in the tube.

The results of the measurements are shown in the figure. It is seen that the rate of cleavage is very rapid in the first few hours and then gradually decreases.

The apparatus used for the measurement of the rate of cleavage is shown in the figure. It consists of a glass tube with a diameter of 1 mm and a length of 10 cm.

The tube is filled with water and the embryo is placed in it. The rate of cleavage is measured by the displacement of the water level in the tube.

The results of the measurements are shown in the figure. It is seen that the rate of cleavage is very rapid in the first few hours and then gradually decreases.

The apparatus used for the measurement of the rate of cleavage is shown in the figure. It consists of a glass tube with a diameter of 1 mm and a length of 10 cm.

The tube is filled with water and the embryo is placed in it. The rate of cleavage is measured by the displacement of the water level in the tube.

The results of the measurements are shown in the figure. It is seen that the rate of cleavage is very rapid in the first few hours and then gradually decreases.

The apparatus used for the measurement of the rate of cleavage is shown in the figure. It consists of a glass tube with a diameter of 1 mm and a length of 10 cm.

The tube is filled with water and the embryo is placed in it. The rate of cleavage is measured by the displacement of the water level in the tube.

The results of the measurements are shown in the figure. It is seen that the rate of cleavage is very rapid in the first few hours and then gradually decreases.

The apparatus used for the measurement of the rate of cleavage is shown in the figure. It consists of a glass tube with a diameter of 1 mm and a length of 10 cm.

The tube is filled with water and the embryo is placed in it. The rate of cleavage is measured by the displacement of the water level in the tube.

The results of the measurements are shown in the figure. It is seen that the rate of cleavage is very rapid in the first few hours and then gradually decreases.

analyzed to provide the pressure spectra as shown in the charts. From these segments one can compare the pressure fluctuations for different flow conditions and observe the change in character as the discharge decreases or, as in the case of Chart 20, when the gate on which the measurements are made is in a relatively protected region.

### 3. Pressure Fluctuations for Various Flow Conditions

In addition to the frequency spectra of the pressure fluctuations on the gates other measurements of pressure fluctuations were made in the Morris Reservoir Turnout Structure in order to compare directly the effects of discharge, water surface elevation in the gate chamber, and transducer location on the pressure patterns. The results of these experiments are shown in Charts 21 through 24. In Chart 21 the results of pressure measurements for several discharges with the transducer mounted in the downstream right gate are presented. For these experiments the headwater elevation was maintained at 1180 ft. The water surface in the chamber between the gates was held at 1150 ft and the tailwater at elevation 1130 ft. The upper chart shows the pressure fluctuations generated by a discharge of 1550 cfs. The middle chart is the result of a discharge of only 420 cfs, while the bottom chart shows the record for 200 cfs through the center gate only. It is quite apparent, as might be expected, that the magnitude of the pressure fluctuations is drastically decreased as the discharge is reduced. In addition, the charts show that the maximum fluctuation for the maximum discharge is approximately  $\pm 2$  ft of water. Chart 22 provides a comparison of the effect of reservoir elevation on the pressure fluctuations on the downstream right gate. In the upper chart the water surface elevation in the gate chamber was at 1150 ft, which corresponds approximately to the minimum elevation of Morris Reservoir, while the bottom chart shows the results of measurements with the water surface in the gate shaft chamber at elevation 1170 ft, which is approximately the maximum elevation of the Morris Reservoir. It is quite clear that the depth of water in the gate chamber influences the magnitude of the pressure fluctuation and that when the water surface elevation is increased the magnitude of the pressure fluctuations is appreciably reduced. Here again it appears that the maximum variation is on the order of  $\pm 2$  ft of water.



#### 4. Pressure Fluctuations with Blind Flange on Morris Drift

In these experiments the tunnel to the Morris Reservoir (Morris Drift) from the turnout structure was closed by means of a blind flange (Photo 14) in order to observe the pressure fluctuations on the flange and on the gate. Chart 23 is a comparison of the pressure fluctuations on the gate and the blind flange for two different water surface elevations in the gate chamber and for a maximum discharge of 1550 cfs through the structure. It appears that the pressure fluctuations on the blind flange are somewhat larger than corresponding pressure fluctuations on the gates. In addition, these pressure fluctuations are greater for the low water surface elevation than for the higher water surface elevation. The maximum pressure fluctuation occurred on the blind flange when the water surface in the gate chamber was at elevation 1150 ft. The minimum pressure was approximately 4 ft below the average and the maximum pressure was approximately 3 ft above the average in prototype dimensions. As the reservoir elevation was increased, these pressures were correspondingly reduced. In Chart 24 are shown the measurements of pressure fluctuations made on the blind flange for a wide range of reservoir elevations. Even here, however, the maximum pressure fluctuation for any flow condition is approximately  $\pm 4$  ft of water (prototype). It is interesting to note that the frequency of the pressure fluctuations appears to increase when the flow is over the emergency weirs and the water surface is at its minimum elevation. This chart clearly shows that the magnitude of the fluctuations increases more or less regularly as the water surface elevation decreases. This would be expected since the reservoir serves as a cushion to absorb some of the forces creating the fluctuations.

### III. CONCLUSIONS

The experimental study of the Morris Reservoir Turnout Structure was concerned with its operating characteristics for both normal and non-normal conditions. The results of this study led to the following conclusions:

- (1) When operating within the control regions the two gate sets can be adjusted so that various percentages of the total head differential can be obtained at any one gate set.

Experimental Results on the Effect of Temperature on the Rate of Diffusion

The rate of diffusion of a gas through a porous medium is known to be dependent on the temperature of the gas. In this experiment, the rate of diffusion of a gas through a porous medium was measured at two different temperatures. The results are shown in the table below.

Temperature (°C)	Rate of Diffusion (cm <sup>3</sup> /min)
20	1.5
30	2.5

The results show that the rate of diffusion increases as the temperature increases. This is because the kinetic energy of the gas molecules increases with temperature, allowing them to move more rapidly through the porous medium.

CONCLUSION

The experimental study of the rate of diffusion of a gas through a porous medium has shown that the rate of diffusion increases as the temperature increases. This is due to the increase in the kinetic energy of the gas molecules, which allows them to move more rapidly through the porous medium.

The results of this study are in agreement with the theoretical predictions. The rate of diffusion is known to be dependent on the temperature of the gas, and the experimental results show that this dependence is indeed present.



- (2) The calibration curves for a particular discharge are independent of the tailwater elevation.
- (3) The velocity measurements show that the flow entering the structure is rather uniformly divided between the several gates, so that the velocity profiles issuing from these upstream gates are very similar.
- (4) With the center gate closed velocity measurements from the center-line of the gate suggest that 51 per cent of the total flow passed through the right upstream gate while 49 per cent of the total passed through the left upstream gate.
- (5) Based upon velocity measurements only the distribution of flow in the downstream gates is quite symmetrical.
- (6) The effect of Morris Drift on the flow pattern appears to be primarily one of energy dissipation through the vortex motion generated by the high velocity jet from the upstream left gate.
- (7) The dye experiments indicate that 49 per cent of the total flow passes through the downstream right gate, 9.6 per cent passes through the center gate, and 41 per cent passes through the downstream left gate.
- (8) Of the flow passing through the upstream left gate 48 per cent goes through the downstream right gate. It is presumed that this portion of the flow from the upstream left gate, upon reaching the nose of the bifurcation, is deflected upward and flows across the chamber in the upper regions and then down into the downstream right gate.
- (9) On the average less than one-half of one per cent of suspended particles 0.75 mm or less are deposited in Morris Drift.
- (10) A discharge of 215 cfs through the Morris Drift appears to be sufficient to transport any deposited particles.
- (11) The pressure fluctuations on the gates generated by the flow were well below the natural frequency of the gate, and consequently would have little influence in forcing the gates to oscillate.

- (2) The velocity of the particles is constant throughout the motion. The velocity is constant.
- (3) The velocity of the particles is constant throughout the motion. The velocity is constant.
- (4) The velocity of the particles is constant throughout the motion. The velocity is constant.
- (5) The velocity of the particles is constant throughout the motion. The velocity is constant.
- (6) The velocity of the particles is constant throughout the motion. The velocity is constant.
- (7) The velocity of the particles is constant throughout the motion. The velocity is constant.
- (8) The velocity of the particles is constant throughout the motion. The velocity is constant.
- (9) The velocity of the particles is constant throughout the motion. The velocity is constant.
- (10) The velocity of the particles is constant throughout the motion. The velocity is constant.
- (11) The velocity of the particles is constant throughout the motion. The velocity is constant.

## LIST OF PHOTOS

- PHOTO 1 (Serial No. 168B-136) View of the Morris Reservoir Turnout Structure Model from upstream showing the tunnel entering or leaving the structure. The tunnel to Morris Reservoir leaves the structure at the left. The manometer board connected to various points in the tunnels is used to measure tunnel pressures and water level in the structure.
- PHOTO 2 (Serial No. 168B-137) This view of the Morris Reservoir Turnout Structure from above shows the relative positions of the three tunnels meeting in the structure and the locations of the two gate sets. The upstream gate set is fitted to a dividing wall which provides an upstream reservoir within the structure independent of the elevation of the Morris Reservoir. The second, or downstream, set of gates is fitted at a point where the Santa Anita Tunnel No. 2 leaves the turnout structure.
- PHOTO 3 (Serial No. 168B-143) This photograph is a close-up of the turnout structure at the gate elevation. Dye injected into the flow upstream of the upstream gate section delineates the flow pattern and shows the high velocity jet through the gate section. This jet appears to approach the downstream gate section without modification.
- PHOTO 4 (Serial No. 168B-144) In this photograph the dye is injected into the flow upstream of the downstream gate section and shows the flow pattern as it enters the downstream tunnel.
- PHOTO 5 (Serial No. 168B-150) In order to delineate the jet boundary and the incoming streamline pattern, a streamer of dye was injected into the upstream tunnel and photographed as the front passed under the upstream gate and before it could become diffused in the overlying water. It shows a rather sharp demarcation at the upper interface of the jet and defines its upper limit. The bottom of the gate can just be made out in the photograph.
- PHOTO 6 (Serial No. 168B-155) This photo was taken slightly later in the stage of jet development than Photo 5. Some of the streamlines can be seen in the upstream reservoir and the upper limit of the jet is still clearly defined, although the high shear in this region is causing a greater degree of diffusion.
- PHOTO 7 (Serial No. 168B-169) In order to delineate the currents within the gate chamber yarns were attached to wands and located at various points to indicate the flow direction of the circulating currents within the tower. It can be seen that the flow is in the upper direction at the downstream wall of the gate chamber, while it is downward at the other locations. For this experiment the discharge was 1550 cfs, the headwater elevation 1180 ft, the water surface elevation in the chamber 1150 ft, and the tailwater elevation 1130 ft.



- PHOTO 8 (Serial No. 168B-156) This photograph shows confetti in the Morris Drift for a discharge of 1550 cfs. The motion of the particles is shown by the directions and lengths of the confetti streaks. In this instance the direction of flow on the front side of the drift is downward so that the rotation is counterclockwise facing the drift. The decrease in velocity and concentration with increasing distances down the drift is apparent.
- PHOTO 9 (Serial No. 168B-157) In this photograph the discharge has been reduced to 1000 cfs. This view shows that, in general, the lengths of the streaks are shorter, suggesting that the rotational velocities are less. This may be due to the decreased thickness of the jet for this discharge flowing past the entrance, since its velocity would be nearly the same as for the higher discharge.
- PHOTO 10 (Serial No. 168B-158) In this photograph the discharge has been reduced to 420 cfs with the same water surface elevation as in Photos 8 and 9. For this low discharge the gates have been nearly closed; the jet issuing from the upstream gates is very thin, and it appears that the rotational velocities have been very considerably reduced. There is no net flow through the Morris Drift Tunnel.
- PHOTO 11 (Serial No. 168B-165) The pressure transducers used in these experiments were of the flexible diaphragm type which could be mounted flush with the surface of the gate. The deflection of the diaphragm was a measure of the local pressure over the area of the transducer. The benefit of a flush mounting in order to eliminate chamber effects is counteracted to a certain extent by the relative size of the transducer when used in the model.
- PHOTO 12 (Serial No. 168B-166) The pressure transducer was mounted in the gate within a chamber on the gate so that only the diaphragm was exposed to the flow. The instrument itself was in the water-tight chamber, from which the leads were carried to the several recorders.
- PHOTO 13 (Serial No. 168B-163) The electrical impulses from the pressure transducers were carried to a moving chart recorder and a magnetic tape recorder. The chart provided an instantaneous visual record of the pressure fluctuations, while the record of the magnetic tape recorder was used for the harmonic analysis.
- PHOTO 14 (Serial No. 168B-161) In these experiments the Morris Drift was removed and the tunnel closed with a blind flange. The photo shows the blind flange in place with the pressure transducer flush mounted on the flange in order to measure pressure fluctuations.

(Section 101) The first step in the process of the...  
with the... of the... and...  
the... of the... and...  
the... of the... and...  
the... of the... and...

(Section 102) The second step in the process of the...  
with the... of the... and...  
the... of the... and...  
the... of the... and...  
the... of the... and...

(Section 103) The third step in the process of the...  
with the... of the... and...  
the... of the... and...  
the... of the... and...  
the... of the... and...

(Section 104) The fourth step in the process of the...  
with the... of the... and...  
the... of the... and...  
the... of the... and...  
the... of the... and...

(Section 105) The fifth step in the process of the...  
with the... of the... and...  
the... of the... and...  
the... of the... and...  
the... of the... and...

(Section 106) The sixth step in the process of the...  
with the... of the... and...  
the... of the... and...  
the... of the... and...  
the... of the... and...

(Section 107) The seventh step in the process of the...  
with the... of the... and...  
the... of the... and...  
the... of the... and...  
the... of the... and...

Handwritten text, possibly a list or notes, located in the upper middle section of the page. The text is very faint and difficult to read.

Handwritten text block in the lower left quadrant, appearing as a list or series of notes.

Handwritten text block in the lower right quadrant, appearing as a list or series of notes.

PHOTO 1 (Serial No. 168B-136) View of the Morris Reservoir Turnout Structure Model from upstream showing the tunnel entering or leaving the structure. The tunnel to Morris Reservoir leaves the structure at the left. The manometer board connected to various points in the tunnels is used to measure tunnel pressure and water level in the structure.

PHOTO 2 (Serial No. 168B-137) This view of the Morris Reservoir Turnout Structure from above shows the relative positions of the three tunnels meeting in the structure and the locations of the two gate sets. The upstream gate set is fitted to a dividing wall which provides an upstream reservoir within the structure independent of the elevation of the Morris Reservoir. The second, or downstream, set of gates is fitted at a point where the Santa Anita Tunnel No. 2 leaves the turnout structure.



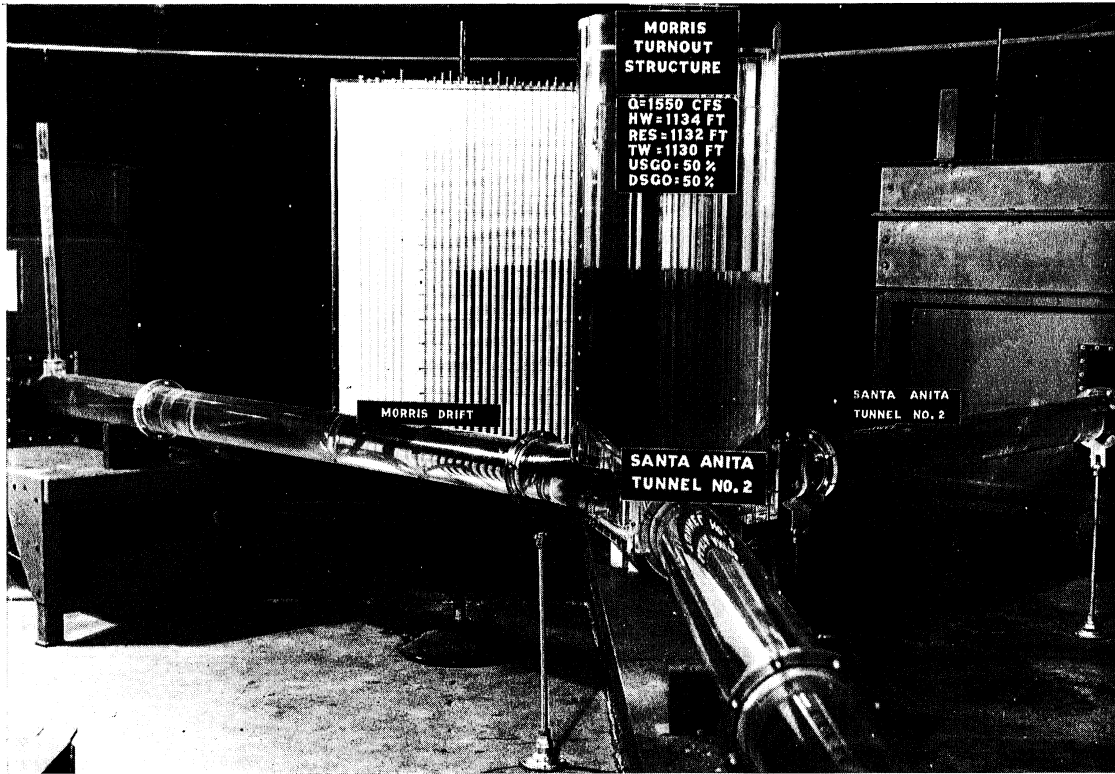


Photo 1

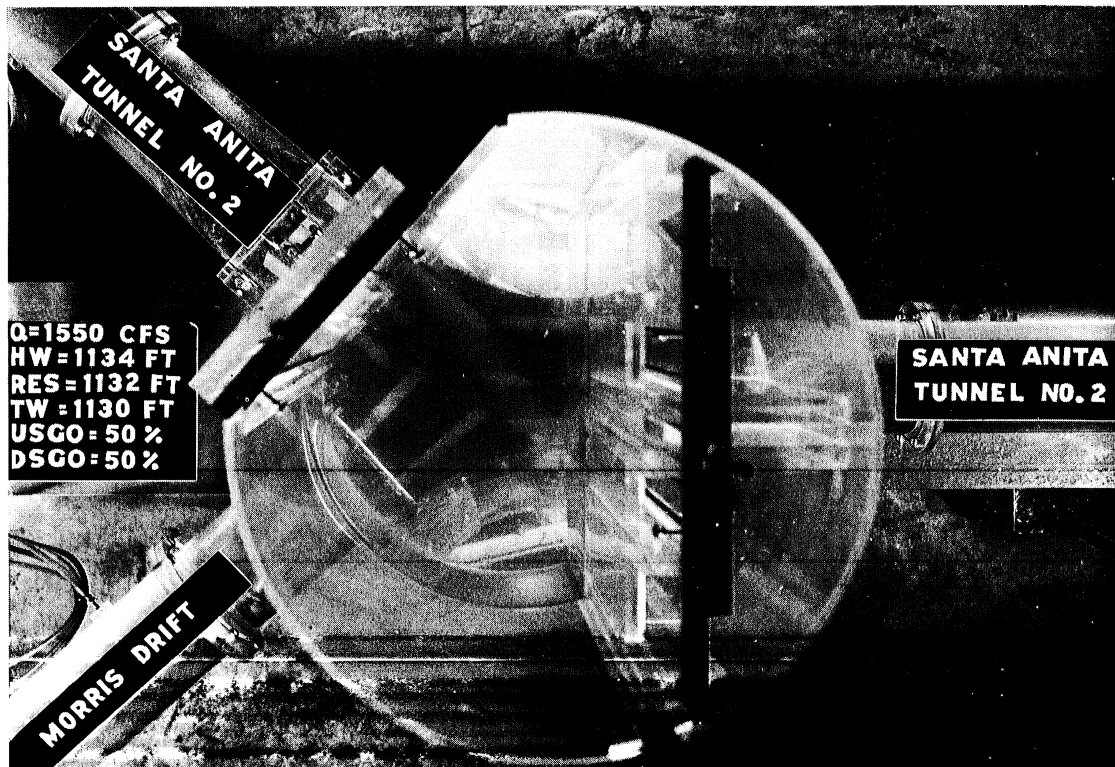


Photo 2



1. The first part of the document discusses the importance of maintaining accurate records of all transactions and activities. It emphasizes that this is crucial for ensuring transparency and accountability in the organization's operations.

2. The second part of the document outlines the various methods and tools used to collect and analyze data. It highlights the need for consistent and reliable data collection processes to support informed decision-making.

3. The third part of the document focuses on the role of technology in data management and analysis. It discusses how modern software solutions can streamline data collection, storage, and reporting, thereby improving efficiency and accuracy.

4. The fourth part of the document addresses the challenges associated with data management, such as data quality, security, and privacy. It provides strategies to mitigate these risks and ensure that data is used responsibly and ethically.

5. The fifth part of the document concludes by summarizing the key findings and recommendations. It stresses the importance of ongoing monitoring and evaluation to ensure that data management practices remain effective and aligned with the organization's goals.

6. The final part of the document provides a list of references and resources for further reading. It includes links to relevant articles, books, and industry reports that offer additional insights into data management best practices.

PHOTO 3 (Serial No. 168B-143) This photograph is a close-up of the turnout structure at the gate elevation. Dye injected into the flow upstream of the upstream gate section delineates the flow pattern and shows the high velocity jet through the gate section. This jet appears to approach the downstream gate section without modification.

PHOTO 4 (Serial No. 168B-144) In this photograph the dye is injected into the flow upstream of the downstream gate section and shows the flow pattern as it enters the downstream tunnel.

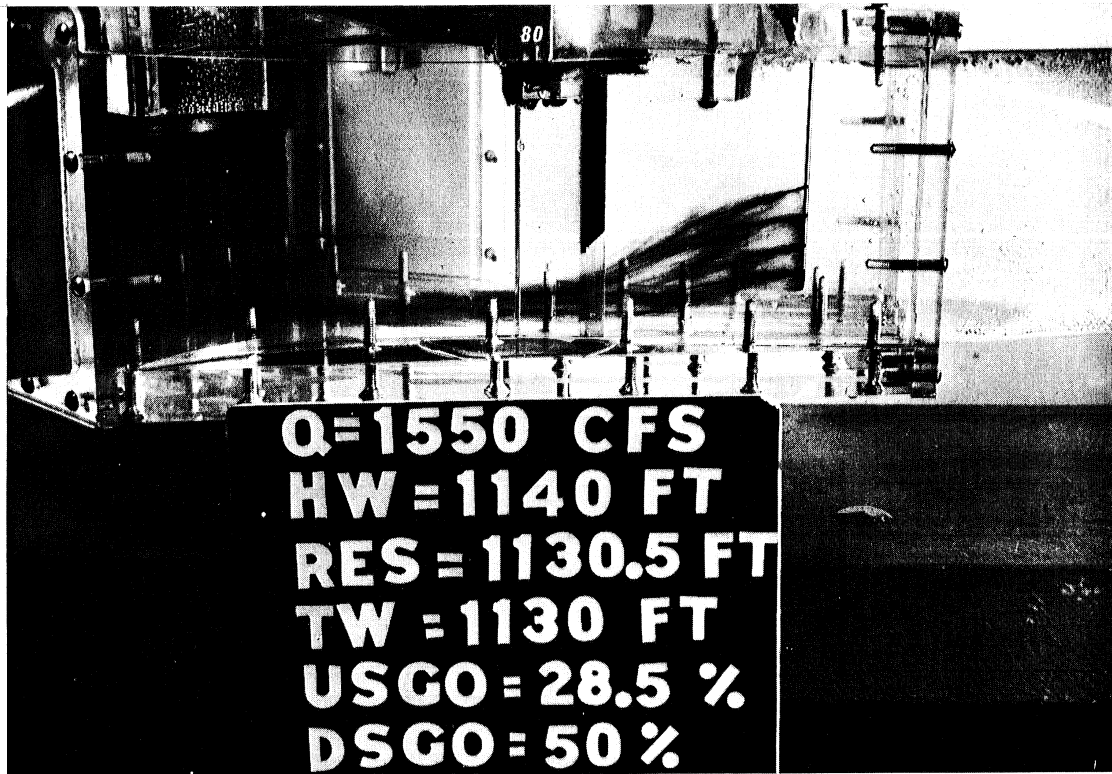


Photo 3

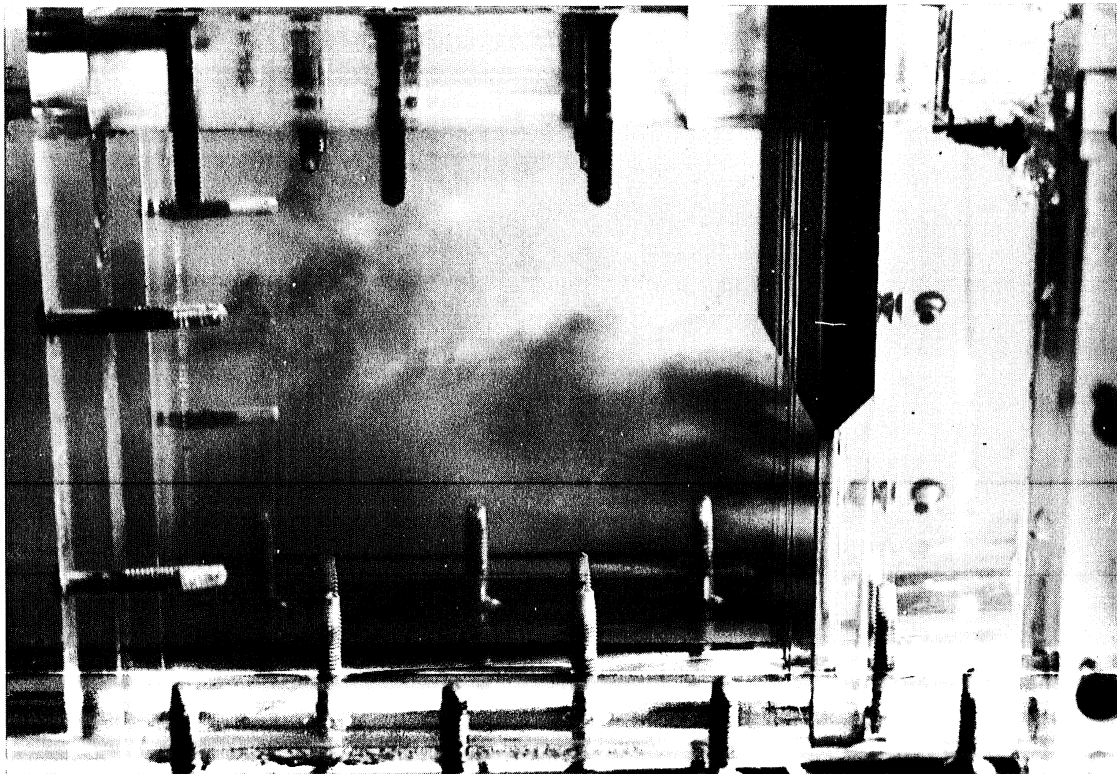


Photo 4





PHOTO 5 (Serial No. 168B-150) In order to delineate the jet boundary and the incoming streamline pattern, a streamer of dye was injected into the upstream tunnel and photographed as the front passed under the upstream gate and before it could become diffused in the overlying water. It shows a rather sharp demarcation at the upper interface of the jet and defines its upper limit. The bottom of the gate can just be made out in the photograph.

PHOTO 6 (Serial No. 168B-155) This photo was taken slightly later in the stage of jet development than Photo 5. Some of the streamlines can be seen in the upstream reservoir and the upper limit of the jet is still clearly defined, although the high shear in this region is causing a greater degree of diffusion.



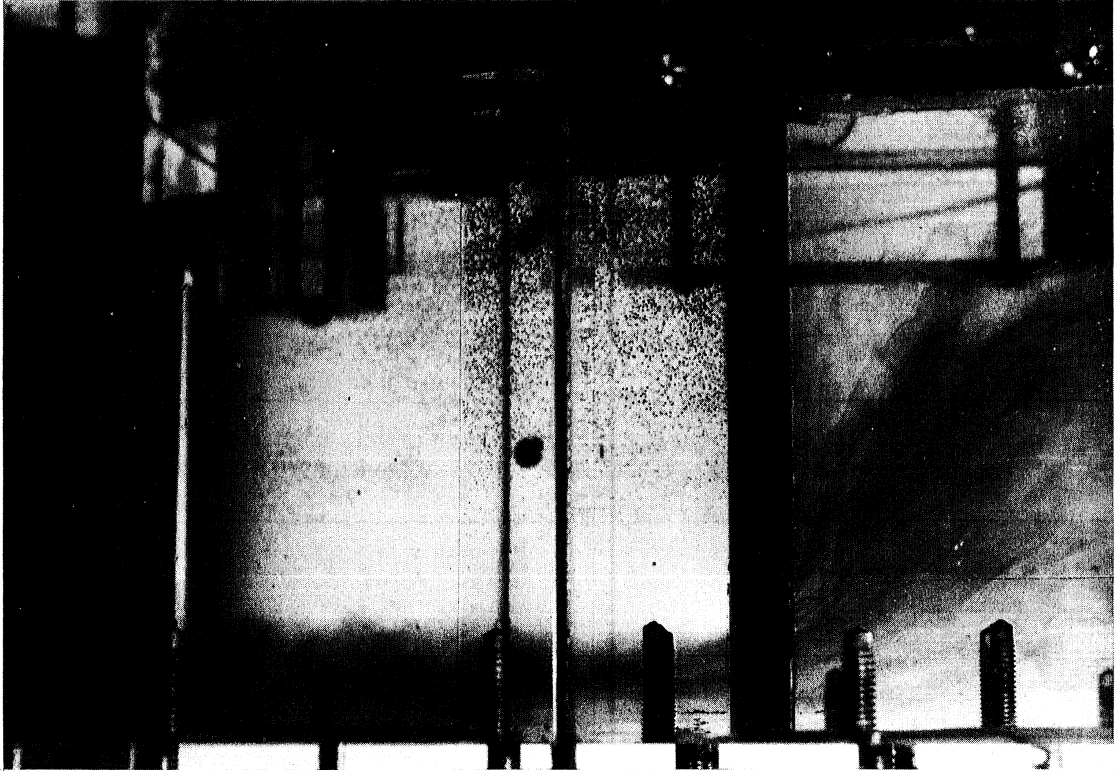


Photo 5

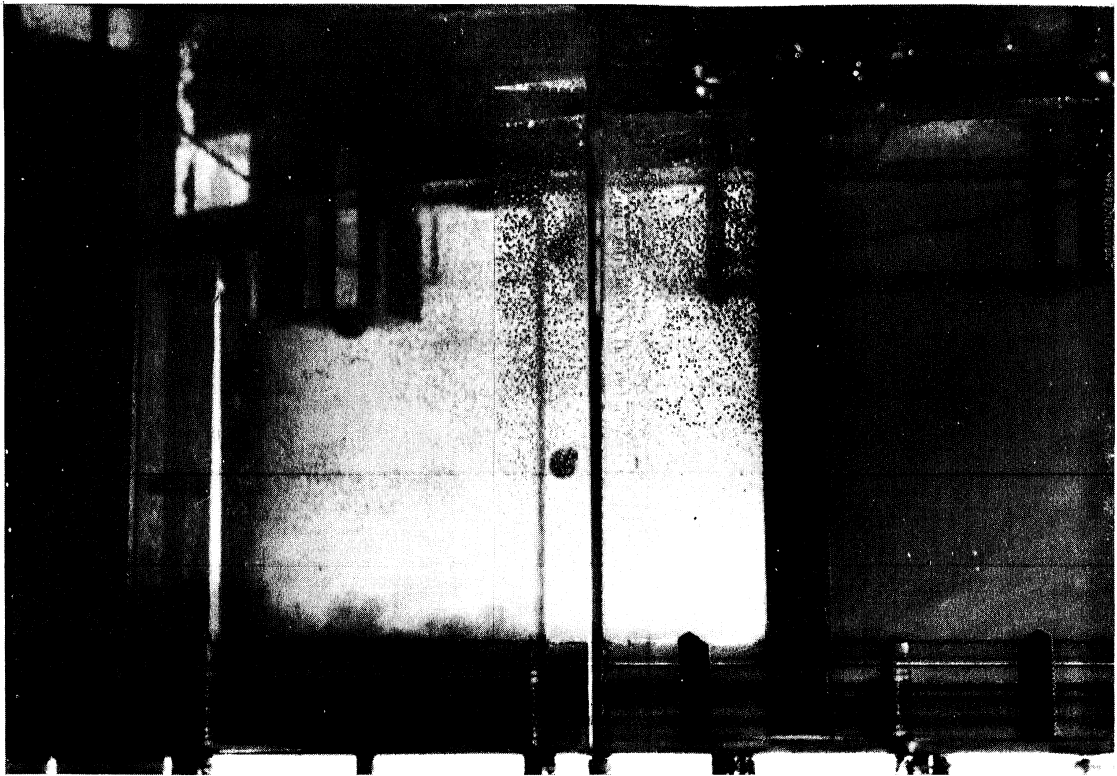


Photo 6



1. The first part of the document discusses the importance of maintaining accurate records of all transactions and activities. It emphasizes that this is crucial for ensuring transparency and accountability in the organization's operations.

2. The second part of the document outlines the various methods and tools used to collect and analyze data. It highlights the need for consistent and reliable data collection processes to support effective decision-making.

3. The third part of the document focuses on the analysis and interpretation of the collected data. It discusses the various statistical and analytical techniques used to identify trends and patterns in the data.

4. The fourth part of the document discusses the importance of communicating the results of the analysis to the relevant stakeholders. It emphasizes the need for clear and concise reporting to ensure that the information is understood and acted upon.

5. The fifth part of the document discusses the importance of reviewing and evaluating the data collection and analysis process. It emphasizes the need for continuous improvement to ensure that the process remains effective and efficient.

6. The sixth part of the document discusses the importance of maintaining the confidentiality and security of the data. It emphasizes the need for robust security measures to protect the organization's sensitive information.

7. The seventh part of the document discusses the importance of ensuring the accuracy and reliability of the data. It emphasizes the need for rigorous quality control measures to minimize errors and ensure that the data is trustworthy.

8. The eighth part of the document discusses the importance of ensuring the integrity and ethical use of the data. It emphasizes the need for clear policies and procedures to guide the organization's data handling practices.

9. The ninth part of the document discusses the importance of ensuring the privacy of the data. It emphasizes the need for strict adherence to data protection regulations to safeguard the personal information of individuals.

10. The tenth part of the document discusses the importance of ensuring the availability and accessibility of the data. It emphasizes the need for robust backup and recovery procedures to ensure that the data is always available when needed.

11. The eleventh part of the document discusses the importance of ensuring the consistency and standardization of the data. It emphasizes the need for clear definitions and standards to ensure that the data is comparable and consistent across different systems and departments.

12. The twelfth part of the document discusses the importance of ensuring the relevance and timeliness of the data. It emphasizes the need for regular updates and reviews to ensure that the data remains current and relevant to the organization's needs.

PHOTO 7 (Serial No. 168B-169) In order to delineate the currents within the gate chamber yarns were attached to wands and located at various points to indicate the flow direction of the circulating currents within the tower. It can be seen that the flow is in the upper direction at the downstream wall of the gate chamber, while it is downward at the other locations. For this experiment the discharge was 1550 cfs, the headwater elevation 1180 ft, the water surface elevation in the chamber 1150 ft, and the tailwater elevation 1130 ft.

PHOTO 8 (Serial No. 168B-156) This photograph shows confetti in the Morris Drift for a discharge of 1550 cfs. The motion of the particles is shown by the directions and lengths of the confetti streaks. In this instance the direction of flow on the front side of the drift is downward so that the rotation is counterclockwise facing the drift. The decrease in velocity and concentration with increasing distances down the drift is apparent.

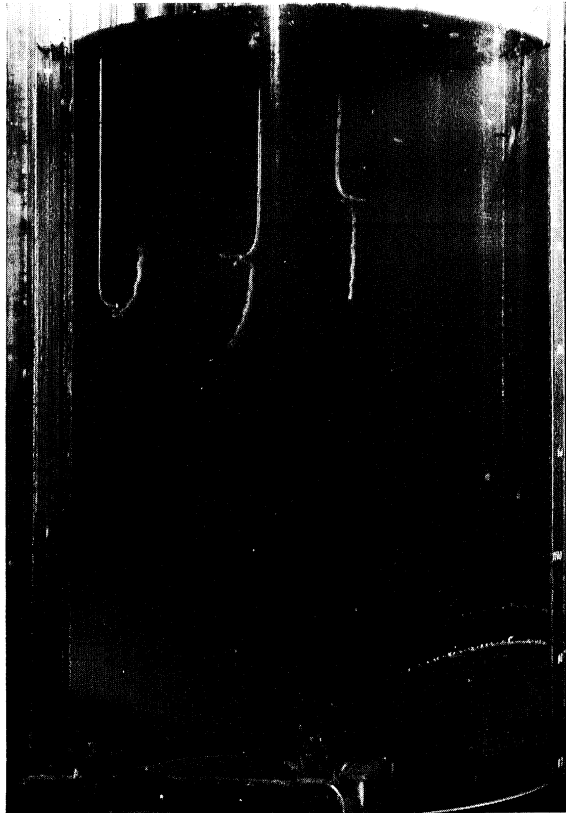


Photo 7

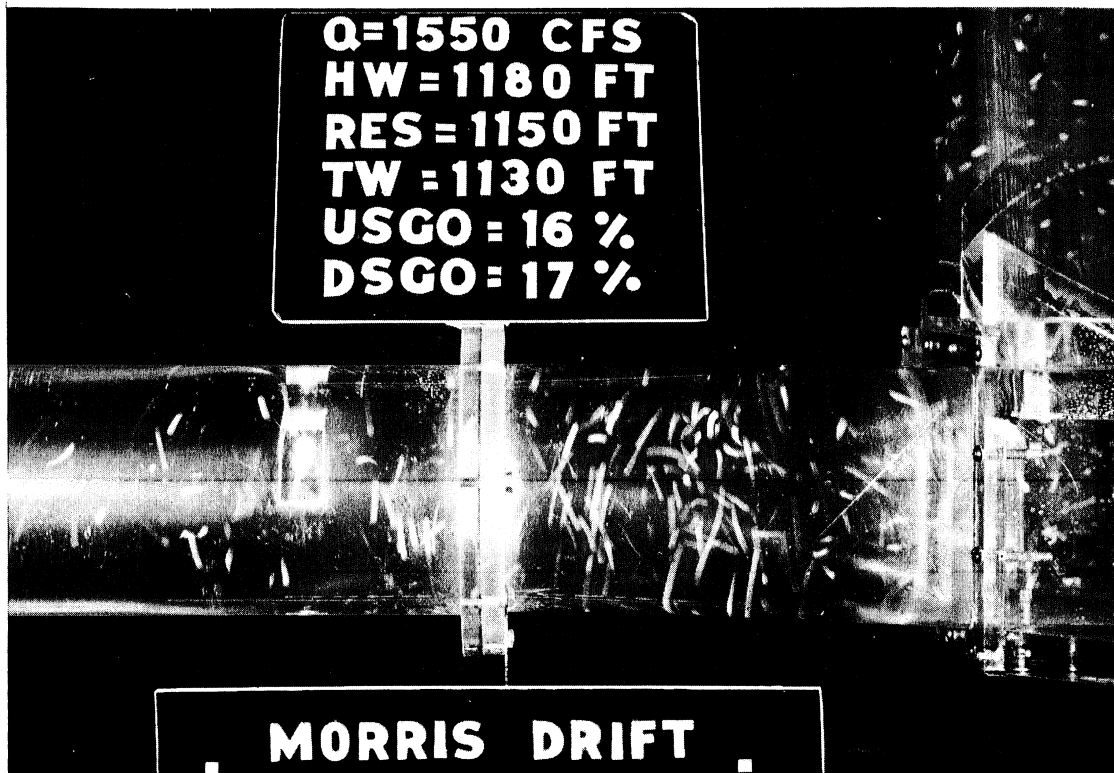


Photo 8



*[The page contains extremely faint and illegible text, likely bleed-through from the reverse side of the document. The text is too light to transcribe accurately.]*

PHOTO 9 (Serial No. 168B-157) In this photograph the discharge has been reduced to 1000 cfs. This view shows that, in general, the lengths of the streaks are shorter, suggesting that the rotational velocities are less. This may be due to the decreased thickness of the jet for this discharge flowing past the entrance, since its velocity would be nearly the same as for the higher discharge.

PHOTO 10 (Serial No. 168B-158) In this photograph the discharge has been reduced to 420 cfs with the same water surface elevation as in Photos 8 and 9. For this low discharge the gates have been nearly closed; the jet issuing from the upstream gates is very thin, and it appears that the rotational velocities have been very considerably reduced. There is no net flow through the Morris Drift tunnel.



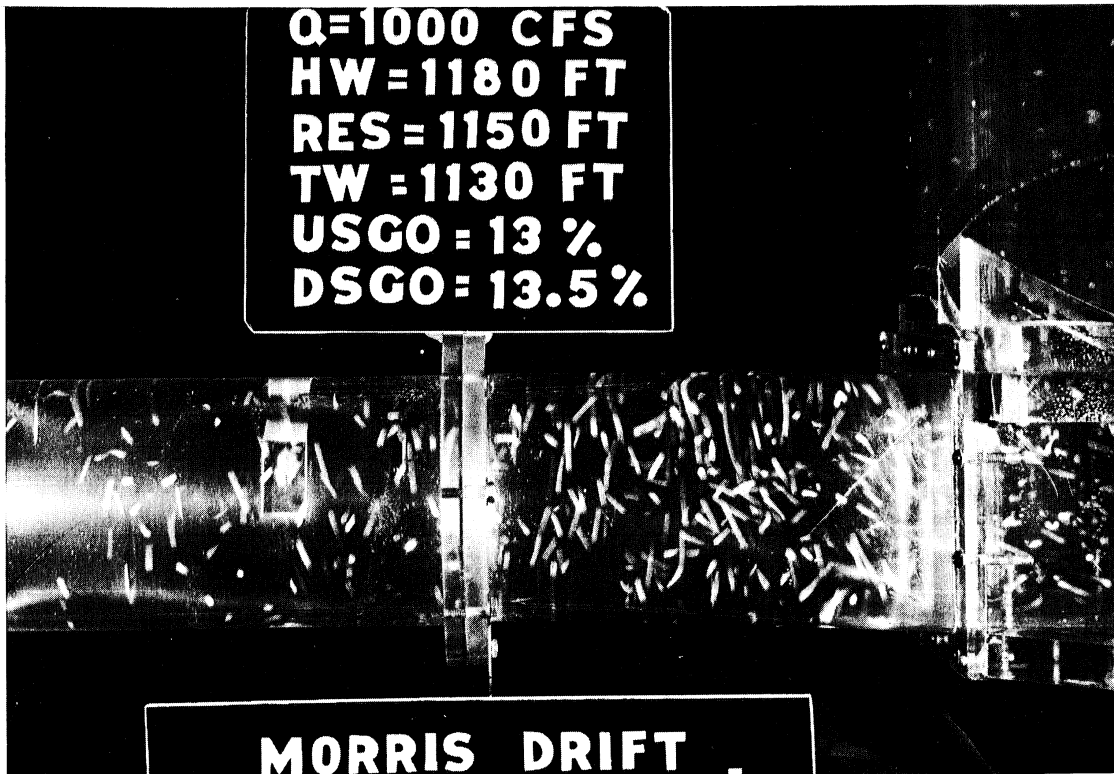


Photo 9

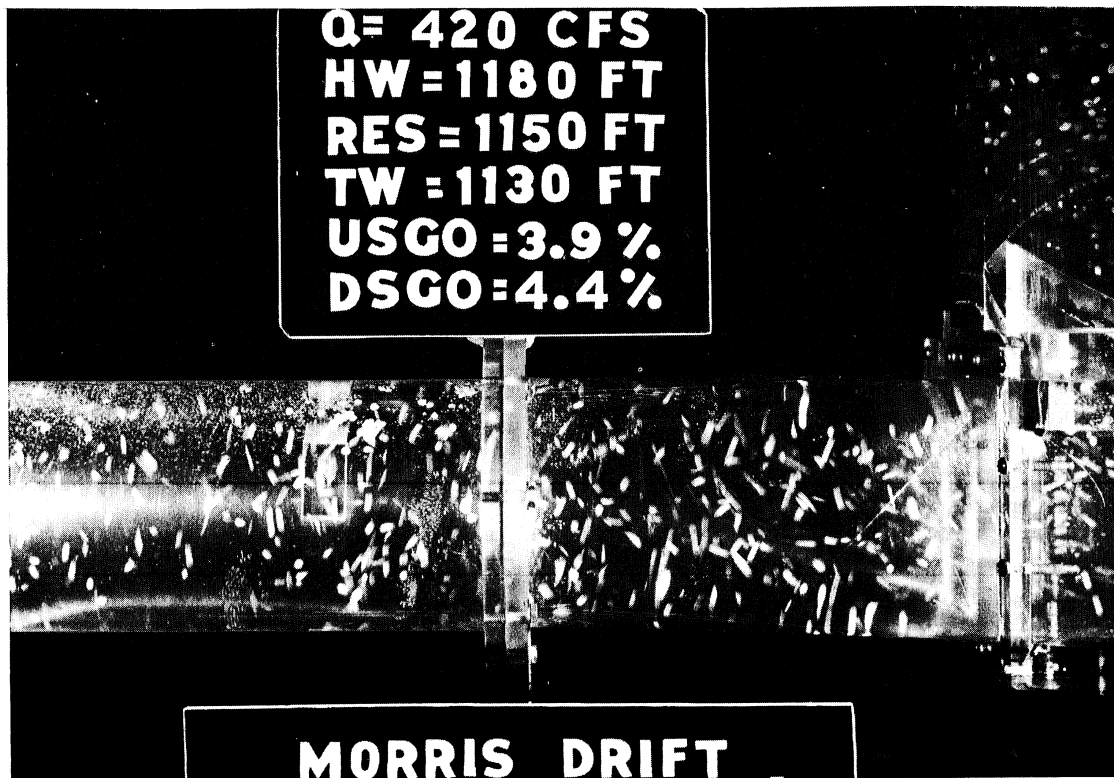
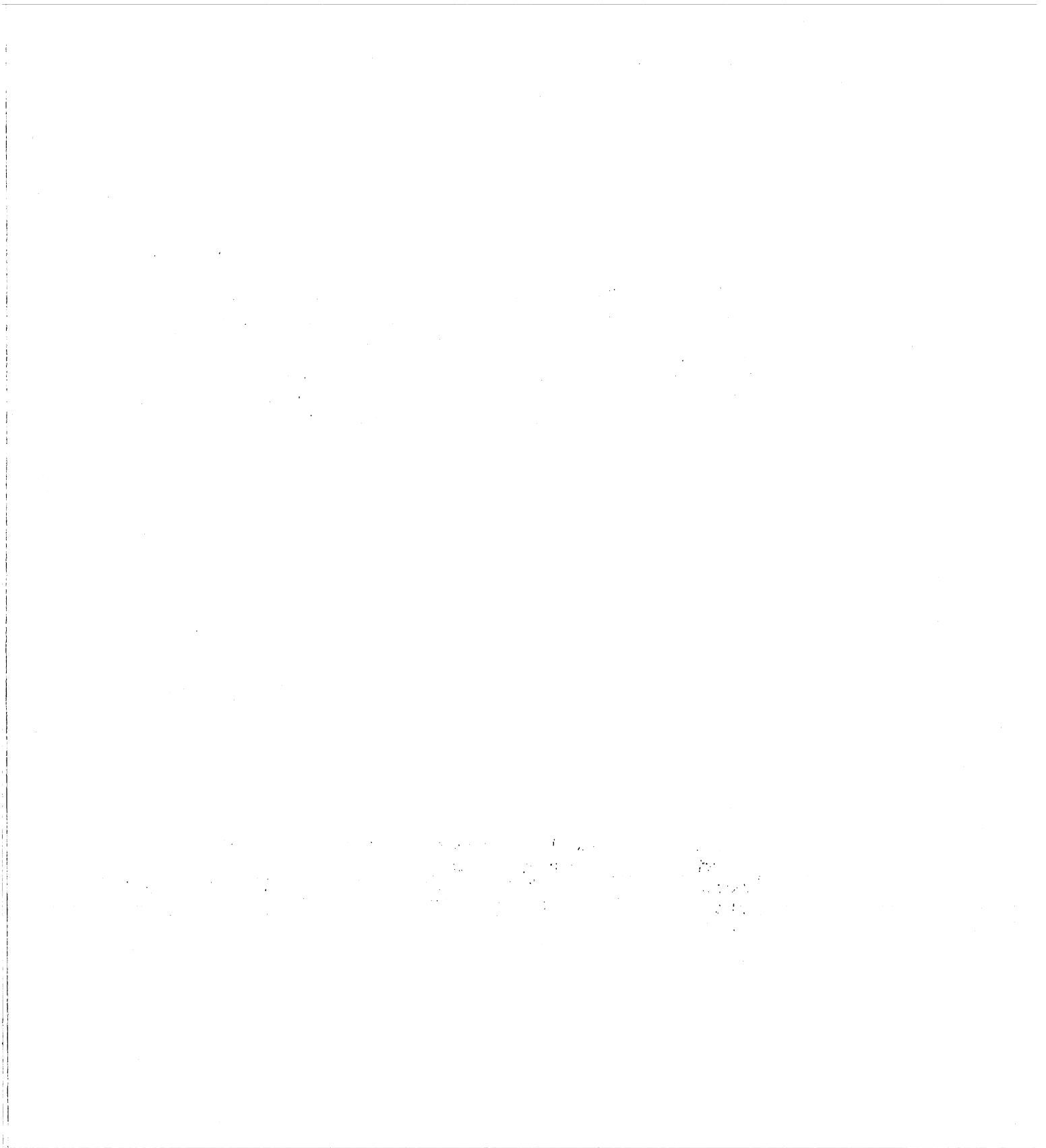


Photo 10







---

1. The first part of the document discusses the importance of maintaining accurate records of all transactions and activities. It emphasizes the need for transparency and accountability in financial reporting.

2. The second part of the document outlines the various methods used to collect and analyze data. It includes a detailed description of the sampling process and the statistical techniques employed to ensure the reliability of the results.

3. The third part of the document presents the findings of the study. It shows that there is a significant correlation between the variables being studied, and that the results are consistent with the theoretical framework proposed in the introduction.

4. The final part of the document discusses the implications of the findings and offers suggestions for future research. It highlights the need for further investigation into the underlying mechanisms that drive the observed relationships.

5. The document concludes by summarizing the key points and reiterating the importance of the research. It expresses the hope that the findings will contribute to a better understanding of the subject matter and inform future decision-making.

PHOTO 13 (Serial No. 168B-163) The electrical impulses from the pressure transducers were carried to a moving chart recorder and a magnetic tape recorder. The chart provided an instantaneous visual record of the pressure fluctuations, while the record of the magnetic tape recorder was used for the harmonic analysis.

PHOTO 14 (Serial No. 168B-161) In these experiments the Morris Drift was removed and the tunnel closed with a blind flange. The photo shows the blind flange in place with the pressure transducer flush mounted on the flange in order to measure pressure fluctuations.

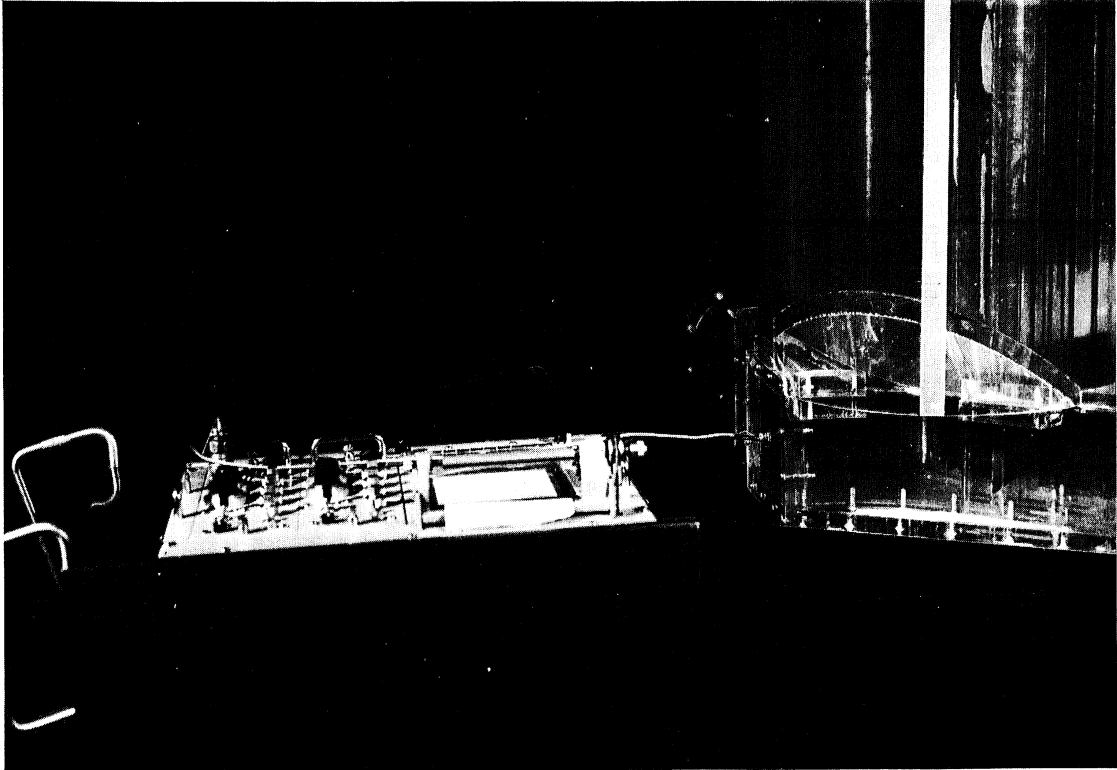


Photo 13

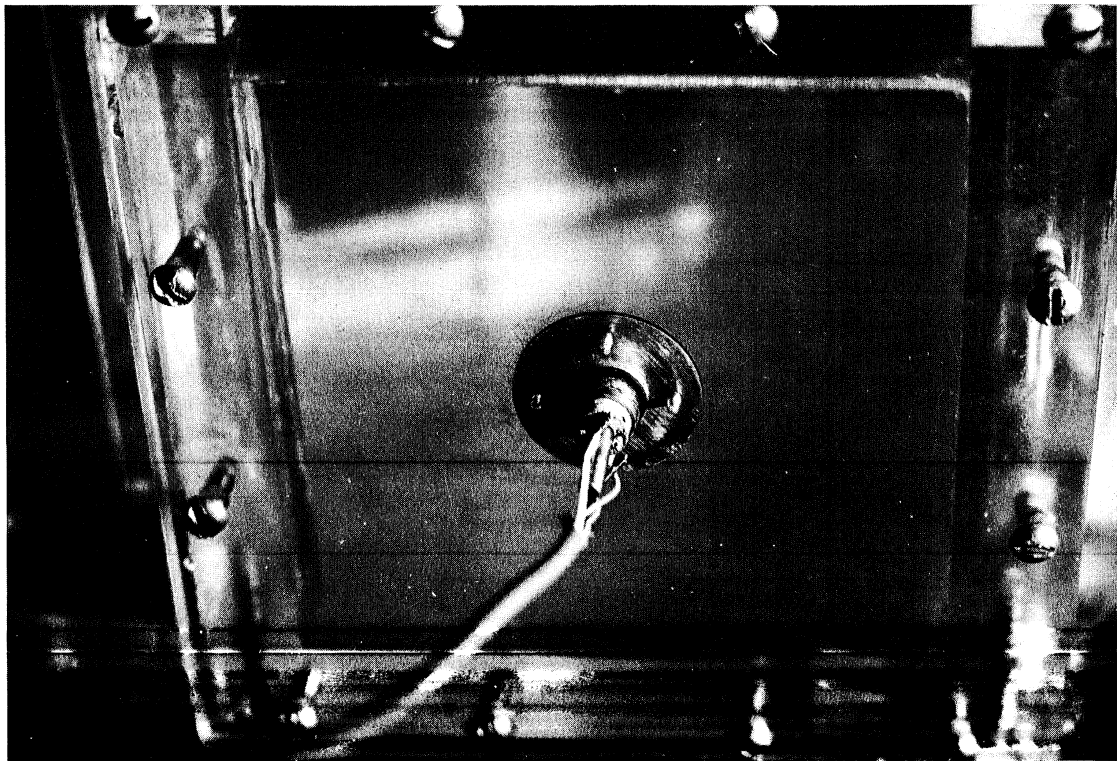


Photo 14





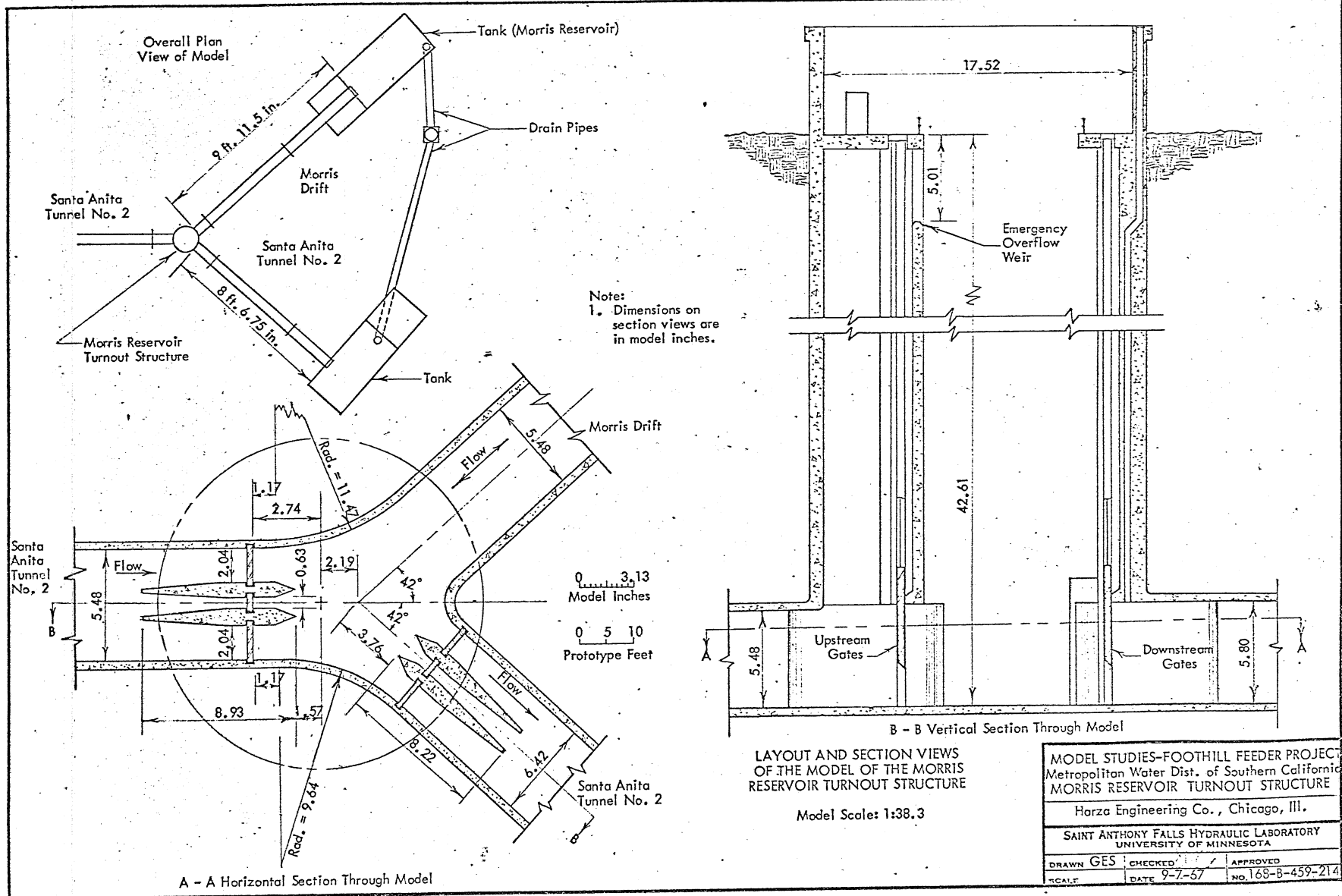
## LIST OF CHARTS

- CHART 1 (168B459-214) Layout and section views of the model of the Morris Reservoir Turnout Structure. Model scale 1:38.3.
- CHART 2 (168B459-215) Theoretical determination of total differential for various gate openings and discharges.
- CHART 3 (168B459-216) Measured total head differential as a function of upstream and downstream gate openings.  $Q = 420$  cfs. Tailwater elevations = 1130 ft, 1150 ft, and 1170 ft.
- CHART 4 (168B459-217) Measured total head differential as a function of the upstream and downstream gate openings.  $Q = 1000$  cfs. Tailwater elevations = 1130 ft, 1150 ft, and 1170 ft.
- CHART 5 (168B459-218) Measured total head differential as a function of the upstream and downstream gate openings.  $Q = 1550$  cfs. Tailwater elevations = 1130 ft, 1150 ft, and 1170 ft.
- CHART 6 (168B459-232) Comparison of velocity profiles with and without the Morris Drift - right upstream gate.  $Q = 1550$  cfs.
- CHART 7 (168B459-233) Comparison of velocity profiles with and without the Morris Drift - left upstream gate.  $Q = 1550$  cfs.
- CHART 8 (168B459-230) Comparison of velocity profiles with and without the Morris Drift - right downstream gate.  $Q = 1550$  cfs.
- CHART 9 (168B459-231) Comparison of velocity profiles with and without the Morris Drift - left downstream gate.  $Q = 1550$  cfs.
- CHART 10 (168B459-219) Velocity profiles in the vicinity of the gates.  $Q = 1550$  cfs. Upstream gate opening 15.2 per cent, downstream gate opening 100 per cent. Velocity profiles taken upstream and downstream along the centerline of the right upstream gate.
- CHART 11 (168B459-220) Velocity profiles in the vicinity of the gates.  $Q = 1550$  cfs. Upstream gate opening 15.2 per cent, downstream gate opening 100 per cent. Velocity profiles upstream and downstream along the centerline of the right upstream gate and upstream of the right downstream gate.
- CHART 12 (168B459-221) Velocity profiles in the vicinity of the gates.  $Q = 1550$  cfs. Upstream gate opening 15.2 per cent, downstream gate opening 100 per cent. Velocity profiles taken at intervals on a line 23.75 ft downstream of the upstream gates and normal to the centerline of the upstream gates.

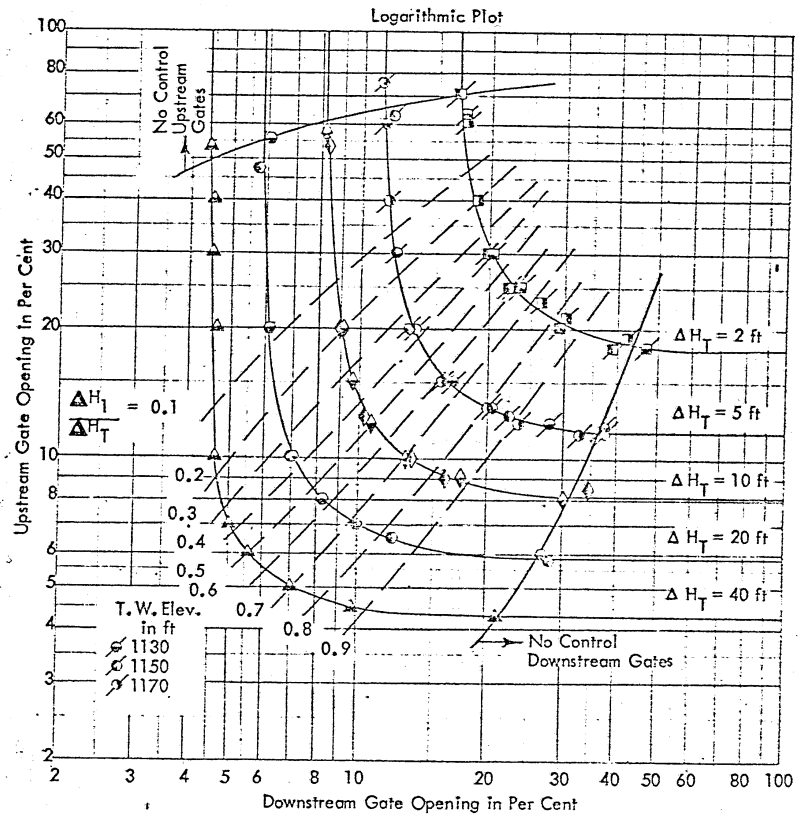
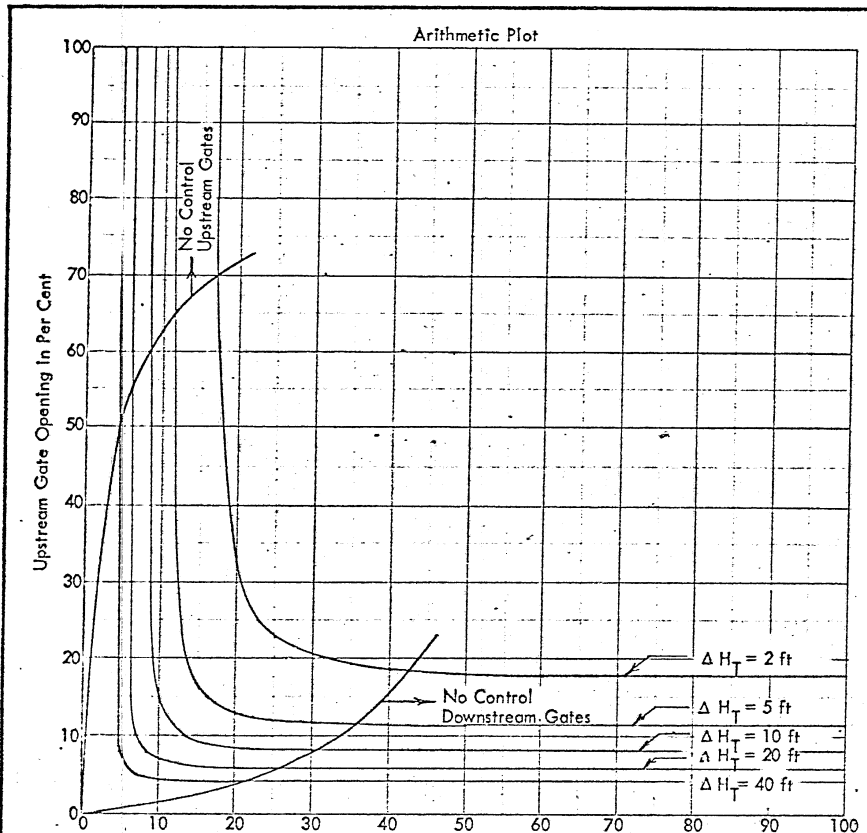
TABLE OF CONTENTS

1	2000	Introduction and Acknowledgements
2	2001	Chapter 1: The History of the Study
3	2002	Chapter 2: Theoretical Framework
4	2003	Chapter 3: Methodology
5	2004	Chapter 4: Data Collection and Analysis
6	2005	Chapter 5: Results and Discussion
7	2006	Chapter 6: Conclusion and Recommendations
8	2007	Appendix A: Questionnaire
9	2008	Appendix B: Interview Schedule
10	2009	Appendix C: Ethical Approval
11	2010	References
12	2011	Bibliography
13	2012	Index
14	2013	Appendix D: Glossary
15	2014	Appendix E: List of Abbreviations
16	2015	Appendix F: List of Figures
17	2016	Appendix G: List of Tables
18	2017	Appendix H: List of Appendices
19	2018	Appendix I: List of References
20	2019	Appendix J: List of Bibliography
21	2020	Appendix K: List of Index
22	2021	Appendix L: List of Appendix
23	2022	Appendix M: List of Glossary
24	2023	Appendix N: List of Abbreviations
25	2024	Appendix O: List of Figures
26	2025	Appendix P: List of Tables
27	2026	Appendix Q: List of Appendices
28	2027	Appendix R: List of References
29	2028	Appendix S: List of Bibliography
30	2029	Appendix T: List of Index
31	2030	Appendix U: List of Appendix
32	2031	Appendix V: List of Glossary
33	2032	Appendix W: List of Abbreviations
34	2033	Appendix X: List of Figures
35	2034	Appendix Y: List of Tables
36	2035	Appendix Z: List of Appendices

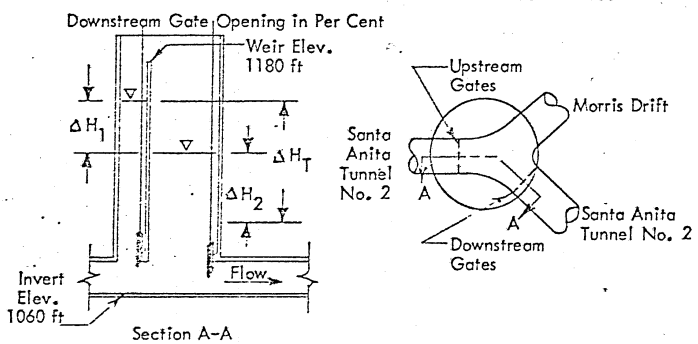
- CHART 13 (168B459-222) Velocity profiles in the vicinity of the gates. Q = 1550 cfs. Upstream gate opening 21.3 per cent, downstream gate opening 17.5 per cent. Velocity profiles taken upstream and downstream along the centerline of the right upstream gate.
- CHART 14 (168B459-223) Velocity profiles in the vicinity of the gates. Q = 1550 cfs. Upstream gates opening 21.3 per cent, downstream gate opening 17.5 per cent. Velocity profiles taken upstream and downstream along the centerline of the right upstream gate and upstream of the right downstream gate.
- CHART 15 (168B459-224) Harmonic wave analysis of pressure pulses on the upstream gates, Q = 1550 cfs over emergency weirs.
- CHART 16 (168B459-225) Harmonic wave analysis of pressure pulses on the downstream right gate, Q = 1550 cfs over emergency weirs.
- CHART 17 (168B459-226) Harmonic wave analysis of pressure pulses on the downstream right gate, Q = 1550 cfs through the gate sections.
- CHART 18 (168B459-227) Harmonic wave analysis of pressure pulses on the downstream right gate, Q = 420 cfs through the gate sections.
- CHART 19 (168B459-228) Harmonic wave analysis of pressure pulses on the downstream right gate, Q = 200 cfs through center gate only.
- CHART 20 (168B459-229) Harmonic wave analysis of pressure pulses on downstream right gate, Q = 1550 cfs through left gates only.
- CHART 21 (168B459-234) Comparison of pressure fluctuations on downstream right gate for various discharges.
- CHART 22 (168B459-235) Comparison of pressure fluctuations on downstream right gate for two reservoir elevations, Q = 1550 cfs.
- CHART 23 (168B459-236) Pressure fluctuations on downstream right gate and blind flange on Morris Drift, Q = 1550 cfs.
- CHART 24 (168B459-237) Comparison of pressure fluctuations on blind flange on Morris Drift for various reservoir elevations, Q = 1550 cfs.



MODEL STUDIES—FOOTHILL FEEDER PROJECT		
Metropolitan Water Dist. of Southern California		
MORRIS RESERVOIR TURNOUT STRUCTURE		
Harza Engineering Co., Chicago, Ill.		
SAINT ANTHONY FALLS HYDRAULIC LABORATORY		
UNIVERSITY OF MINNESOTA		
DRAWN	GES	CHECKED
SCALE	DATE	APPROVED
	9-7-57	NO. 168-B-459-214



Symbol	$\Delta H_T$ in ft
○	80
□	60
△	40
○	20
◇	10
◇	5
◇	2



- Notes:
1. The three gates of each set are opened equally.
  2. No flow in Morris Drift.
  3.  $\Delta H_T$  is the total head differential across both gate sets.
- $\Delta H_T = \Delta H_1 + \Delta H_2$

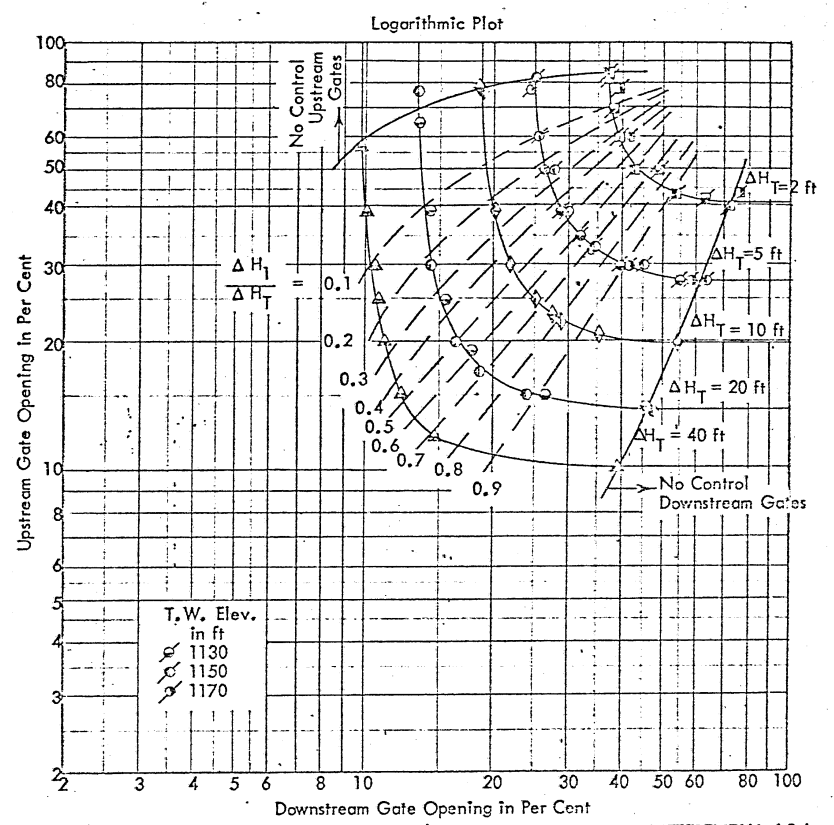
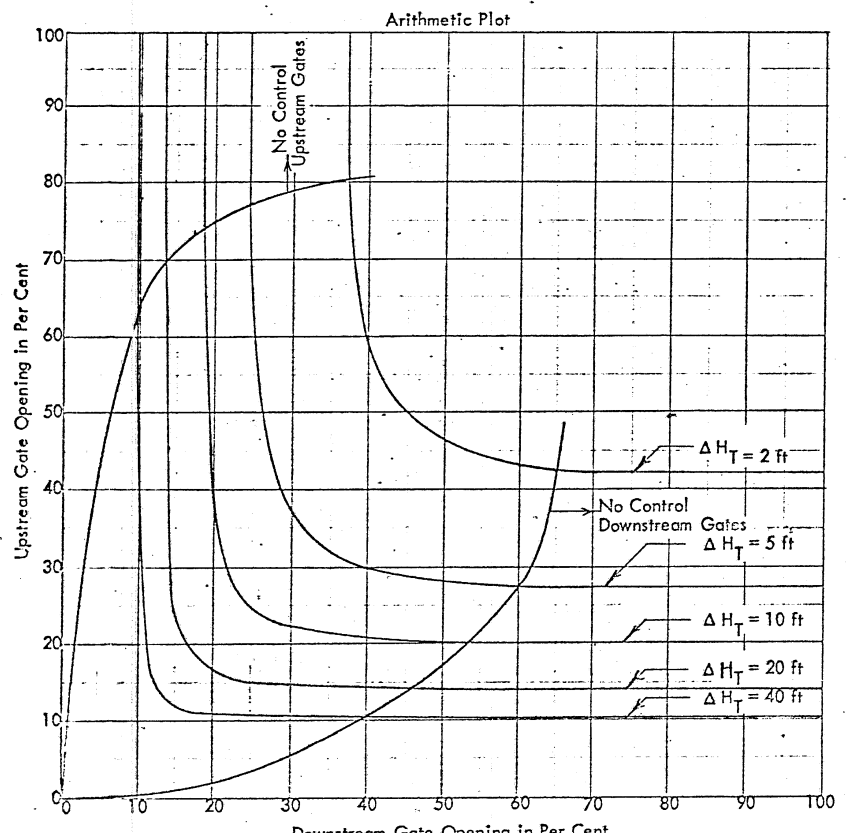
TOTAL HEAD DIFFERENTIAL AS A FUNCTION OF THE UPSTREAM AND DOWNSTREAM GATE OPENINGS  
 $Q = 420$  cfs  
 T.W. Elev. = 1130 ft, 1150 ft and 1170 ft  
 Model Scale 1:38.3

MODEL STUDIES-FOOTHILL FEEDER PROJECT  
 Metropolitan Water Dist. of Southern California  
 MORRIS RESERVOIR TURNOUT STRUCTURE

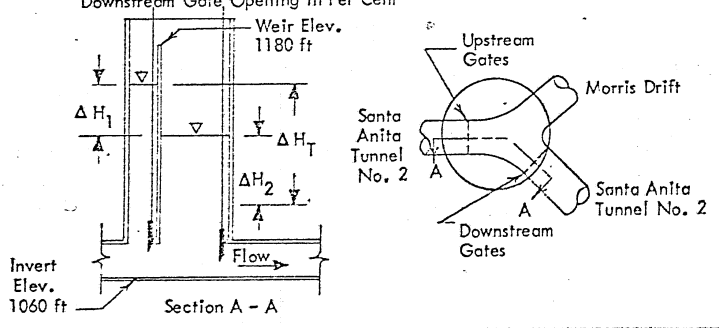
Harza Engineering Co., Chicago, Ill.

SAINT ANTHONY FALLS HYDRAULIC LABORATORY  
 UNIVERSITY OF MINNESOTA

DRAWN D.M.N. CHECKED [initials] APPROVED [initials]  
 SCALE 1 DATE 10-17-57 NO 53-3-459-215



$\Delta H_T$ in ft
○
□
△
◇
◇
◇
◇
◇



- Notes:
- The three gates of each set are opened equally.
  - No flow in Morris Drift.
  - $\Delta H_T$  is the total head differential across both gate sets.
- $\Delta H_T = \Delta H_1 + \Delta H_2$

TOTAL HEAD DIFFERENTIAL AS A FUNCTION OF THE UPSTREAM AND DOWNSTREAM GATE OPENINGS

$Q = 1000$  cfs

T.W. Elev. = 1130 ft, 1150 ft and 1170 ft

Model Scale 1:38.3

MODEL STUDIES-FOOTHILL FEEDER PROJECT

Metropolitan Water Dist. of Southern California

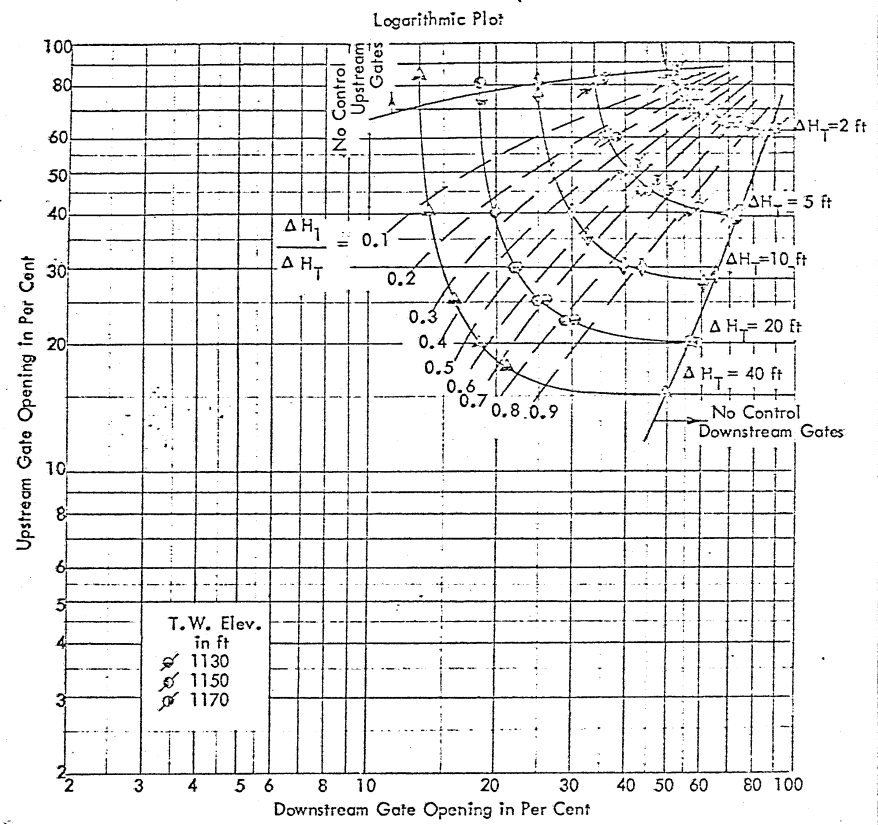
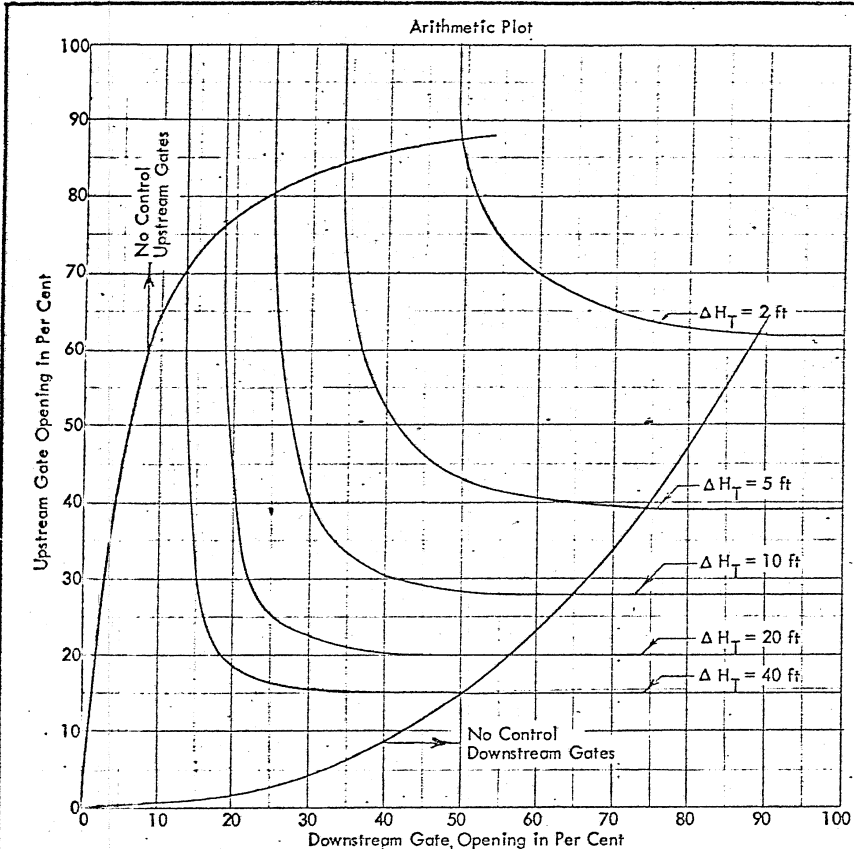
MORRIS RESERVOIR TURNOUT STRUCTURE

Harza Engineering Co., Chicago, Ill.

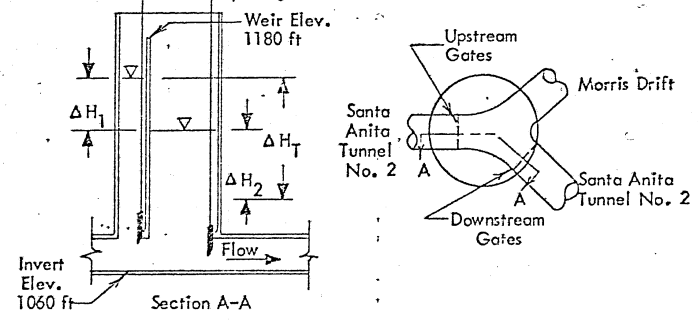
SAINT ANTHONY FALLS HYDRAULIC LABORATORY

UNIVERSITY OF MINNESOTA

DRAWN DJA CHECKED DATE 10-16-57 APPROVED NO. 165-3-459-217



$\Delta H_T$ in ft	Symbol
80	○
60	□
40	△
20	◇
10	◇
5	◇
2	◇



- Notes:
1. The three gates of each set are opened equally.
  2. No flow in Morris Drift.
  3.  $\Delta H_T$  is the total head differential across both gate sets.  
 $\Delta H_T = \Delta H_1 + \Delta H_2$

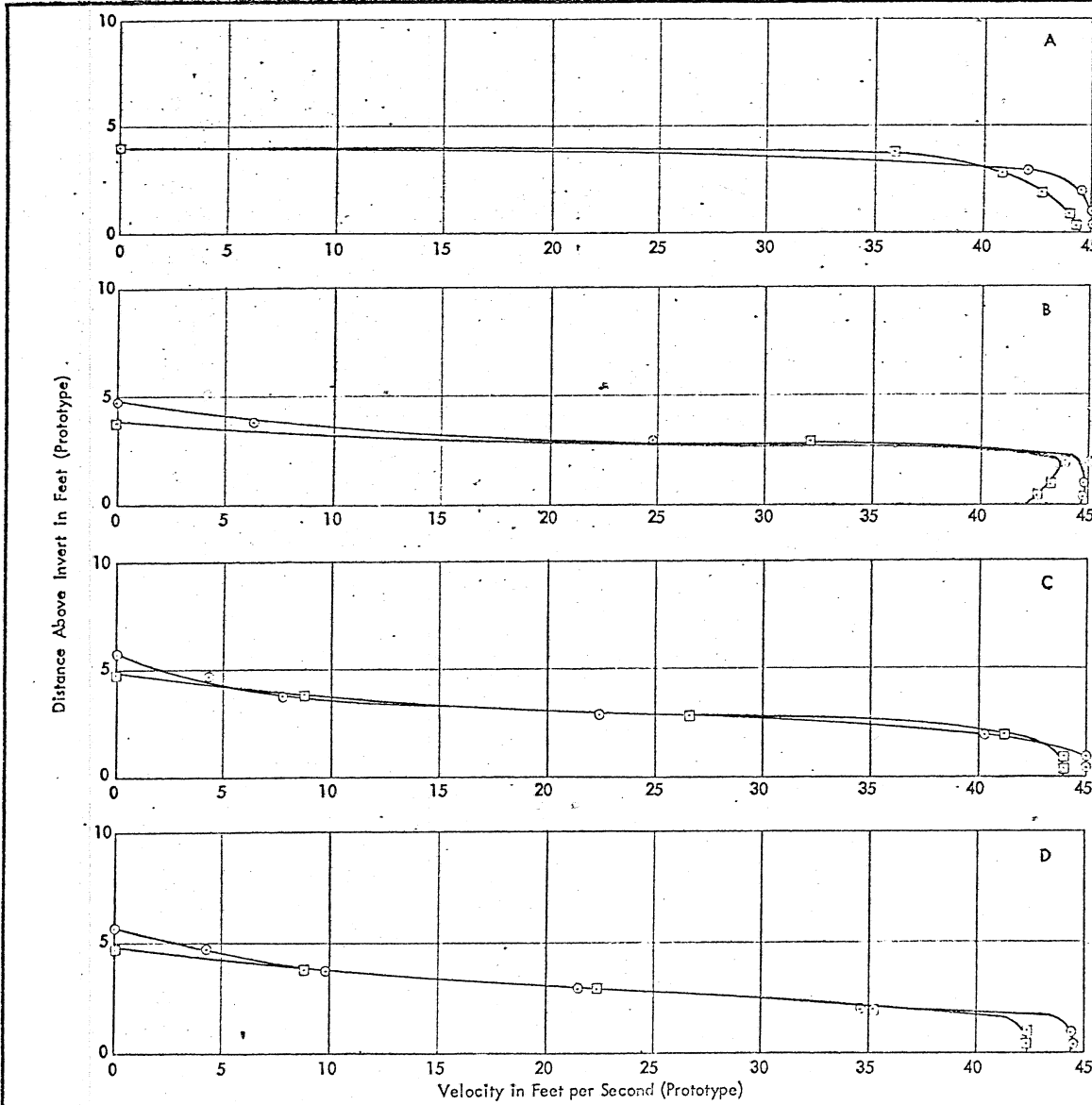
TOTAL HEAD DIFFERENTIAL AS A FUNCTION OF THE UPSTREAM AND DOWNSTREAM GATE OPENINGS  
 $Q = 1550$  cfs  
 T.W. Elev. = 1130 ft, 1150 ft and 1170 ft  
 Model Scale 1:38.3

MODEL STUDIES—FOOTHILL FEEDER PROJECT  
 Metropolitan Water Dist. of Southern California  
 MORRIS RESERVOIR TURNOUT STRUCTURE

Harza Engineering Co., Chicago, Ill.

SAINT ANTHONY FALLS HYDRAULIC LABORATORY  
 UNIVERSITY OF MINNESOTA

DRAWN: DMN CHECKED: [ ] APPROVED: [ ]  
 SCALE: [ ] DATE: 10-17-67 NO. 100-3-457-215



- With Morris Drift
- Without Morris Drift

Notes:

1. Center gates closed, outer gates of each set opened equally.
2. Velocities were measured using special, calibrated pitot tubes.
3. Profiles were taken at successive points on the centerline downstream of the right upstream gate as follows:

Profile	Location - distance downstream of gate feet prototype
A	0
B	5.75
C	11.50
D	17.25

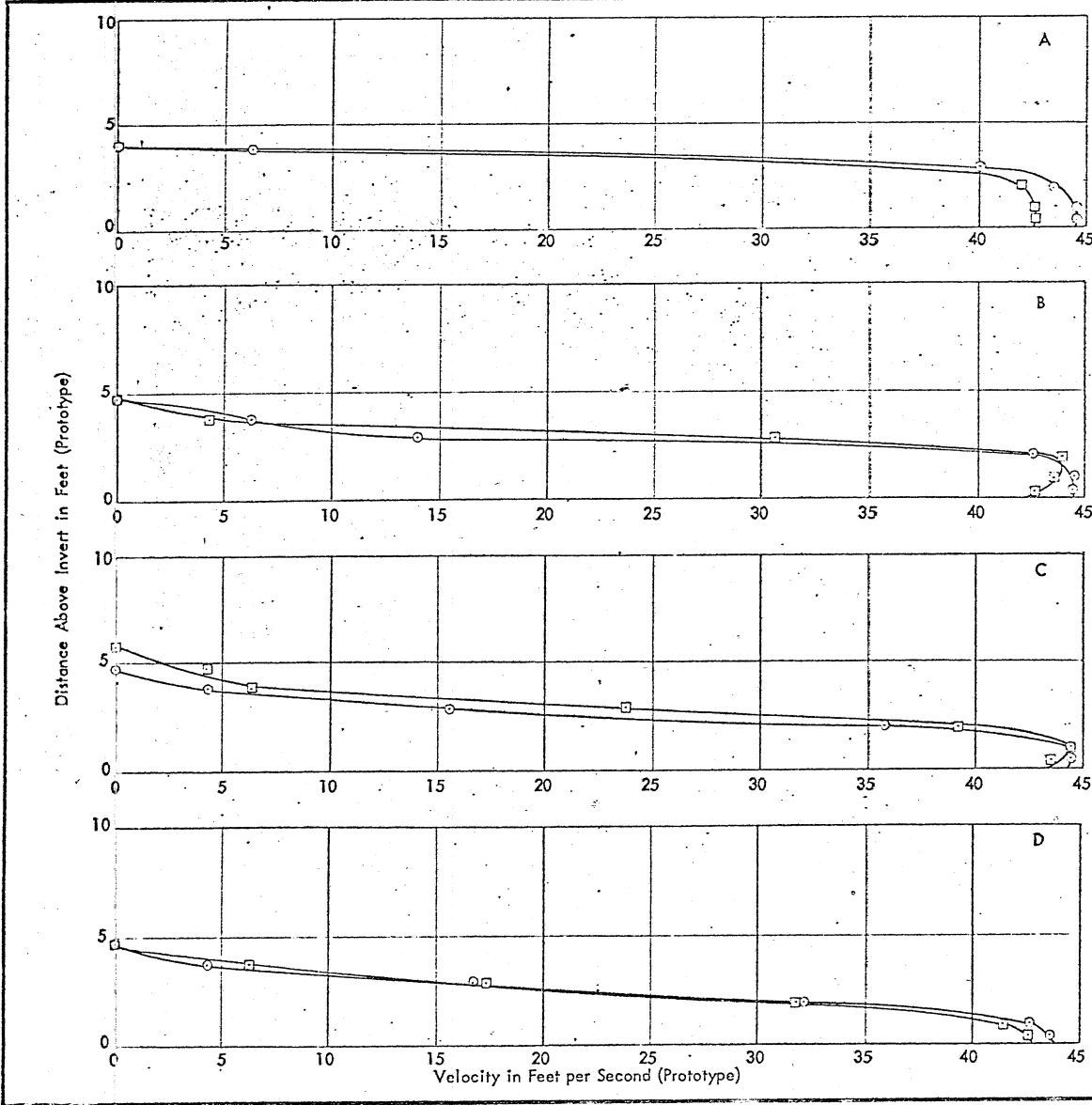
COMPARISON OF VELOCITY PROFILES WITH AND WITHOUT MORRIS DRIFT - RIGHT UPSTREAM GATE

$Q = 1550$  cfs  
 $HW = 1180$  ft.  
 $RES = 1150$  ft.  
 $TW = 1130$  ft.

$USGO = 21.6\%$   
 $DSGO = 21.6\%$   
 (Center Gates Closed)  
 Model Scale 1:38.3

MODEL STUDIES-FOOTHILL FEEDER PROJECT		
Metropolitan Water Dist. of Southern California		
MORRIS RESERVOIR TURNOUT STRUCTURE		
Herza Engineering Co., Chicago, Ill.		
SAINT ANTHONY FALLS HYDRAULIC LABORATORY		
UNIVERSITY OF MINNESOTA		
DRAWN DWN	CHECKED	APPROVED
DATE	DATE	DATE
2-8-68		1653-459-202





- With Morris Drift
- Without Morris Drift

Notes:

1. Center gates closed, outer gates of each set opened equally.
2. Velocities were measured using special, calibrated pitot tubes.
3. Profiles were taken at successive points on the centerline downstream of the left upstream gate as follows:

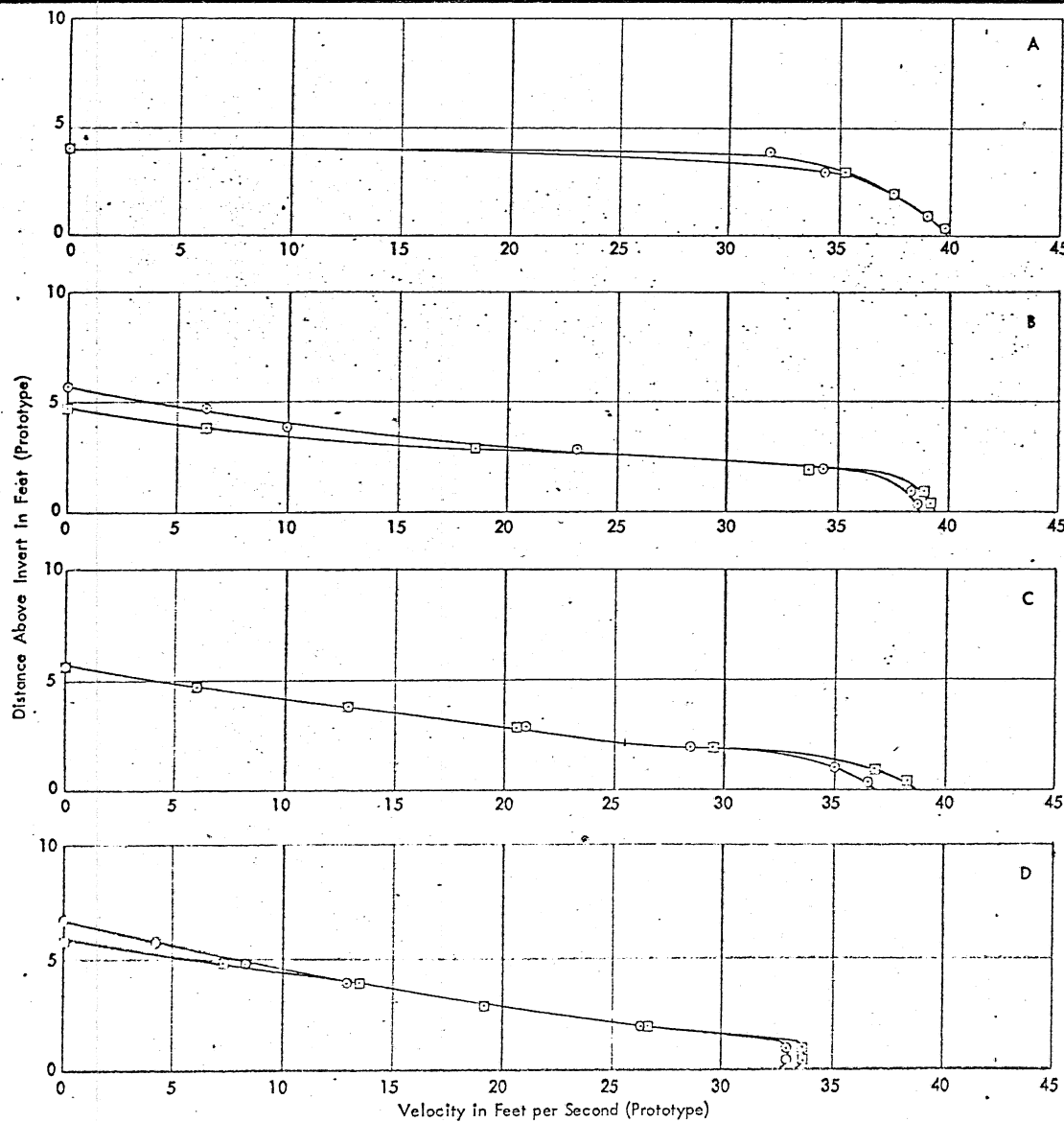
Profile	Location - distance downstream of gate feet prototype
A	0
B	5.75
C	11.50
D	17.25

COMPARISON OF VELOCITY PROFILES WITH AND WITHOUT MORRIS DRIFT - LEFT UPSTREAM GATE

Q = 1550 cfs  
 HW = 1180 ft.  
 RES = 1150 ft.  
 TW = 1130 ft.

USGO = 21.6 %  
 DSGO = 21.6 %  
 (Center Gates Closed)  
 Model Scale 1:38.3

MODEL STUDIES-FOOTHILL FEEDER PROJECT Metropolitan Water Dist. of Southern California MORRIS RESERVOIR TURNOUT STRUCTURE		
Harza Engineering Co., Chicago, Ill.		
SAINT ANTHONY FALLS HYDRAULIC LABORATORY UNIVERSITY OF MINNESOTA		
DRAWN GES	CHECKED [initials]	APPROVED [initials]
SCALE	DATE 2-9-48	NO. 1653-459-233



- With Morris Drift
- Without Morris Drift

Notes:

1. Center gates closed, outer gates of each set opened equally.
2. Velocities were measured using special, calibrated pitot tubes.
3. Profiles were taken at successive points on the centerline downstream of the right downstream gate as follows:

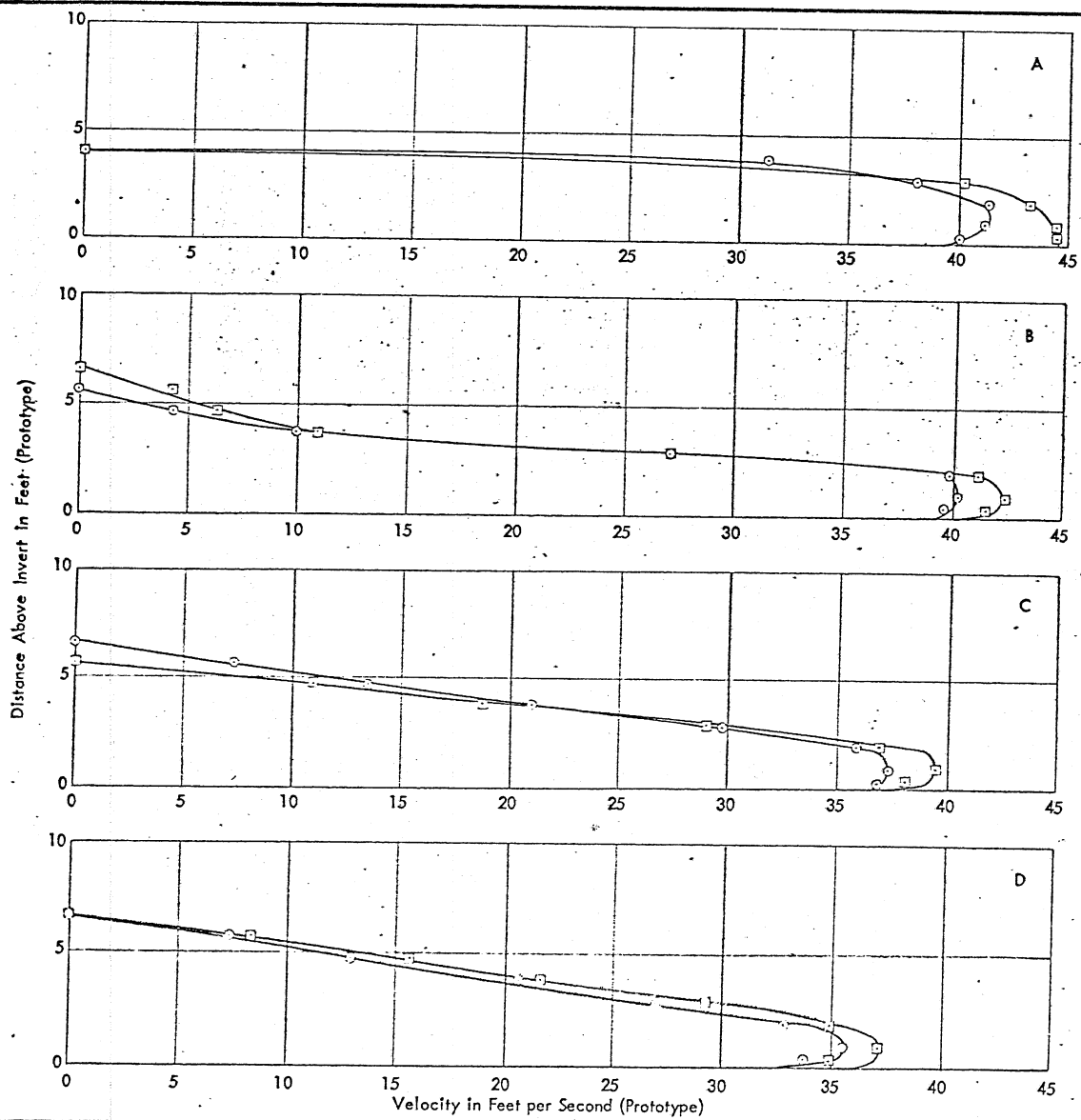
Profile	Location - distance downstream of gate feet prototype
A	0
B	5.75
C	11.50
D	17.25

COMPARISON OF VELOCITY PROFILES WITH AND WITHOUT MORRIS DRIFT - RIGHT DOWNSTREAM GATE

Q = 1550 cfs  
 HW = 1180 ft.  
 RES = 1150 ft.  
 TW = 1130 ft.

USGO = 21.6 %  
 DSGO = 21.6 %  
 (Center Gates Closed)  
 Model Scale 1:38.3

MODEL STUDIES-FOOTHILL FEEDER PROJECT Metropolitan Water Dist. of Southern California MORRIS RESERVOIR TURNOUT STRUCTURE		
Harza Engineering Co., Chicago, Ill.		
SAINT ANTHONY FALLS HYDRAULIC LABORATORY UNIVERSITY OF MINNESOTA		
DRAWN DMN	CHECKED [initials]	APPROVED [initials]
SCALE	DATE 2-8-68	NO 1688-459-230



- With Morris Drift
- Without Morris Drift

Notes:

1. Center gates closed, outer gates of each set opened equally.
2. Velocities were measured using special, calibrated pitot tubes.
3. Profiles were taken at successive points on the centerline downstream of the left downstream gate as follows:

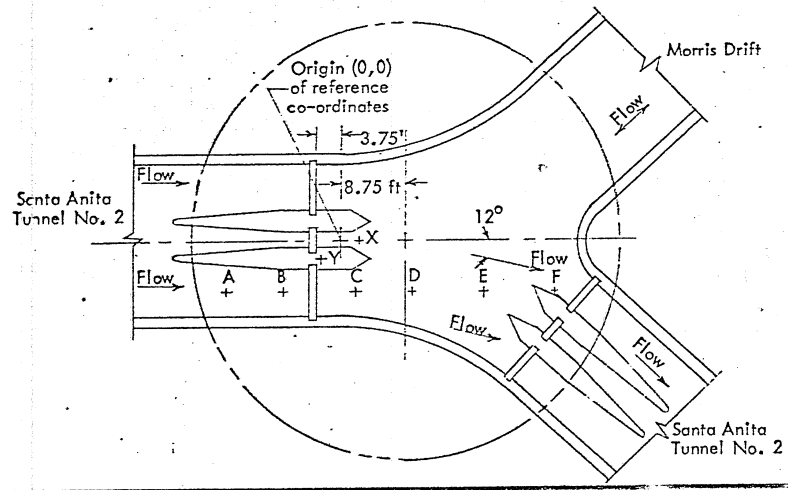
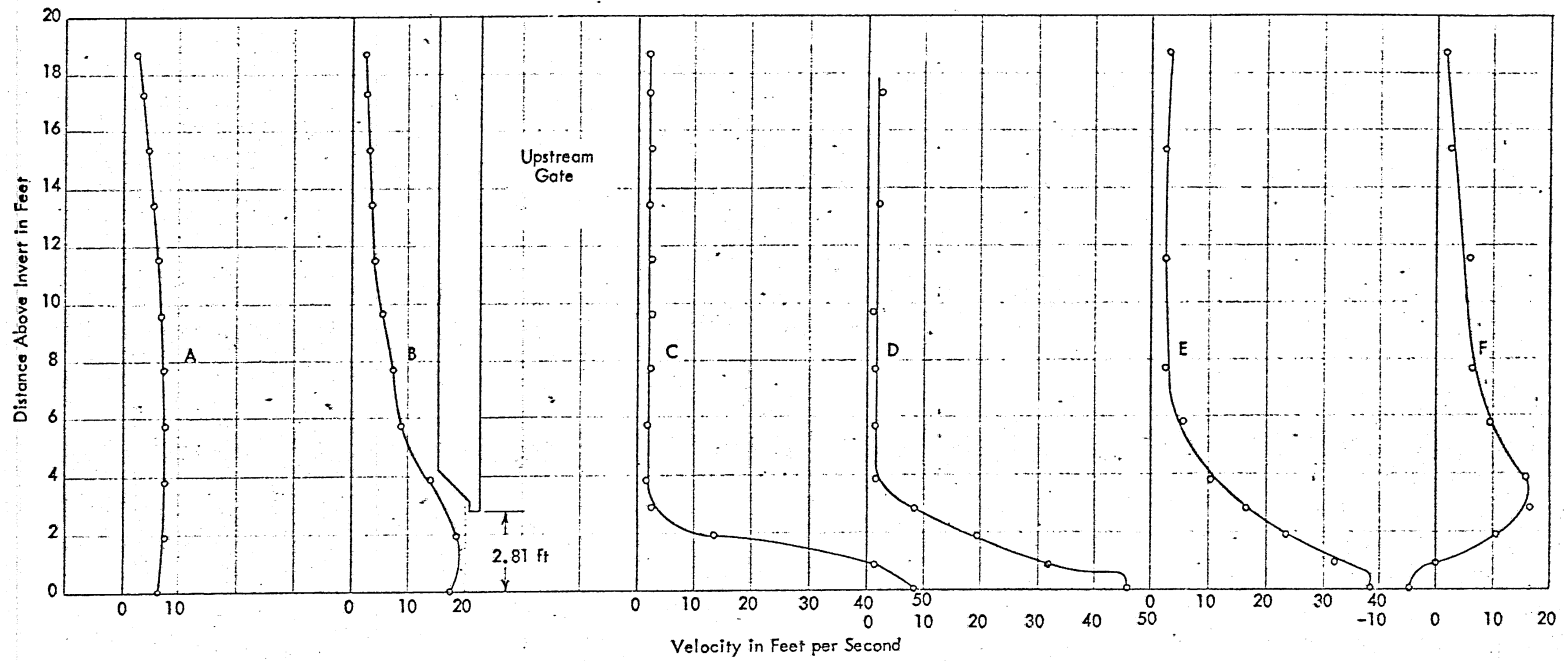
Profile	Location - distance downstream of gate feet prototype
A	0
B	5.75
C	11.50
D	17.25

COMPARISON OF VELOCITY PROFILES WITH AND WITHOUT MORRIS DRIFT - LEFT DOWNSTREAM GATE

Q = 1550 cfs  
 HW = 1180 ft.  
 RES = 1150 ft.  
 TW = 1130 ft.

USGO = 21.6%  
 DSGO = 21.6%  
 (Center Gates Closed)  
 Model Scale 1:38.3

MODEL STUDIES-FOOTHILL FEEDER PROJECT		
Metropolitan Water Dist. of Southern California		
MORRIS RESERVOIR TURNOUT STRUCTURE		
Harza Engineering Co., Chicago, Ill.		
SAINT ANTHONY FALLS HYDRAULIC LABORATORY		
UNIVERSITY OF MINNESOTA		
DRAWN DMN	CHECKED	APPROVED
SCALE	DATE 2-8-68	NO. 1083-459-231



- Notes:
1. See sketch for location of the origin (0,0) of the reference co-ordinate system.
  2. No flow in Morris Drift.
  3. The three gates of each set are opened equally.

Position	X in Feet	Y in Feet
A	-16	+7
B	-8	+7
C	+2	+7
D	+10	+7
E	+20	+7
F	+30	+7

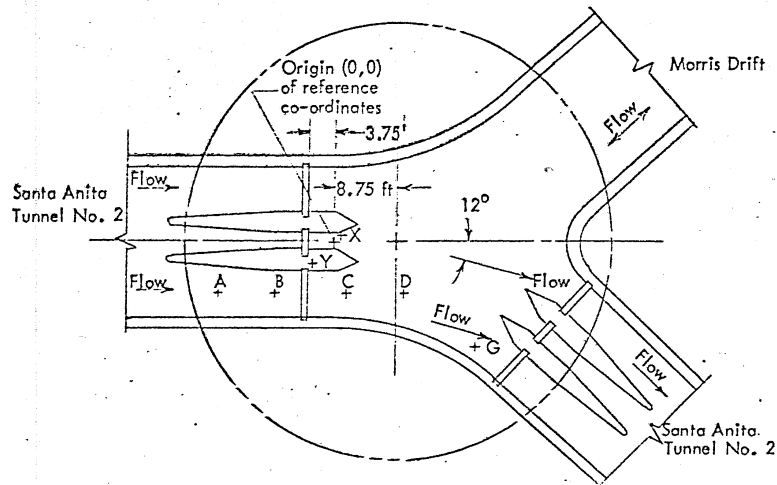
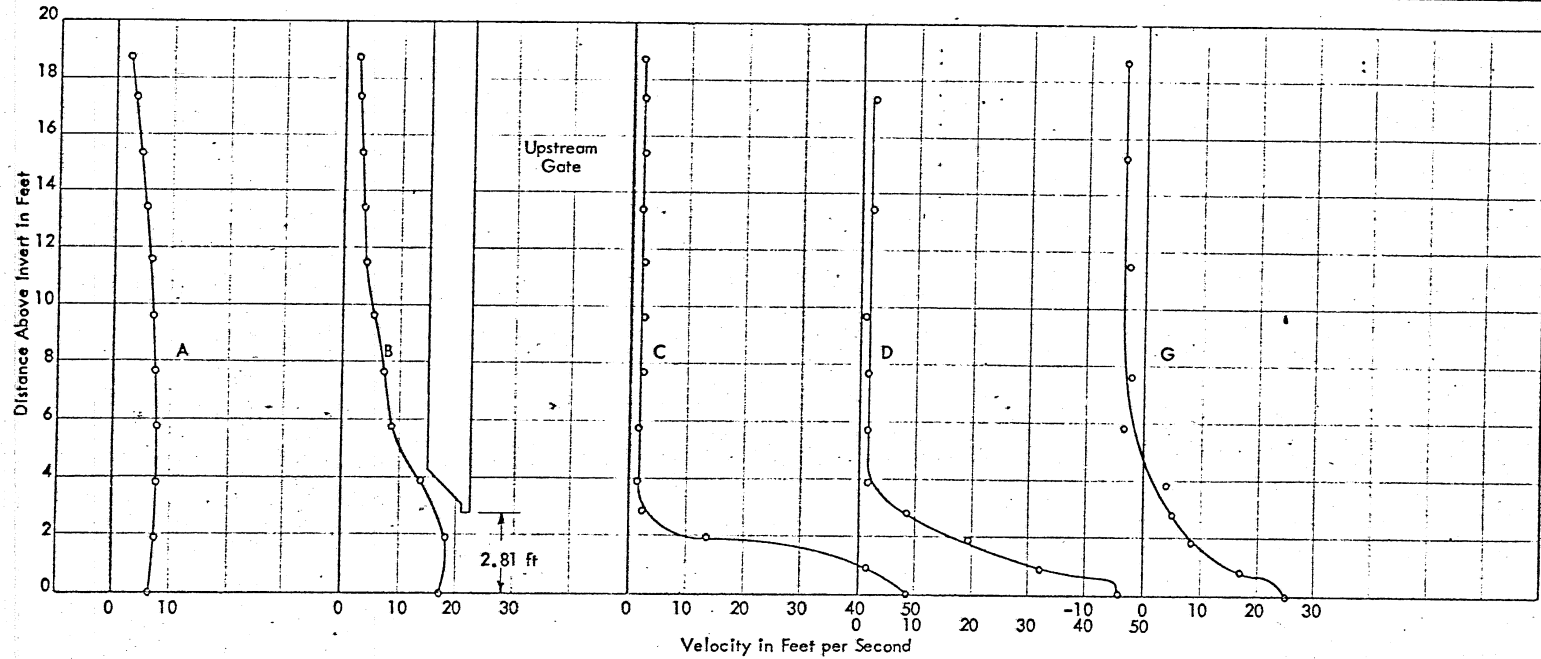
VELOCITY PROFILES IN THE VICINITY OF THE GATES

$Q = 1550$  cfs  
 H.W. Elev. = 1170 ft  
 Res. Elev. = 1131 ft  
 T. W. Elev. = 1130 ft  
 Upstream Gate Opening = 15.2%  
 Downstream Gate Opening = 100%  
 Model Scale = 1:38.3

MODEL STUDIES-FOOTHILL FEEDER PROJECT  
 Metropolitan Water Dist. of Southern California  
 MORRIS RESERVOIR TURNOUT STRUCTURE

Harza Engineering Co., Chicago, Ill.  
 SAINT ANTHONY FALLS HYDRAULIC LABORATORY  
 UNIVERSITY OF MINNESOTA

DRAWN GES	CHECKED	APPROVED
SCALE	DATE 11-28-67	NO. 168-B-459-219



Notes:

1. See sketch for location of the origin (0,0) of the reference co-ordinate system.
2. No flow in Morris Drift.
3. The three gates of each set are opened equally.

Position	X in Feet	Y in Feet
A	-16	+7
B	-8	+7
C	+2	+7
D	+10	+7
G	+20	+14

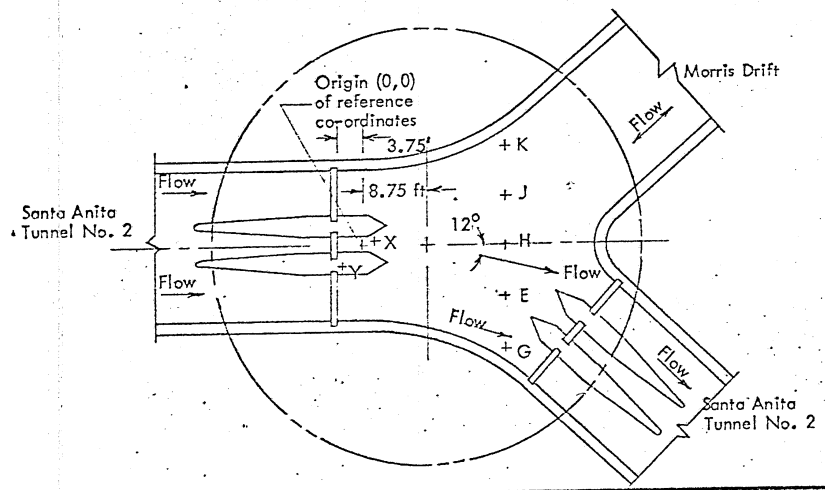
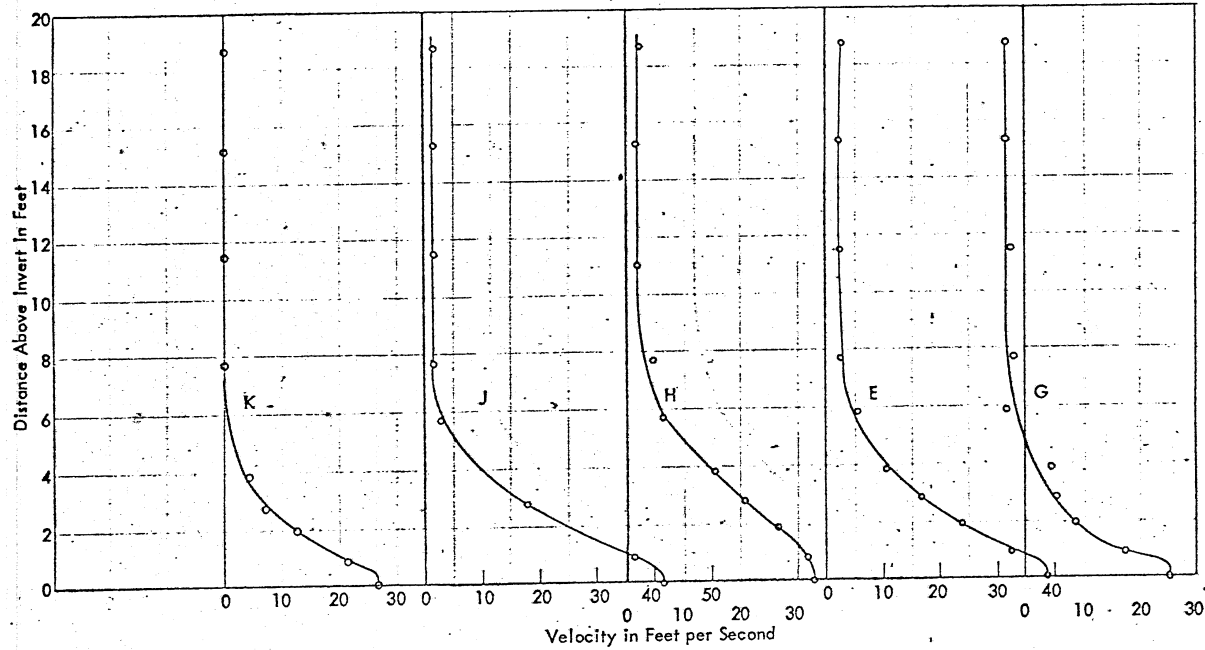
VELOCITY PROFILES IN THE VICINITY OF THE GATES

$Q = 1550$  cfs  
 H.W. Elev. = 1170 ft  
 Res. Elev. = 1131 ft  
 T.W. Elev. = 1130 ft  
 Upstream Gate Opening = 15.2%  
 Downstream Gate Opening = 100%  
 Model Scale = 1:38.3

MODEL STUDIES-FOOTHILL FEEDER PROJECT  
 Metropolitan Water Dist. of Southern California  
 MORRIS RESERVOIR TURNOUT STRUCTURE

Harza Engineering Co., Chicago, Ill.  
 SAINT ANTHONY FALLS HYDRAULIC LABORATORY  
 UNIVERSITY OF MINNESOTA

DRAWN GES    CHECKED    APPROVED  
 SCALE    DATE 11-28-67    NO. 168-5-459-220



- Notes:
1. See sketch for location of the origin (0,0) of the reference co-ordinates.
  2. No flow in Morris Drift.
  3. The three gates of each set are opened equally.

Position	X in Feet	Y in Feet
K	20	-14
J	20	-7
H	20	0
E	20	7
G	20	14

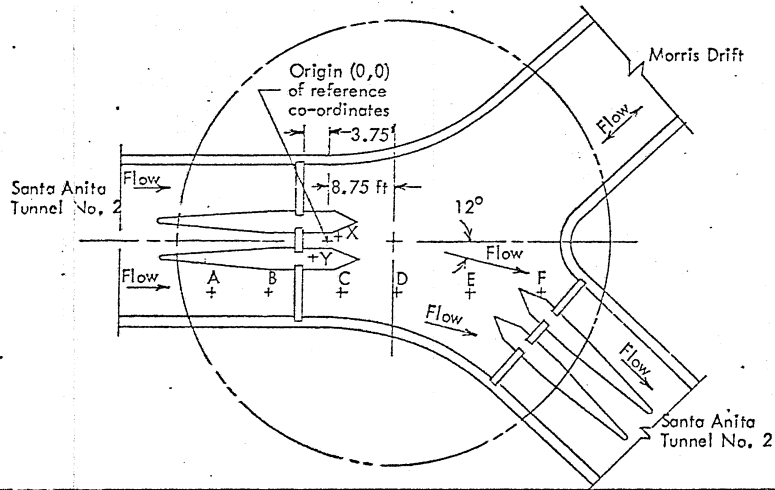
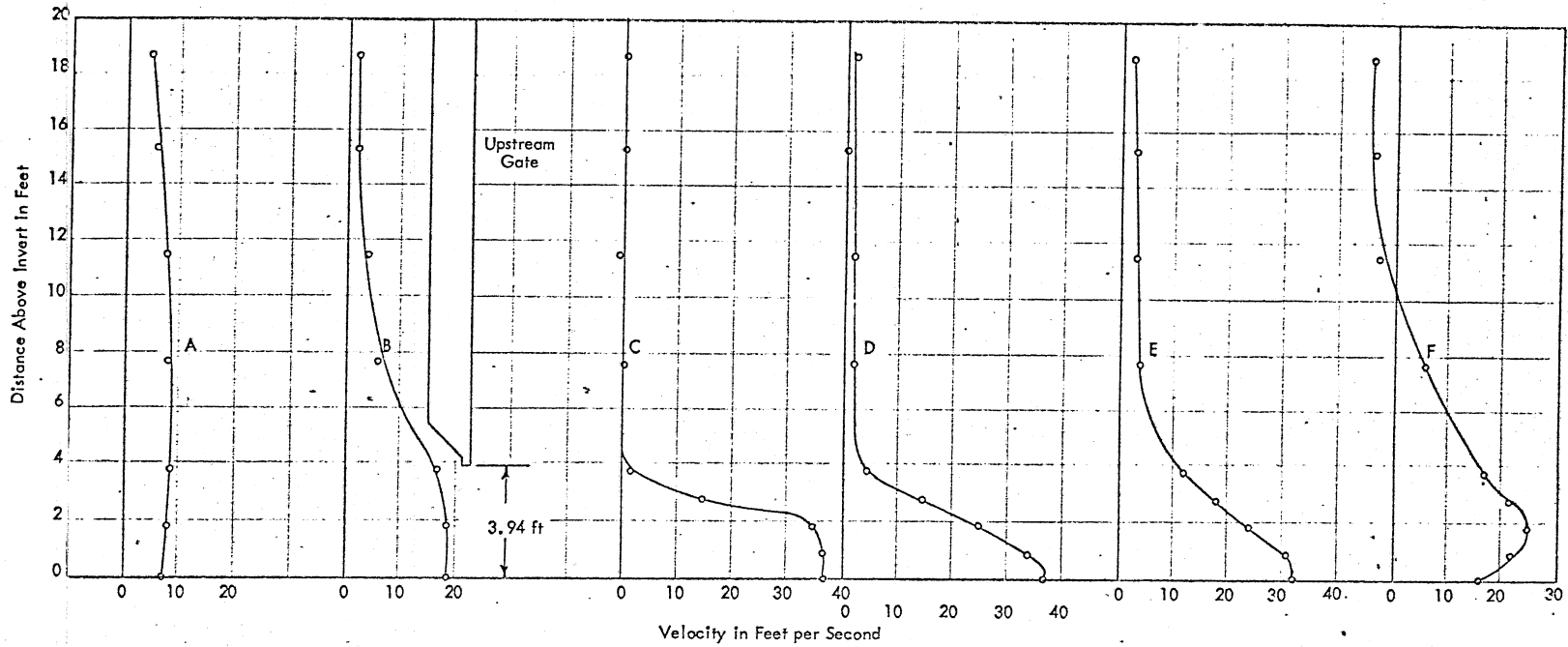
VELOCITY PROFILES IN THE VICINITY OF THE GATES  
 Q = 1550 cfs  
 H. W. Elev. = 1170 ft  
 Res. Elev. = 1131 ft  
 T. W. Elev. = 1130 ft  
 Upstream Gate Opening = 15.2%  
 Downstream Gate Opening = 100%  
 Model Scale = 1:38.3

MODEL STUDIES-FOOTHILL FEEDER PROJECT  
 Metropolitan Water Dist. of Southern California  
 MORRIS RESERVOIR TURNOUT STRUCTURE

Harza Engineering Co., Chicago, Ill.

SAINT ANTHONY FALLS HYDRAULIC LABORATORY  
 UNIVERSITY OF MINNESOTA

DRAWN	DJA	CHECKED	[initials]	APPROVED	[initials]
SCALE	DATE	11-28-67	NO.	16S-8-459-221	



Notes:

1. See sketch for location of the origin (0,0) of the reference co-ordinate system.
2. No flow in Morris Drift.
3. The three gates of each set are opened equally.

Position	X in Feet	Y in Feet
A	-16	+7
B	-8	+7
C	+2	+7
D	+10	+7
E	+20	+7
F	+30	+7

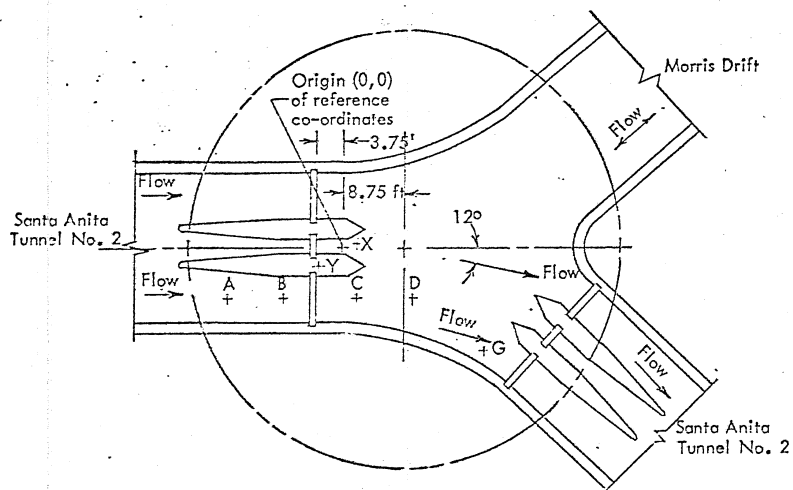
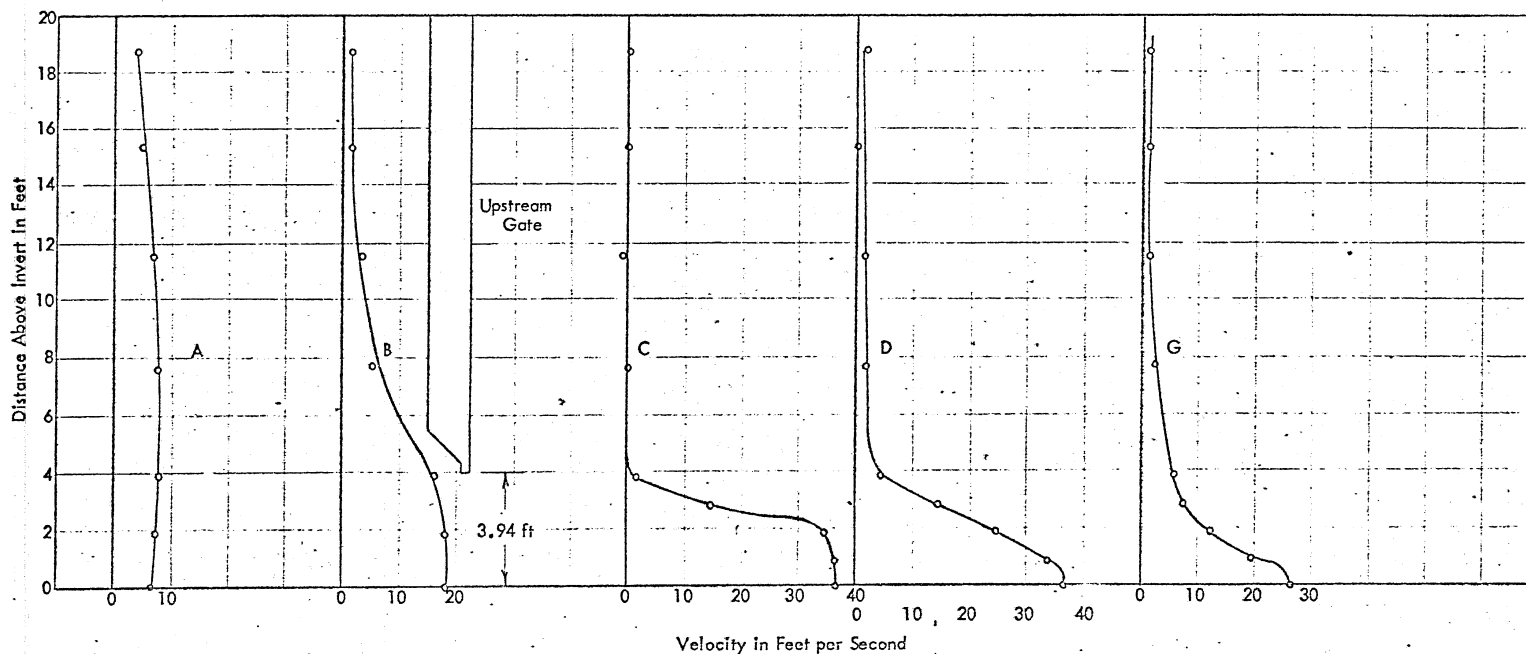
VELOCITY PROFILES IN THE VICINITY OF THE GATES

Q = 1550 cfs  
 H. W. Elev. = 1170 ft  
 Res. Elev. = 1150 ft  
 T. W. Elev. = 1130 ft  
 Upstream Gate Opening = 21.3%  
 Downstream Gate Opening = 17.5%  
 Model Scale = 1:38.2

MODEL STUDIES-FOOTHILL FEEDER PROJECT  
 Metropolitan Water Dist. of Southern California  
 MORRIS RESERVOIR TURNOUT STRUCTURE

Harza Engineering Co., Chicago, Ill.  
 SAINT ANTHONY FALLS HYDRAULIC LABORATORY  
 UNIVERSITY OF MINNESOTA

DRAWN	GES	CHECKED	APPROVED
SCALE	DATE	11-23-67	NO. 163-B-459-222



- Notes:
1. See sketch for location of the origin (0,0) of the reference co-ordinate system.
  2. No flow in Morris Drift.
  3. The three gates of each set are opened equally.

Position	X in Feet	Y in Feet
A	-16	+7
B	-8	+7
C	+2	+7
D	+10	+7
G	+20	+14

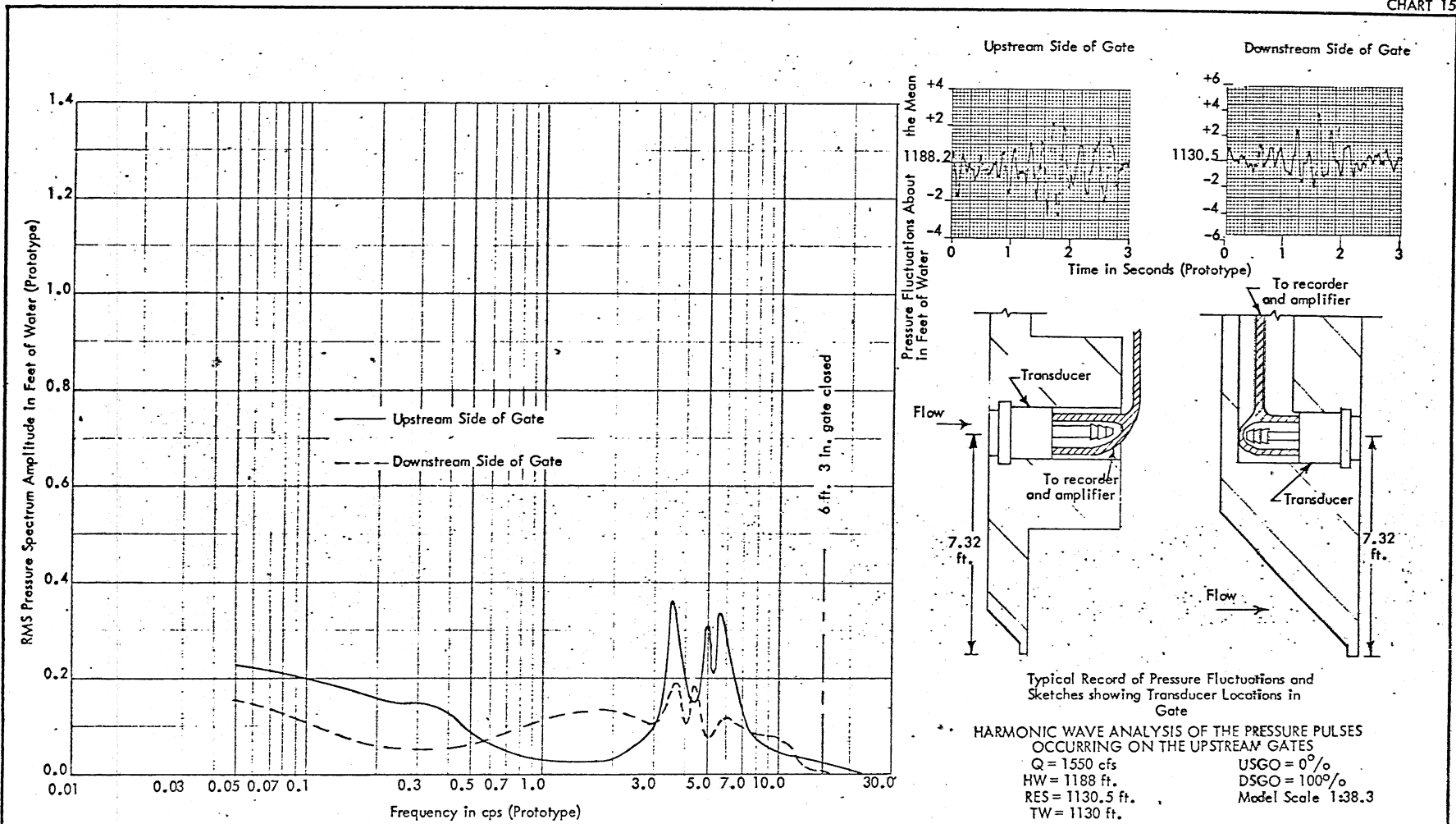
VELOCITY PROFILES IN THE VICINITY OF THE GATES

Q = 1550 cfs  
 H.W. Elev. = 1170 ft  
 Res. Elev. = 1150 ft  
 T.W. Elev. = 1130 ft  
 Upstream Gate Opening = 21.3 %  
 Downstream Gate Opening = 17.5 %  
 Model Scale = 1:38.3

MODEL STUDIES-FOOTHILL FEEDER PROJECT  
 Metropolitan Water Dist. of Southern California  
 MORRIS RESERVOIR TURNOUT STRUCTURE

Herza Engineering Co., Chicago, Ill.  
 SAINT ANTHONY FALLS HYDRAULIC LABORATORY  
 UNIVERSITY OF MINNESOTA  
 DRAWN DMN CHECKED [initials] APPROVED [initials]  
 SCALE 11-23-67 NO. 168-B-459-22



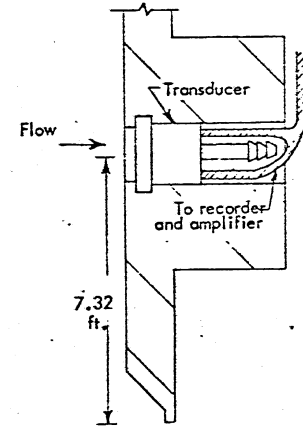
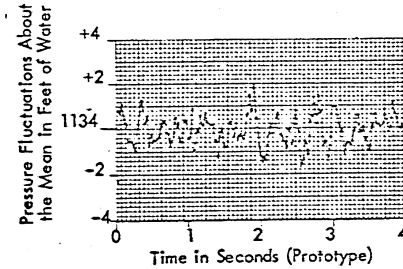
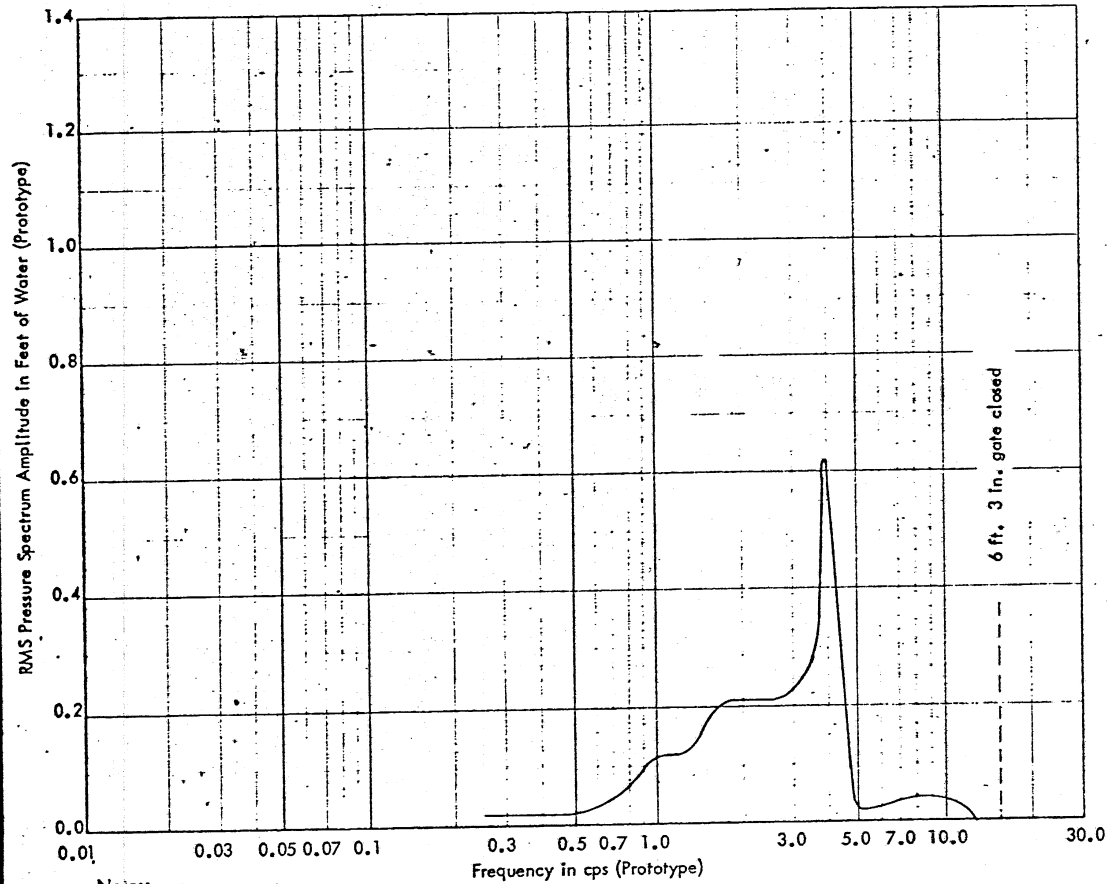


Notes:

1. Transducers used were 2.5 psi C.E.C., flush mounted type.
2. Upstream gates closed, downstream gates completely open, no flow in Morris Drift.
3. The transducers were mounted so as to record fluctuating pressures 7.32 ft. above the bottom of the gate.
4. The spectrum was obtained by analysis of records similar to that shown (above right). The graph above shows the RMS value of the amplitudes of the pressure pulses occurring with the indicated frequencies.
5. Dashed line on graph indicates natural frequency of the gate as designed by Harza Engineering Co. and shown on Harza drawings. 380-SKC-165 and 166.
6. Entire discharge was passed over the emergency weir.

HARMONIC WAVE ANALYSIS OF THE PRESSURE PULSES OCCURRING ON THE UPSTREAM GATES  
 Q = 1550 cfs                      USGO = 0%  
 HW = 1188 ft.                    DSGO = 100%  
 RES = 1130.5 ft.                Model Scale 1:38.3  
 TW = 1130 ft.

MODEL STUDIES-FOOTHILL FEEDER PROJECT		
Metropolitan Water Dist. of Southern California		
MORRIS RESERVOIR TURNOUT STRUCTURE		
Harza Engineering Co., Chicago, Ill.		
SAINT ANTHONY FALLS HYDRAULIC LABORATORY		
UNIVERSITY OF MINNESOTA		
DRAWN DMN	CHECKED [Signature]	APPROVED [Signature]
SCALE	DATE 12-18-67	NO 1685-459-224



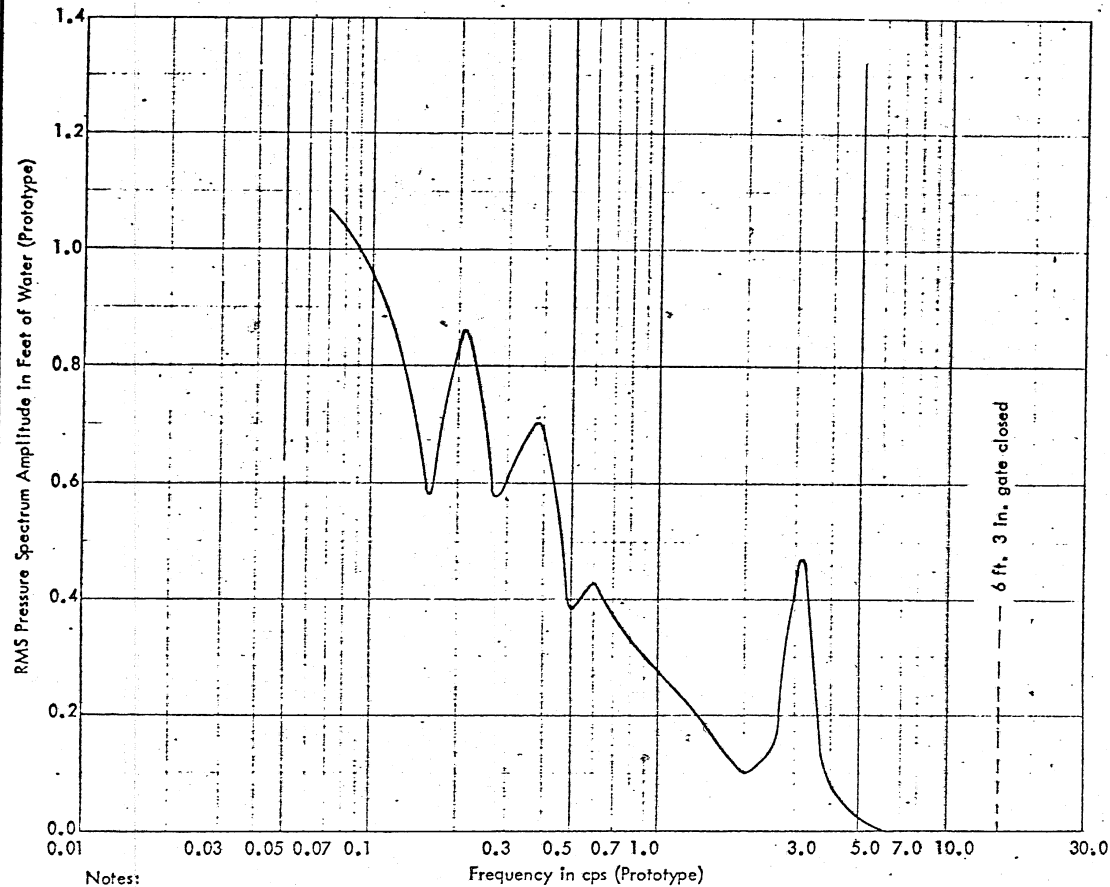
Typical Record of Pressure Fluctuations and Sketch showing Transducer Location in Gate

HARMONIC WAVE ANALYSIS OF THE PRESSURE PULSES OCCURRING ON THE DOWNSTREAM RIGHT GATE  
 Q = 1550 cfs  
 HW = 1188 ft.  
 RES = 1134 ft.  
 TW = 1130 ft.  
 USGO = 0%  
 DSGO = 37.8%  
 Model Scale 1:38.3

Notes:

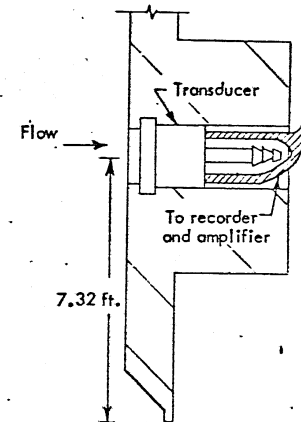
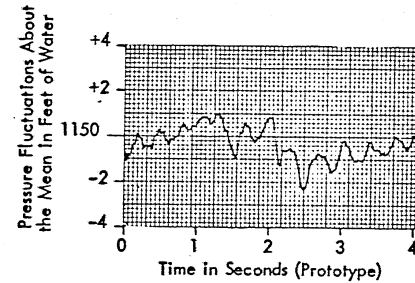
1. Transducers used were 2.5 psi C.E.C., flush mounted type.
2. Upstream gates closed, downstream gates open 37.8%, no flow in Morris Drift.
3. The transducers were mounted so as to record fluctuating pressures 7.32 ft. above the bottom of the gate.
4. The spectrum was obtained by analysis of records similar to that shown (above right). The graph above shows the RMS value of the amplitudes of the pressure pulses occurring with the indicated frequencies.
5. Dashed line on graph indicates natural frequency of the gate as designed by Harza Engineering Co. and shown on Harza drawings. 380-SKC-165 and 166.
6. Entire discharge was passed over the emergency weir.

MODEL STUDIES-FOOTHILL FEEDER PROJECT Metropolitan Water Dist. of Southern California		
MORRIS RESERVOIR TURNOUT STRUCTURE		
Harza Engineering Co., Chicago, Ill.		
SAINT ANTHONY FALLS HYDRAULIC LABORATORY UNIVERSITY OF MINNESOTA		
DRAWN DMNI	CHECKED <i>[Signature]</i>	APPROVED
SCALE	DATE 12-19-67	NO. 1688-459-225



Notes:

- Transducers used were 2.5 psi C.E.C., flush mounted type.
- Upstream gates open 16%, downstream gates open 17%, no flow in Morris Drift.
- The transducers were mounted so as to record fluctuating pressures 7.32 ft. above the bottom of the gate.
- The spectrum was obtained by analysis of records similar to that shown (above right). The graph above shows the RMS value of the amplitudes of the pressure pulses occurring with the indicated frequencies.
- Dashed line on graph indicates natural frequency of the gate as designed by Harza Engineering Co. and shown on Harza drawings. 380-SKC-165 and 166.



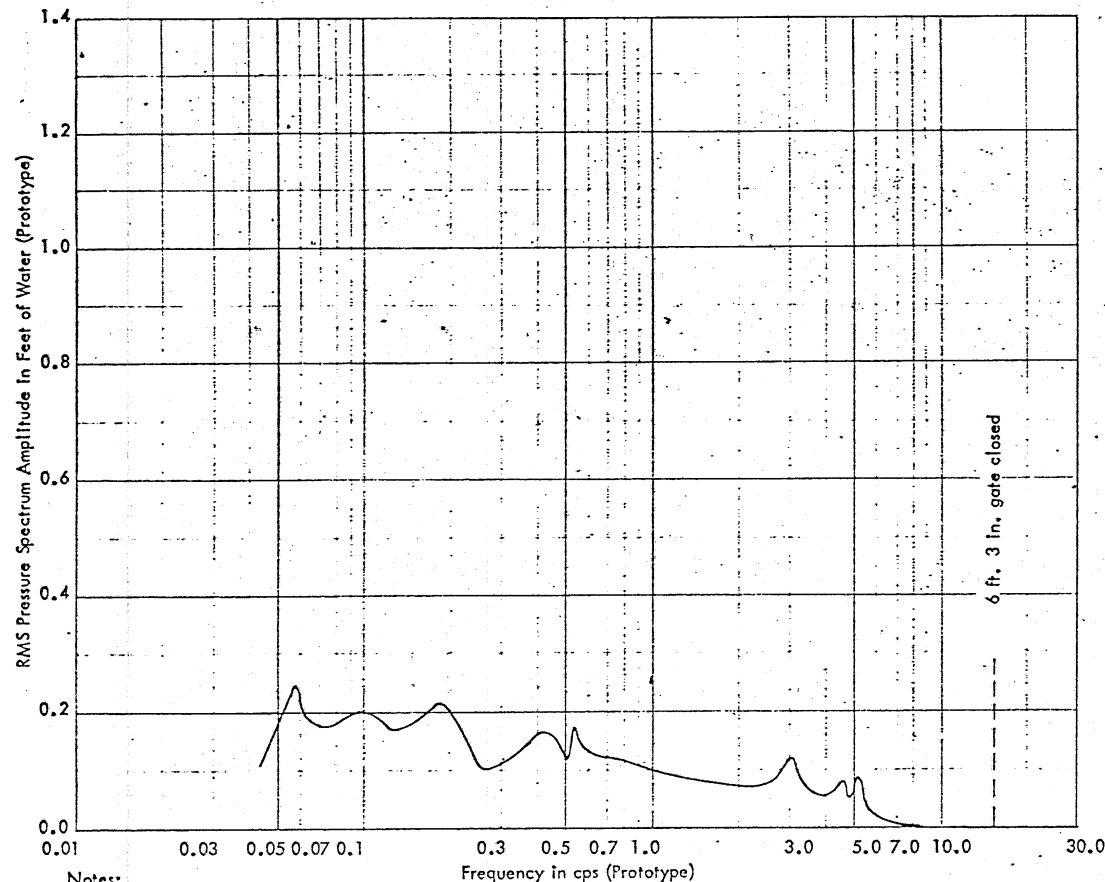
Typical Record of Pressure Fluctuations and Sketch showing Transducer Location in Gate

HARMONIC WAVE ANALYSIS OF THE PRESSURE PULSES OCCURRING ON THE DOWNSTREAM RIGHT GATE

Q = 1550 cfs  
 HW = 1180 ft.  
 RES = 1150 ft.  
 TW = 1130 ft.  
 USGO = 16%

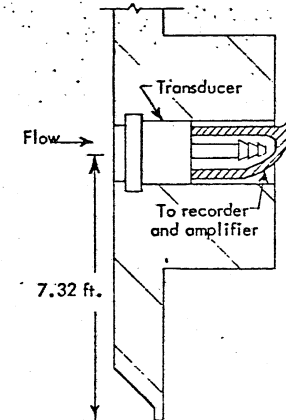
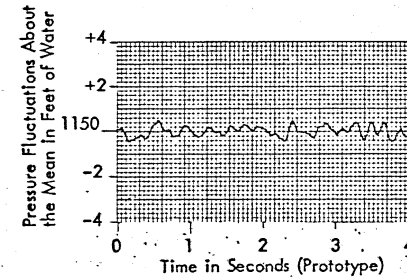
DSGO 17%  
 Model Scale 1:38.3

MODEL STUDIES-FOOTHILL FEEDER PROJECT		
Metropolitan Water Dist. of Southern California		
MORRIS RESERVOIR TURNOUT STRUCTURE		
Harza Engineering Co., Chicago, Ill.		
SAINT ANTHONY FALLS HYDRAULIC LABORATORY		
UNIVERSITY OF MINNESOTA		
DRAWN D.V.N.	CHECKED	APPROVED
SCALE	DATE 12-14-67	NO. 1688-439-226



Notes:

1. Transducers used were 2.5 psi C.E.C., flush mounted type.
2. Upstream gates open 3.9%, downstream gates open 4.4%, no flow in Morris Drift.
3. The transducers were mounted so as to record fluctuating pressures 7.32 ft. above the bottom of the gate.
4. The spectrum was obtained by analysis of records similar to that shown (above right). The graph above shows the RMS value of the amplitudes of the pressure pulses occurring with the indicated frequencies.
5. Dashed line on graph indicates natural frequency of the gate as designed by Harza Engineering Co. and shown on Harza drawings. 380-SKC-165 and 166.



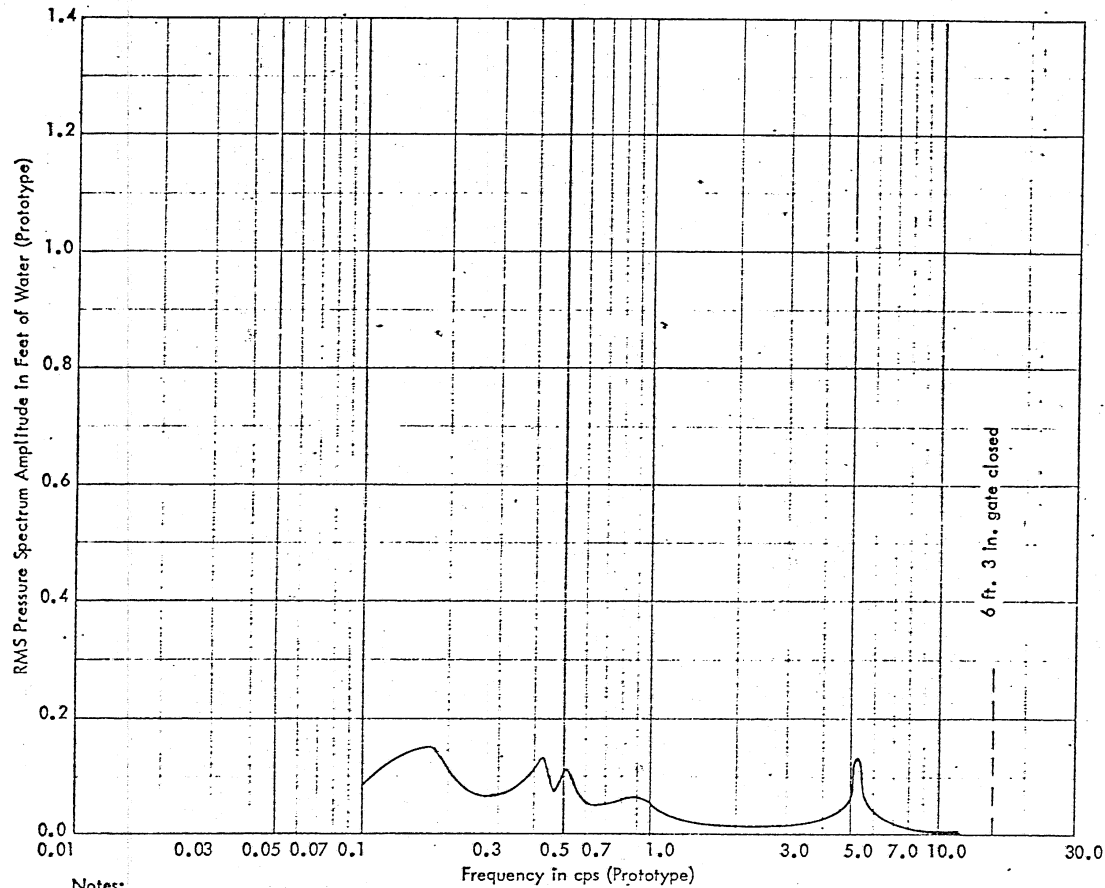
Typical Record of Pressure Fluctuations and Sketch showing Transducer Location in Gate

HARMONIC WAVE ANALYSIS OF THE PRESSURE PULSES OCCURRING ON THE DOWNSTREAM RIGHT GATE

Q = 420 cfs  
 HW = 1180 ft.  
 RES = 1150 ft.  
 TW = 1130 ft.  
 USGO = 3.9%

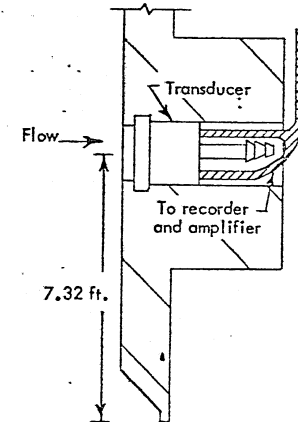
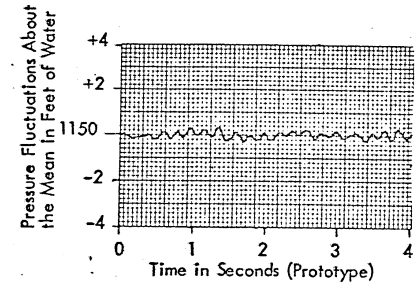
DSGO = 4.4%  
 Model Scale 1:38.3

MODEL STUDIES-FOOTHILL FEEDER PROJECT		
Metropolitan Water Dist. of Southern California		
MORRIS RESERVOIR TURNOUT STRUCTURE		
Harza Engineering Co., Chicago, Ill.		
SAINT ANTHONY FALLS HYDRAULIC LABORATORY		
UNIVERSITY OF MINNESOTA		
DRAWN	CHECKED	APPROVED
SCALE	DATE 12-19-67	NO 1688-459-227



Notes:

1. Transducers used were 2.5 psi C. E. C., flush mounted type.
2. Upstream gate open 15.8%, downstream gate open 18.1% (center gates only), no flow in Morris Drift.
3. The transducers were mounted so as to record fluctuating pressures 7.32 ft. above the bottom of the gate.
4. The spectrum was obtained by analysis of records similar to that shown (above right). The graph above shows the RMS value of the amplitudes of the pressure pulses occurring with the indicated frequencies.
5. Dashed line on graph indicates natural frequency of the gate as designed by Harza Engineering Co. and shown on Harza drawings. 380-SKC-165 and 166.



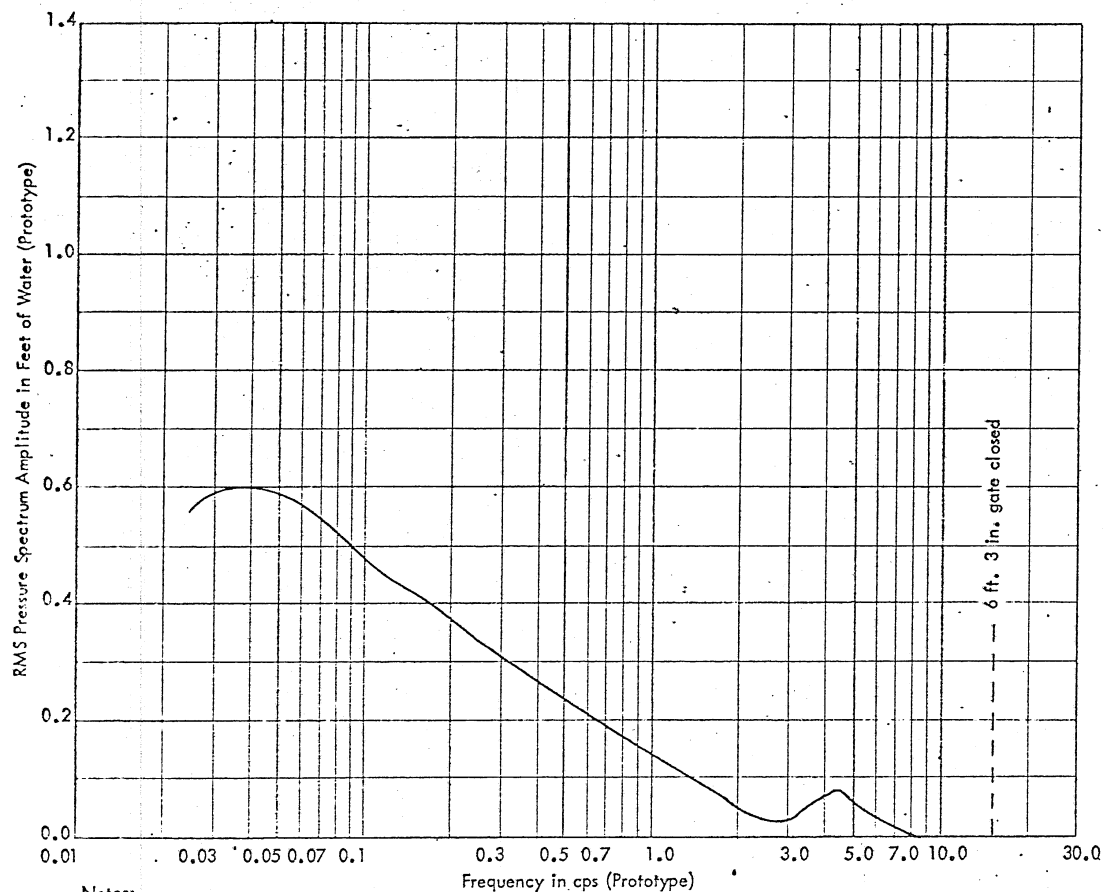
Typical Record of Pressure Fluctuations and Sketch showing Transducer Location in Gate

HARMONIC WAVE ANALYSIS OF THE PRESSURE PULSES OCCURRING ON THE DOWNSTREAM RIGHT GATE

Q = 200 cfs  
 HW = 1180 ft.  
 RES = 1150 ft.  
 TW = 1130 ft.

DSGO = 18.1% (Center Gate Only)  
 Model Scale 1:38:3  
 USGO = 15.8% (Center Gate Only)

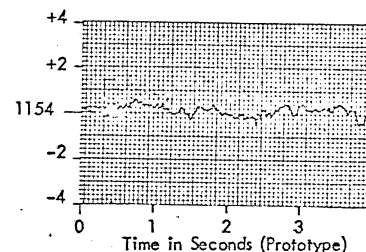
MODEL STUDIES-FOOTHILL FEEDER PROJECT		
Metropolitan Water Dist. of Southern California		
MORRIS RESERVOIR TURNOUT STRUCTURE		
Harza Engineering Co., Chicago, Ill.		
SAINT ANTHONY FALLS HYDRAULIC LABORATORY		
UNIVERSITY OF MINNESOTA		
DRAWN D.W.N.	CHECKED /	APPROVED /
SCALE	DATE 12-19-67	NO 1698-459-228



Notes:

1. Transducers used were 2.5 psi C.E.E., flush mounted type.
2. Upstream gate open 33.5%, downstream gate open 34.5% (Left gates only), no flow in Morris Drift.
3. The transducers were mounted so as to record fluctuating pressures 7.32 ft. above the bottom of the gate.
4. The spectrum was obtained by analysis of the records similar to that shown (above right). The graph above shows the RMS value of the amplitudes of the pressure pulses occurring with the indicated frequencies.
5. Dashed line on graph indicates natural frequency of the gate as designed by Harza Engineering Co. and shown on Harza drawings. 380-SKC-165 and 166.

Pressure Fluctuations About the Mean in Feet of Water

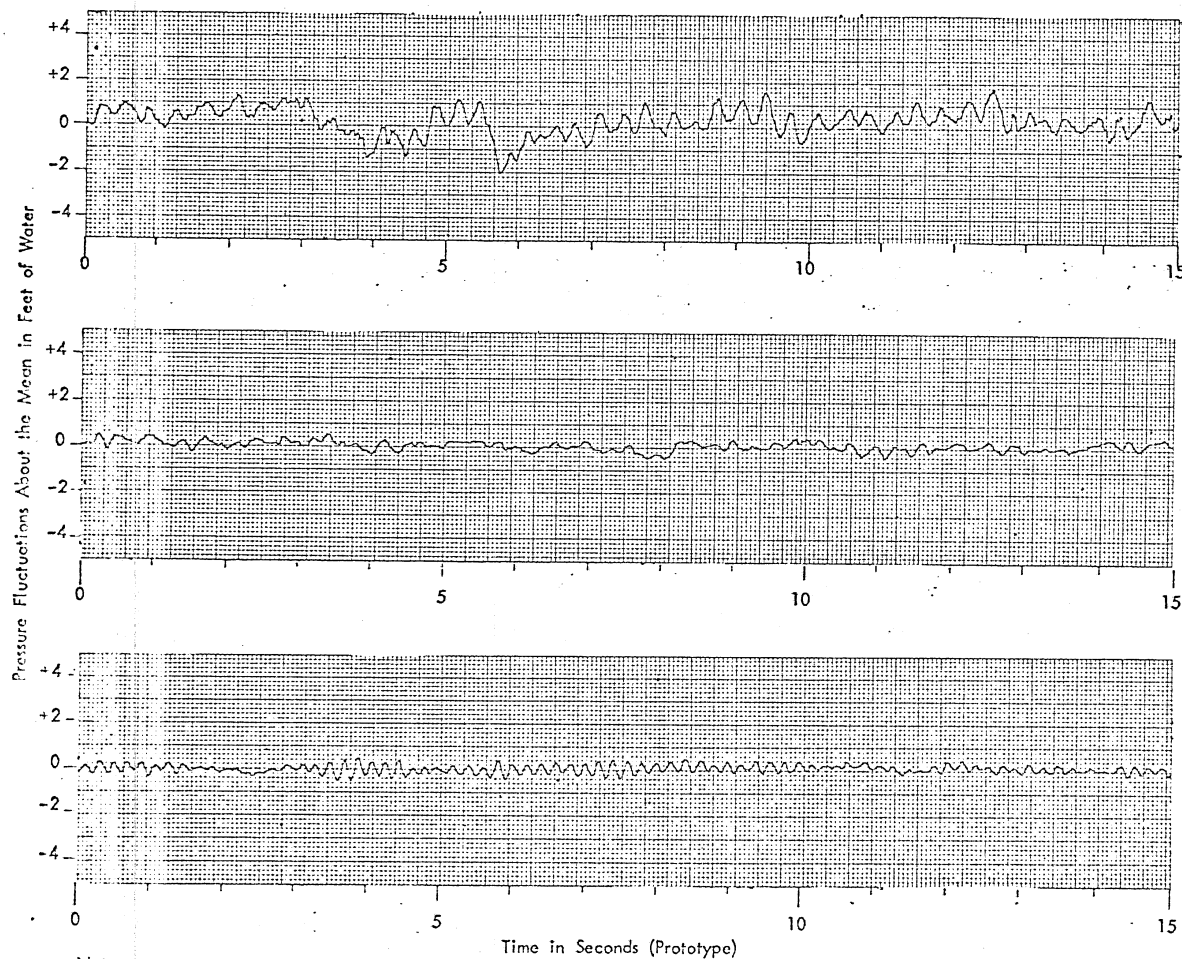


Typical Record of Pressure Fluctuations and Sketch showing Transducer Location in Gate

HARMONIC WAVE ANALYSIS OF THE PRESSURE PULSES OCCURRING ON THE DOWNSTREAM RIGHT GATE

Q = 1550 cfs  
 HW = 1180 ft.  
 RES = 1154 ft.  
 TW = 1130 ft.  
 USGO = 33.5% (Left Only)  
 DSGO = 34.5% (Left Only)  
 Model Scale 1:38.3

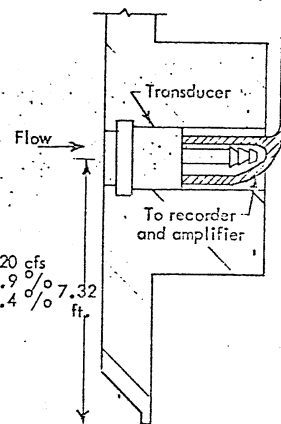
MODEL STUDIES-FOOTHILL FEEDER PROJECT		
Metropolitan Water Dist. of Southern California		
MORRIS RESERVOIR TURNOUT STRUCTURE		
Harza Engineering Co., Chicago, Ill.		
SAINT ANTHONY FALLS HYDRAULIC LABORATORY		
UNIVERSITY OF MINNESOTA		
DRAWN	CHECKED	APPROVED
DMN	LL	
SCALE	DATE 12-14-67	NO 1688-459-229



Q = 1550 cfs  
USGO = 16 %  
DSGO = 17 %

Q = 420 cfs  
USGO = 3.9 %  
DSGO = 4.4 %

Q = 200 cfs  
USGO = 15.8 %  
DSGO = 18.1 %  
(Center Gates Only)



Sketch showing transducer location in the gate

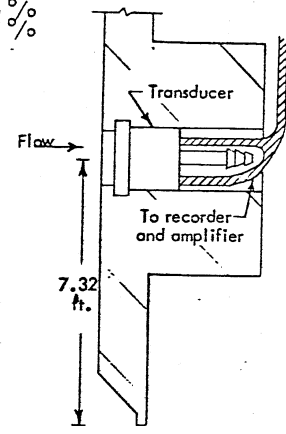
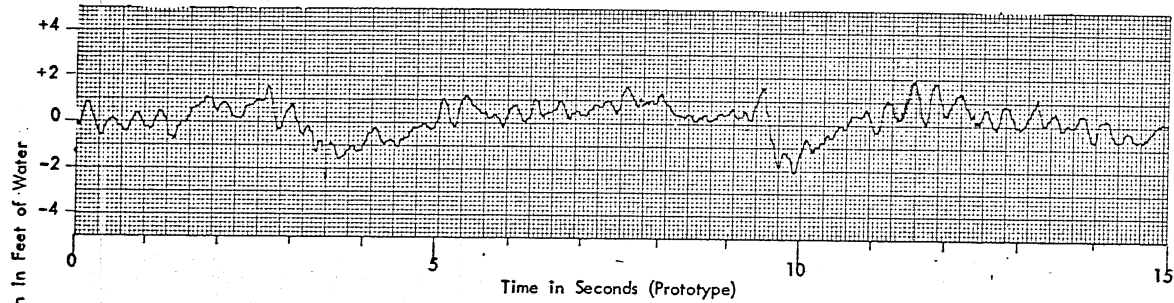
COMPARISON OF PRESSURE FLUCTUATIONS ON THE DOWNSTREAM RIGHT GATE FOR VARIOUS DISCHARGES

HW = 1180 ft.  
RES = 1150 ft.  
TW = 1130 ft.  
Model Scale 1:38.3

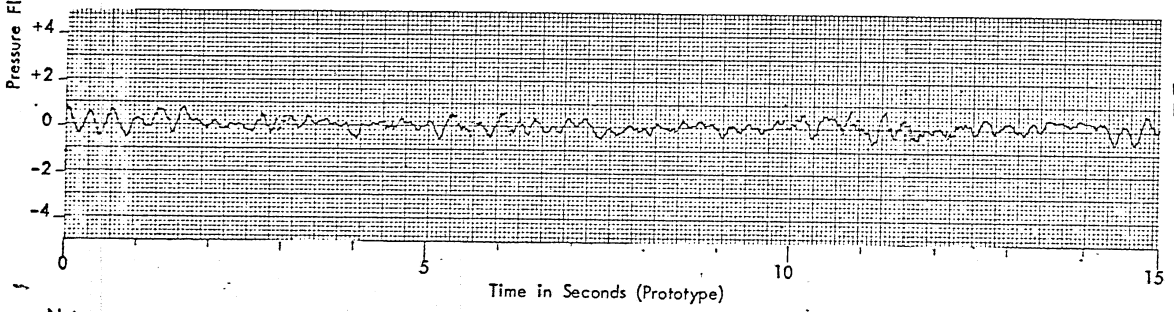
Notes:

1. Transducer used was a 2.5 psi C.E.C., flush mounted type.
2. Pressure fluctuations are shown with reference to gage zero which corresponds to a reservoir elevation of 1150 ft.

MODEL STUDIES-FOOTHILL FEEDER PROJECT Metropolitan Water Dist. of Southern California MORRIS RESERVOIR TURNOUT STRUCTURE		
Harza Engineering Co., Chicago, Ill.		
SAINT ANTHONY FALLS HYDRAULIC LABORATORY UNIVERSITY OF MINNESOTA		
DRAWN DIMN	CHECKED	APPROVED
DATE 2-8-68		NO 1688-459-234



Sketch showing transducer location in the gate



COMPARISON OF PRESSURE FLUCTUATIONS ON THE DOWNSTREAM RIGHT GATE FOR TWO RESERVOIR ELEVATIONS

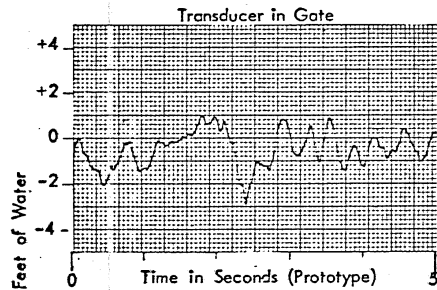
Q = 1550 cfs  
HW = 1180 ft.  
TW = 1130 ft.  
Model Scale 1:38.3

Notes:

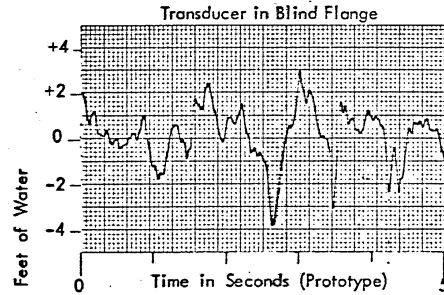
1. Transducer used was a 2.5 psi C.E.C., flush mounted type.
2. Pressure fluctuations are shown with reference to gage zero which corresponds to the reservoir elevations listed.

MODEL STUDIES-FOOTHILL FEEDER PROJECT			
Metropolitan Water Dist. of Southern California			
MORRIS RESERVOIR TURNOUT STRUCTURE			
Harza Engineering Co., Chicago, Ill.			
SAINT ANTHONY FALLS HYDRAULIC LABORATORY			
UNIVERSITY OF MINNESOTA			
DRAWN	DMN	CHECKED	APPROVED
SCALE	DATE 2-8-55	ING	1408-459-235





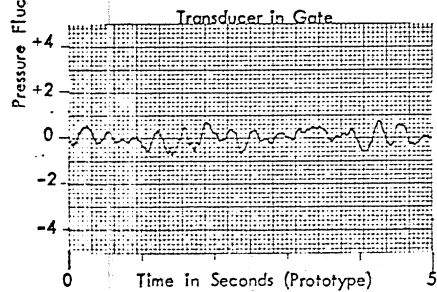
(A)  
RES = 1150 ft.  
USGO = 16%  
DSGO = 17%



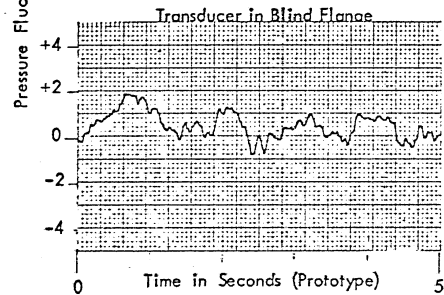
(C)  
RES = 1150 ft.  
USGO = 21.6%  
DSGO = 21.6%  
(Center Gates Closed)

Notes:

1. Transducers used were 2.5 psi C.E.C., flush mounted type.
2. The transducer in the gate was mounted on the centerline 7.32 ft. above the gate lip.
3. The transducer in the blind flange was mounted at the center.
4. Pressure fluctuations are shown with reference to gage zero which corresponds to the reservoir elevations listed.
5. Comparison of tape A to tape B and of tape C to tape D should be made.



(B)  
RES = 1170 ft.  
USGO = 24%  
DSGO = 13%



(D)  
RES = 1170 ft.  
USGO = 33.6%  
DSGO = 15.5%  
(Center Gates Closed)

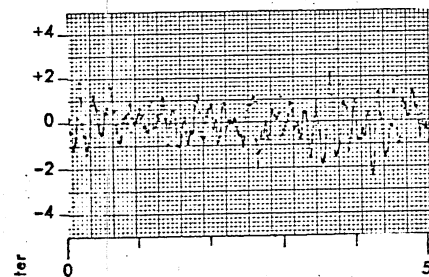
PRESSURE FLUCTUATIONS ON DOWNSTREAM RIGHT GATE AND BLIND FLANGE ON MORRIS DRIFT

Q = 1550 cfs-  
HW = 1180 ft.  
TW = 1130 ft.  
Model Scale 1:38.3

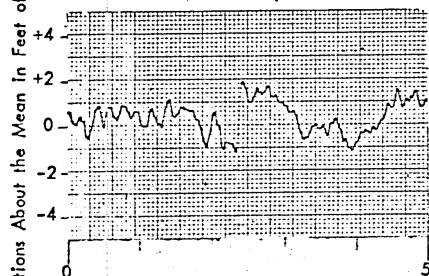
MODEL STUDIES-FOOTHILL FEEDER PROJECT  
Metropolitan Water Dist. of Southern California  
MORRIS RESERVOIR TURNOUT STRUCTURE

Harzo Engineering Co., Chicago, Ill.  
SAINT ANTHONY FALLS HYDRAULIC LABORATORY  
UNIVERSITY OF MINNESOTA

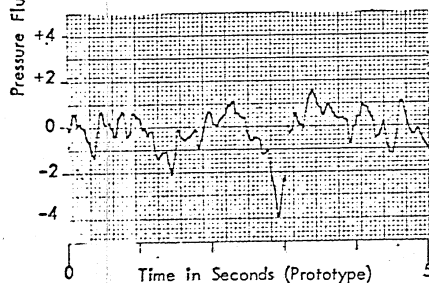
DRAWN DMN	CHECKED	APPROVED
SCALE	DATE 2-8-68	NO 1658-459-236



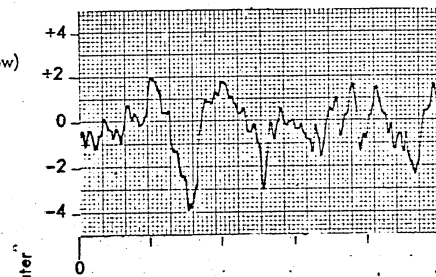
HW = 1188 ft.  
(Emergency Weir Overflow)  
RES = 1130.5 ft.  
USGO = 0%  
DSGO = 100%  
Max. Fluctuation  
is 6.6 ft. of water.



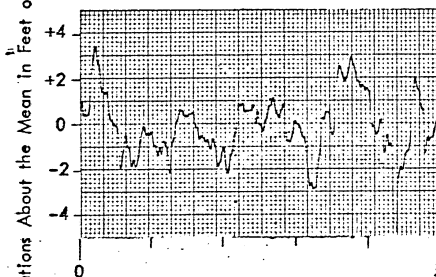
HW = 1180 ft.  
RES = 1170 ft.  
USGO = 33.6%  
DSGO = 15.5%  
Max. Fluctuation  
is 4.2 ft. of water.



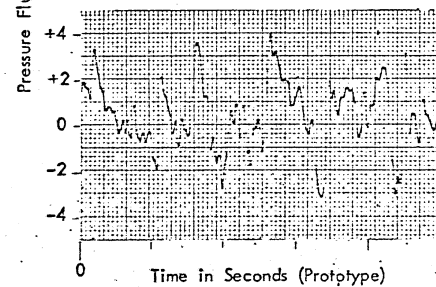
HW = 1180 ft.  
RES = 1160 ft.  
USGO = 25.4%  
DSGO = 19.8%  
Max. Fluctuation  
is 6.0 ft. of water.



HW = 1180 ft.  
RES = 1150 ft.  
USGO = 21.6%  
DSGO = 21.6%  
Max. Fluctuation  
is 8.8 ft. of water.



HW = 1180 ft.  
RES = 1140 ft.  
USGO = 18.1%  
DSGO = 28.4%  
Max. Fluctuation  
is 9.8 ft. of water.



HW = 1180 ft.  
RES = 1130.5 ft.  
USGO = 16.8%  
DSGO = 100%  
Max. Fluctuation  
is 9.6 ft. of water.

Notes:

1. Transducer used was a 2.5 psi C. E. C., flush mounted type.
2. The transducer was mounted at the center of the blind flange.
3. Pressure fluctuations are shown with reference to gage zero which corresponds to the reservoir elevations listed.
4. Maximum fluctuations listed are those found when examining data from entire test run.

COMPARISON OF THE PRESSURE FLUCTUATIONS ON THE BLIND FLANGE ON MORRIS DRIFT FOR VARIOUS RESERVOIR ELEVATIONS

Q = 1550 cfs  
Model Scale 1:38.3

MODEL STUDIES-FOOTHILL FEEDER PROJECT  
Metropolitan Water Dist. of Southern California  
MORRIS RESERVOIR TURNOUT STRUCTURE

Harza Engineering Co., Chicago, Ill.

SAINT ANTHONY FALLS HYDRAULIC LABORATORY  
UNIVERSITY OF MINNESOTA

DRAWN DMN	CHECKED	APPROVED
SCALE	DATE 2-8-68	NO. 1688-459-237